Mapping Erosion from Space

2007

Promotor: Prof. dr. ir. L. Stroosnijder
Hoogleraar Erosie en Bodem & Waterconservering
Wageningen Universiteit

Co-promotor: dr. ir. G. Sterk
Universitair docent bij de leerstoelgroep Erosie en
Bodem- & Waterconservering
Wageningen Universiteit

Promotiecommissie: Prof. dr. M.E. Schaepman (Wageningen Universiteit)
Prof. dr. S.M. de Jong (Utrecht Universiteit)
Prof. dr. J. Poesen (Katholieke Universiteit Leuven)
dr. ir. J.J. Stoorvogel (Wageningen Universiteit)

Mapping Erosion from Space

Anton Vrieling

Acknowledgements

Remote sensing may be defined as acquiring information about objects or phenomena from a distance. In that light, it seems inappropriate that while performing my PhD on remote sensing for soil erosion studies, a large amount of time was spent 40 to 60 cm from a computer screen. From a nuclear physicist's point of view this distance is remote, but from the human perspective the term 'close sensing' may be more suitable. Nevertheless, images that I have been observing on the screen were acquired from a greater distance, typically between 400 and 800 km above the earth surface. As we are not all that lucky to become astronauts, cosmonauts, or taikonauts, orbiting satellites are a good alternative for acquiring space-based earth observations. I must say though that I feel far from unlucky, but rather privileged that I have had the opportunity to perform this study, which left me not only in front of the computer, but also took me to a number of remote places on this planet that I could observe at very high resolution. In remote sensing, the mere observation is not the final goal, because valuable information is only obtained through active interaction with the data. Interaction is indeed what makes things interesting, whether it is in remote sensing, in music, or in daily life. I am therefore grateful to everybody that in some way or another contributed to the finalization of this thesis.

First, I would like to acknowledge the constant support of the Erosion and Soil & Water Conservation (ESW) Group of Wageningen University. In particular, I want to thank my daily supervisor and co-promotor Geert Sterk who has continuously encouraged me and made many constructive comments on my research and manuscripts. Geert, you have been a determining factor in starting and finishing this PhD research and I learned a lot from you. I hope we will share at least the number of beers that we already shared and I am looking forward to a bicycle ride to Twente! It has been a pleasure to work at the ESW group and share ideas and personal matters in an open atmosphere. My promotor Leo Stroosnijder is acknowledged for his institutional support. I express my gratitude to Dirk Meindertsma who never got tired of explaining how to fill in declaration forms and helped me in many other matters. A special word of thanks to Aad Kessler who recently gave me much highly-appreciated advice (although in many cases I was too stubborn to follow it). I want to thank Saskia, Jakolien, Huiberdien, Luuk, Monique, Jan, Wim, Piet, Michel, Ferko, Helena, Jolanda, Tony, and the many international PhD-students for their company during these years.

In the Netherlands, I would like to acknowledge the contribution of several other persons. At the start of the PhD, my idea was to use a specific remote sensing technique called SAR interferometry for erosion detection. Interferometric processing was done at Delft University of Technology in collaboration with Ramon Hanssen, which unfortunately showed that for my study areas conditions were not ideal to apply the technique. Ramon, thank you for teaching me the potentials and limits of this interesting technique. I would like to thank Harm Bartholomeus of the Centre for Geo-Information of WU for the stimulating cooperation in finding ways for automatic gully detection. Steven de Jong of Utrecht

through the EO-1223 Category-1 project submitted to the European Space Agency, although these data unfortunately did not make it into this thesis. Furthermore, a lot of free satellite data was obtained through NASA, including processed products of ASTER, MODIS, and TRMM. The QuickBird and the Landsat scene were commercially acquired.

I would like to finish by thanking all the people that have endured my presence (or absence) during off-work moments and offered their hospitability and friendship when needed. I will name here but a few, although there are many more that have made life an enjoyable experience over the past years. I want to thank my housemates from the Herenstraat for their understanding in busy times. I express my gratitude to Maryory, Fatima, and Daniela that made me feel at home in Uberlândia (Brazil), which in Lushoto (Tanzania) holds equally for Agnes. The bigband Sound of Science is acknowledged for the weekly two-hours of relaxation on Tuesday afternoon. Frank, I highly appreciate our frequent visits to the bar and the cinema during the past couple of years. Thijs and Joyce, you have a special place even though I managed to forget your first wedding anniversary. I hope to visit you soon in Germany and I will bring my Laura to your Laura! Linda, I am happy that you are back in town and maybe this year we should try to make it finally to the TT in Assen. Esther, also good that you are back and we will enjoy more beers than we have been doing lately. Silvia Elena, although our communication has become less during the past years, you mean a lot to me and I hope to visit you again in Colombia. Compadre John, I expect you to come back soon to immerse again together into the Wageningen nightlife. Resy, thanks for the various stimulating talks before several departures from Schiphol. Three persons have been very close to me during the PhD-period, although the physical distance has often been great. Patricia, remote feeling turned out to be difficult, especially with an ocean between us. However, I am grateful for knowing you and having spent an important moment of my life together. Sara, thank you for all the love and energy you have given me. Although our timing turned out not to be optimal, it has been a wonderful time. Mia piccola principessa Laura, I am very happy to be with you. Thank you for all your support and understanding, and simply for being the way you are.

Last but not least, I would like to express my gratitude to my family that formed a stable basis during all these years. Alina, thank you for the continuous hospitality whenever I had to catch an early flight from Schiphol, and of course for your concern about work and private matters. Don't worry too much about the finalization of your PhD: it will surely happen when the time is ripe. Andree, thank you for all the car rides to the north, your help whenever needed, and the many enjoyable cycle tours: it is great to have you in the family. Jans and Gezina, you are the best parents one could desire. You have always had faith in me, were always open to talk about the things on my mind, offered great hospitality to the persons I brought home, and never complained when another plan to go abroad came up. Our telephone calls and the relaxing weekends in Smilde are of important value to me. I am very grateful for your persistent support.

Anton

Contents

Chapter 1

INTRODUCTION

1. Introduction

1.1 Soil erosion by water

Mankind adapts its environment to meet its demands (UNEP, 2005). Its interventions can be radical, and may cause disequilibrium of the natural system. The search for a new dynamic equilibrium implies the action of natural processes on the changed circumstances. These processes frequently involve negative impacts on the valuable natural resources that humans require for their living. Exponential growth of the human population during the last centuries in combination with increasingly demanding consumption patterns is putting a strong pressure on these resources (Cohen, 1995; Ehrlich et al., 1993; Meyer and Turner, 1992). Global awareness about the consequences of our conduct on the environment is however rising. Worldwide, efforts are being taken to mitigate the negative impacts of our interventions and to obtain a situation in which the human utilisation of natural resources is in equilibrium with their long-term ecological functions (e.g. Hannam and Boer, 2001; United Nations, 2002). The ideal situation for the earth and mankind would be a sustainable system in which ecological and production functions are in balance and which can be maintained for an indefinite number of years to come. However, at the global level this ideal seems distant as alarming reports indicating strong imbalances reach us regularly, e.g. on melting of ice sheets (Bindschadler, 2006), large-scale river flooding (Kundzewicz et al., 2005), and decline of biodiversity (Dirzo and Raven, 2003).

Soil erosion is one of the menaces to the sustainability ideal. It is a natural process that detaches and transports soil material through the action of an erosive agent. Possible agents are water, wind, gravity, and anthropogenic perturbations (Lal, 2001). At geological time-scales there is a balance between erosion and soil formation (Tricart and KiewietdeJonge, 1992), but at many locations worldwide a disequilibrium currently exists between the two processes. This disequilibrium is called accelerated soil erosion and is principally caused by anthropogenic land use changes like deforestation and agricultural practices. At the global scale soil erosion by water is the most important land degradation problem (Eswaran et al., 2001). It generates strong environmental impacts and high economic costs by its on-site effects on agricultural production and off-site effects on infrastructure and water quality (Ananda and Herath, 2003; Lal, 1998; Pimentel et al., 1995). To mitigate these effects and reduce soil erosion, soil and water conservation strategies are required at different spatial scales and at different organizational levels (Morgan, 2005). Spatial information on the importance of erosion at different scales is necessary for defining effective strategies and prioritizing conservation efforts.

Soil erosion processes by water comprise: *splash erosion*, which occurs when soil particles are detached and transported as a result of the impact of falling raindrops; *sheet or interrill erosion*, which removes soil in thin layers and is caused by the combined effects of

splash erosion and surface runoff; *rill erosion*, which is the disappearance of soil particles caused by concentrations of flowing water; and *gully erosion*, that occurs when the flow concentration becomes large and the incision deeper and wider than with rills (Morgan, 2005). Gully dynamics are however not limited to runoff processes only, but can be greatly influenced by sub-surface flow, tunnelling and side-wall failures (Bocco, 1991). Biophysical factors that regulate erosion processes include climate, soil, terrain and ground cover (Lal, 2001). The importance of each individual factor is not always the same, but depends on regional characteristics, the specific erosion process under consideration, and the spatial and temporal scale studied.

1.2   Spatial erosion assessment

Spatial assessment of soil erosion can basically be done in three different ways. The first is to measure soil erosion rates at different locations using some measuring device or erosion plots (Hudson, 1993; Loughran, 1989). However, accurate measurements are generally expensive and time-consuming, standard equipment is hardly available (Stroosnijder, 2005), and measurement results may be highly variable under similar circumstances (Nearing et al., 1999). Field measurements are mostly used for assessing the role of a specific erosion factor, model development, or validation purposes, but not for spatial evaluation of erosion.

The second approach is the execution of erosion field surveys in which features are identified that formed due to erosion processes, such as pedestals or rills (Herweg, 1996). Although quantitative information may be obtained through repeated measurement of feature dimensions, surveys are often performed in a qualitative sense thus classifying the amount of erosion based on the features encountered. Survey timing is important, because features may not be visible throughout the year due to e.g. management practices like ploughing. Surveys may allow spatial erosion mapping for small catchments of about 2-km^2 (Vigiak et al., 2005), but for larger regions this becomes difficult. However, systematic visual identification of certain features from aerial photographs would be another form of erosion survey that could be performed for larger areas up to 50-km^2 (Bergsma, 1974).

The third and most common method for spatial erosion assessment is through integrating spatial data on erosion factors. Widely-used is the Universal Soil Loss Equation (USLE: Wischmeier and Smith, 1978), although many other erosion models exist that allow spatial mapping of erosion (Merritt et al., 2003). However, erosion models are all developed for a certain region and scale, and transferring a model to other scales or regions is not straightforward and may give poor or erroneous results (Brazier et al., 2000; Jetten et al., 2003; Kirkby et al., 1996; Schoorl et al., 2000). Furthermore, many erosion models require a large amount of detailed data on a wide variety of rainfall, soil, vegetation, and slope parameters. In data-poor environments like e.g. developing countries, these data are often not readily available, or only at very coarse scales. Qualitative data integration methods that allow some flexibility in the selection and combination of erosion factors can provide a good

alternative to erosion models. Selection of erosion factors can be region-specific, depending on the processes that occur and the key parameters that explain the variability of these processes within the region. Local or expert knowledge can provide important input to such qualitative approaches (De la Rosa et al., 1999; Sonneveld, 2003). Outcomes of these methods are generally a qualitative measure of erosion risk, which is the relative risk that erosion will occur at a certain location as compared to other locations in the region mapped.

Spatial data are needed for the application of both erosion models and qualitative methods. The scale or resolution of these data should correspond with the desired output scale of the mapping exercise (Woodcock and Strahler, 1987). For example, at the national scale it would make no sense to work with field-scale data, whereas for erosion assessment in small catchments (e.g. 10 km^2) national soil inventories are of little value. Two types of spatial data are required for erosion mapping: (1) input data on erosion factors that allow the application of the mapping method, (2) validation data to assess how accurate and reliable the results of the method are. Relevant spatial data may be derived from a variety of sources like e.g. existing soil, land use, and topographic maps, weather stations, field measurements and surveys, aerial photographs, and satellite imagery.

1.3   Satellite remote sensing

Observations of environmental variables are required for assessing the status of the earth's resources and for monitoring their dynamics. Space technology, in particular satellite remote sensing, currently offers an important contribution to the synoptic and timely evaluation of natural resources over large areas. The term *remote sensing* means that information about objects or phenomena is acquired from a distance, without having physical contact with the object or phenomenon under study (Colwell, 1983). In practice, the term is mostly used for the acquisition, processing, and interpretation of data which are recorded by a sensing device mounted on an aircraft or satellite. Although military purposes have been the driving factor for its development, satellite remote sensing is currently an important source of information for environmental studies on the atmosphere, oceans, and land surfaces. At present, hundreds of artificial satellites are orbiting our planet that record and transmit valuable information on our environment using a wide range of sensors.

Information needs to be derived however from the recorded image data. Sensors onboard satellites record electromagnetic radiation, which is subsequently transmitted to the ground where it is stored in electronic form. Radiation can be measured at different wavelengths (e.g. visible light, infrared, thermal), depending on the specific sensor characteristics. The sun is the most common source of radiation, but in some cases like for imaging radar the satellite system itself provides its own radiation source by transmitting energy pulses to the earth surface. Satellite images thus merely show spatial differences of how electromagnetic radiation has interacted with the atmosphere and the earth surface at a specific moment in time. From the recorded imagery, information on environmental variables

may be inferred using physical models or empirical approaches. The variable of interest in a particular study dictates the choice of the image type (sensor and satellite) to be used. Besides the recorded wavelength(s), also other sensor characteristics like spatial and temporal resolution may be important. Temporal resolution refers to how often an image with the same characteristics can be recorded, and is generally inversely related to spatial resolution. Spatial resolution depends on the sensor and the height of the satellite orbit. Methods for extracting environmental variables from satellite data are thus based on the specific image type chosen. Independent *in situ* observations of the variable of interest are needed for the development and validation of these methods (Jensen, 2004). Variables obtained from satellite data may subsequently be combined with additional spatial data to extract new or more accurate information (e.g. He et al., 1998; Lubczynski and Gurwin, 2005; Saha et al., 2002).

1.4   Mapping erosion from space

Through the variety of spaceborne sensors currently orbiting the earth, satellite remote sensing can offer an important input to erosion assessments at various spatial scales. Particularly for data-poor regions, satellite data may assist in rapid mapping of erosion over large areas, while otherwise this could only be done through expensive and time-consuming surveying methods. Many types of satellite images and image-derived products obtained from earth-observing space missions are presently available to the general public. Although some image types are still costly, a lot of data is inexpensive or free of charge, which facilitates its use for a wide community. Satellite imagery is therefore increasingly being used for regional erosion studies. This can be done either through the detection of erosion features and eroded areas, or through assessing erosion factors like vegetation cover or slope.

Eroded areas larger than 1 ha may in some cases be distinguished from its surroundings because vegetation cover is reduced (Pickup and Nelson, 1984), soil properties have changed (Hill et al., 1995a), or random changes of the earth surface have occurred (Lee and Liu, 2001). However, successful application of satellite remote sensing to detect eroded areas is generally limited to (semi-) arid natural and rangeland environments or extensive areas suffering gully erosion (badlands). In more humid regions vegetation cover often obscures the visibility of the soil, whereas agricultural activities may furthermore greatly influence vegetation cover, soil properties, and surface roughness. For humid and agricultural areas these variables can thus not be directly related to soil erosion occurrence. Besides eroded areas also individual erosion features like gullies and large rills may be identified from satellite imagery. This is partly due to distinct properties such as subsoil exposure and reduced vegetation cover, but perhaps more importantly because of the clear spatial structure of rills and gullies. Spatial resolution of the imagery should however correspond with the size of the features. Visual interpretation has been a common method for detecting individual gullies from aerial photographs (Martínez-Casasnovas, 2003; Nachtergaele and Poesen, 1999) and satellite images (Bocco and Valenzuela, 1993). Automatic retrieval of gullies from

satellite images would provide fast insight in the importance of gully erosion and the consequent loss of productive land for large regions, although some authors have questioned the feasibility of this exercise due to the spectral heterogeneity of gullies themselves and of their surroundings (King et al., 2005; Zinck et al., 2001).

Information on a variety of erosion factors can be obtained from satellite imagery, including climate, soil, terrain, and vegetation characteristics. Important climate parameters for erosion studies are rainfall amount and intensity, which may at coarse scales be assessed e.g. using data of the spaceborne Tropical Rainfall and Measurement Mission (TRMM). Terrain attributes such as slope are generally assessed using digital elevation models (DEMs), which can be obtained from stereo images (Toutin, 2001) or advanced techniques like radar interferometry (Toutin and Gray, 2000). The spatial distribution of various soil properties may be evaluated with satellite data, although often this is restricted to arid or semi-arid regions due to the disturbing influence of vegetation (Huete, 2004). To assess vegetation cover, satellite data can be applied for land use classification or the extraction of continuous measures of vegetation abundance and structure (Hall et al., 1995). Erosion factors are not static, but change with time. The most dynamic factors are rainfall and vegetation, although soil properties may also be altered on short time-scales due to e.g. tillage or crusting. The temporal variability of erosion factors needs to be accounted for in satellite-based erosion assessments one way or another. One option for this is to assess the factors at different moments of the year using multi-temporal satellite imagery (e.g. De Jong et al., 1999). A second option is to ascertain that a mono-temporal satellite image represents conditions of the factor under study at the moment of highest erosion risk. Image timing can thus be relevant for obtaining accurate spatial erosion patterns, although rationales for image selection are often not clearly defined in erosion studies.

Despite the vast amount of existing studies on the remote sensing of variables that are of importance for erosion studies, little work has been done on developing methodologies for mapping soil erosion based specifically on these remotely-sensed variables. Instead, often an erosion model such as the USLE, developed for small erosion plots (1.8 by 22.1 m) in the eastern United States, is simply applied to larger scales and different regions, while satellite data merely provides vegetation information as an input (e.g. CORINE, 1992; Kim et al., 2005; Lu et al., 2004). Some exceptions are the modelling work of De Jong et al. (1999) and a few erosion studies using qualitative data integration methods (e.g. Haboudane et al., 2002; Hill et al., 1995b; Liu et al., 2004; Metternicht, 1996). However, these studies were all performed for semi-arid regions and rely on specific observables in these environments. Erosion mapping methodologies based on remotely-sensed variables could however also be valuable for more humid environments. Local experts may assist in defining suitable methodologies for region-specific erosion mapping through defining the locally-important variables which can explain the spatial differences of erosion and can be obtained from satellite data.

Any erosion mapping methodology will result in a nice-looking map, but without validation of the results it is unknown whether the obtained results are accurate (Favis-

Mortlock et al., 1996). To assess the performance of methodologies for a specific region, spatial results should therefore be compared with independent data such as derived from field measurements or surveys. Validation data may also be obtained through visual identification of erosion features from high-resolution (about 1 m) airborne or spaceborne data. Besides aerial photographs, good options for this are currently offered by high-resolution satellites like QuickBird and IKONOS. However, due to the time-consuming nature of obtaining validation data, and the lack of standard validation approaches especially for larger regions, many erosion studies merely performed map construction without questioning the outcomes (e.g. Anys et al., 1994; Fan et al., 2004; Jürgens and Fander, 1993; Reusing et al., 2000; Sekhar and Rao, 2002). To advance the ability of accurately mapping erosion risk, the validation effort should however be made and clear options for collecting proper spatial validation data at regional scales need to be defined.

1.5   Aim

The aim of the research described in this thesis is to develop new methodologies for qualitative regional erosion mapping using satellite remote sensing. The methodologies should be easily applicable in tropical environments and not rely on erosion models which were developed for different scales and regions. Especially options are envisaged for regions (50-10.000 km^2) which besides satellite imagery have poor data availability at a sufficiently detailed scale. The specific objectives of this study are:

- to provide a detailed overview of how satellite data have been used previously for the assessment of soil erosion;
- to determine whether automatic identification of large erosion features from satellite imagery is possible under certain circumstances;
- to develop methodologies that integrate satellite and additional data for accurate qualitative erosion risk mapping, and explore the potential role of expert knowledge;
- to assess the importance of temporal dynamics of vegetation cover and rainfall for the selection of satellite images that are used to describe the spatial variability of erosion risk.

1.6   Study outline

This thesis presents a number of studies that apply satellite remote sensing data for assessing soil erosion in three different tropical regions, namely the Brazilian Cerrados, the Colombian Eastern Plains, and the West Usambara Mountains of Tanzania. The thesis starts with a literature review of existing methodologies for soil erosion assessment using satellite data (Chapter 2). It covers the detection of erosion features and eroded areas, the evaluation of

off-site impacts such as water quality of inland lakes, and the assessment of erosion factors. Furthermore data integration techniques and validation methods are discussed.

Chapter 3 addresses the detection of erosion features with satellite imagery. Bi-temporal ASTER (Advanced Spaceborne Thermal Emission and Reflection Radiometer) imagery was applied to evaluate whether automatic identification of large permanent erosion gullies is possible for an area in the Brazilian Cerrados.

Chapters 4 to 6 explore new options for qualitative erosion risk mapping, in which satellite data is used to obtain information on one or more erosion factors. In Chapter 4 a decision-tree approach to erosion risk mapping is presented for a municipality (about 7000 km^2) in the Colombian Eastern Plains. It uses expert knowledge for defining and combining the locally-important variables for different erosion factors. Land use and vegetation cover were evaluated with a Landsat image, while additional data sources used include a soil and geology map and a DEM derived from a topographic map.

Chapter 5 presents a different erosion risk mapping approach for a 70-km^2 watershed in the West Usambara Mountains of Tanzania. For the watershed, spatial information at a proper scale was scarce. Therefore, the question was raised whether an accurate erosion risk map may be created using only satellite information. The chapter presents two data integration methods that merely use information on vegetation cover and slope derived from a well-timed Landsat image and a DEM of the Shuttle Radar Topography Mission (SRTM).

The issue of image timing is further explored in Chapter 6. For the Brazilian study area multi-temporal coarse-resolution satellite data were applied to determine when high rainfall intensities coincide with a limited vegetation cover. The implication of this timing was assessed with a time-series of six medium-resolution ASTER images. Six different mono-temporal erosion risk maps were derived from the images by relating erosion risk to vegetation cover patterns. The optimal timing of the ASTER imagery was evaluated by comparing the maps with the presence of erosion features that were visually delineated from a fine-resolution QuickBird image.

Finally, in Chapter 7 the major findings of this thesis are discussed and general directions for future work are given.

References

Ananda J, and Herath G. 2003. Soil erosion in developing countries: a socio-economic appraisal. *Journal of Environmental Management* 68 (4): 343-353.

Anys H, Bonn F, and Merzouk A. 1994. Remote sensing and GIS based mapping and modeling of water erosion and sediment yield in a semi-arid watershed of Morocco. *Geocarto International* 9 (1): 31-40.

Bergsma E. 1974. Soil erosion sequences on aerial photographs. *ITC Journal* 3: 342-376.

Bindschadler R. 2006. Hitting the ice sheets where it hurts. *Science* 311 (5768): 1720-1721.

Bocco G. 1991. Gully erosion: processes and models. *Progress in Physical Geography* 15 (4): 392-406.

Bocco G, and Valenzuela CR. 1993. Integrating satellite remote sensing and Geographic Information Systems technologies in gully erosion research. *Remote Sensing Reviews* 7: 233-240.

Brazier RE, Beven KJ, Freer JF, and Rowan JS. 2000. Equifinality and uncertainty in physically based soil erosion models: application of the GLUE methodology to WEPP - the Water Erosion Prediction Project - for sites in the UK and USA. *Earth Surface Processes and Landforms* 25 (8): 825-845.

Cohen JE. 1995. Population growth and earth's human carrying capacity. *Science* 269 (5222): 341-346.

Colwell RN (Editor). 1983. Manual of Remote Sensing, 2nd Edition. American Society for Photogrammetry, Falls Church, Virginia: 2240 pp.

CORINE. 1992. Soil Erosion Risk and Important Land Resources in the Southern Regions of the European Community. EUR 13233. Office for Offical Publications of the European Communities, Luxembourg: 97 pp.

De Jong SM, Paracchini ML, Bertolo F, Folving S, Megier J, and De Roo APJ. 1999. Regional assessment of soil erosion using the distributed model SEMMED and remotely sensed data. *Catena* 37 (3-4): 291-308.

De la Rosa D, Mayol F, Moreno JA, Bonsón T, and Lozano S. 1999. An expert system/neural network model (ImpelERO) for evaluating agricultural soil erosion in Andalucia region, southern Spain. *Agriculture, Ecosystems and Environment* 73 (3): 211-226.

Dirzo R, and Raven PH. 2003. Global state of biodiversity and loss. *Annual Review of Environment and Resources* 28: 137-167.

Ehrlich PR, Ehrlich AH, and Daily GC. 1993. Food security, population, and environment. *Population & Development Review* 19 (1): 1-32.

Eswaran H, Lal R, and Reich PF. 2001. Land degradation: an overview. *In*: Bridges EM, Hannam ID, Oldeman LR, Penning de Vries FWT, Scherr SJ, and Sombatpanit S (Editors), Response to land degradation. Science Publishers Inc., Enfield, NH, USA: pp. 20-35.

Fan JR, Zhang JH, Zhong XH, Liu SZ, and Tao HP. 2004. Monitoring of soil erosion and assessment for contribution of sediments to rivers in a typical watershed of the Upper Yangtze River Basin. *Land Degradation & Development* 15 (4): 411-421.

Favis-Mortlock DT, Quinton JN, and Dickinson WT. 1996. The GCTE validation of soil erosion models for global change studies. *Journal of Soil and Water Conservation* 51 (5): 397-403.

Haboudane D, Bonn F, Royer A, Sommer S, and Mehl W. 2002. Land degradation and erosion risk mapping by fusion of spectrally-based information and digital geomorphometric attributes. *International Journal of Remote Sensing* 23 (18): 3795-3820.

Hall FG, Townshend JR, and Engman ET. 1995. Status of remote-sensing algorithms for estimation of land-surface state parameters. *Remote Sensing of Environment* 51 (1): 138-156.

Hannam ID, and Boer BW. 2001. Land degradation and international environmental law. *In*: Bridges EM, Hannam ID, Oldeman LR, Penning de Vries FWT, Scherr SJ, and Sombatpanit S (Editors), Response to land degradation. Science Publishers Inc., Enfield, NH, USA: pp. 429-438.

He HS, Mladenoff DJ, Radeloff VC, and Crow TR. 1998. Integration of GIS data and classified satellite imagery for regional forest assessment. *Ecological Applications* 8 (4): 1072-1083.

Herweg K. 1996. Field Manual for Assessment of Current Erosion Damage. SCRP Ethiopia, and Centre for Development and Environment, University of Berne, Switzerland: 69 pp.

Hill J, Mégier J, and Mehl W. 1995a. Land degradation, soil erosion and desertification monitoring in Mediterranean ecosystems. *Remote Sensing Reviews* 12: 107-130.

Hill J, Sommer S, Mehl W, and Mégier J. 1995b. Towards a satellite-observatory for mapping and monitoring the degradation of Mediterranean ecosystems. *In*: Askne J (Editor), Sensors and environmental application of remote sensing. Balkema, Rotterdam: pp. 53-61.

Hudson NW. 1993. Field measurement of soil erosion and runoff. FAO Soils Bulletin, 68. Food and Agriculture Organization, Rome, Italy.

Huete A. 2004. Remote sensing of soils and soil processes. *In*: Ustin SL (Editor), Remote Sensing for Natural Resources Management and Environmental Monitoring: Manual of Remote Sensing. John Wiley & Sons, Hoboken, NJ, USA: pp. 3-52.

Jensen JR. 2004. Introductory digital image processing: a remote sensing perspective (3rd edition). Pearson Prentice Hall, Upper Saddle River, NJ, USA: 526 pp.

Jetten V, Govers G, and Hessel R. 2003. Erosion models: quality of spatial predictions. *Hydrological Processes* 17 (5): 887-900.

Jürgens C, and Fander M. 1993. Soil erosion assessment and simulation by means of SGEOS and ancillary digital data. *International Journal of Remote Sensing* 14 (15): 2847-2855.

Kim JB, Saunders P, and Finn JT. 2005. Rapid assessment of soil erosion in the Rio Lempa Basin, Central America, using the universal soil loss equation and geographic information systems. *Environmental Management* 36 (6): 872-885.

King C, Baghdadi N, Lecomte V, and Cerdan O. 2005. The application of remote-sensing data to monitoring and modelling of soil erosion. *Catena* 62 (2-3): 79-93.

Kirkby MJ, Imeson AC, Bergkamp G, and Cammeraat LH. 1996. Scaling up processes and models from the field plot to the watershed and regional areas. *Journal of Soil and Water Conservation* 51 (5): 391-396.

Kundzewicz ZW, Ulbrich U, Bru?cher T, Graczyk D, Kru?ger A, Leckebusch GC, Menzel L, Pin?skwar I, Radziejewski M, and Szwed M. 2005. Summer floods in Central Europe - Climate change track? *Natural Hazards* 36 (1-2): 165-189.

Lal R. 1998. Soil erosion impact on agronomic productivity and environment quality. *Critical Reviews in Plant Sciences* 17 (4): 319-464.

Lal R. 2001. Soil degradation by erosion. *Land Degradation & Development* 12 (6): 519-39.

Lee H, and Liu JG. 2001. Analysis of topographic decorrelation in SAR interferometry using ratio coherence imagery. *IEEE Transactions on Geoscience and Remote Sensing* 39 (2): 223-232.

Liu JG, Mason P, Hilton F, and Lee H. 2004. Detection of rapid erosion in SE Spain: A GIS approach based on ERS SAR coherence imagery. *Photogrammetric Engineering and Remote Sensing* 70 (10): 1179-1185.

Loughran RJ. 1989. The measurement of soil erosion. *Progress in Physical Geography* 13 (2): 216-233.

Lu D, Li G, Valladares GS, and Batistella M. 2004. Mapping soil erosion risk in Rondonia, Brazilian Amazonia: Using RUSLE, remote sensing and GIS. *Land Degradation & Development* 15 (5): 499-512.

Lubczynski MW, and Gurwin J. 2005. Integration of various data sources for transient groundwater modeling with spatio-temporally variable fluxes - Sardon study case, Spain. *Journal of Hydrology* 306 (1-4): 71-96.

Martínez-Casasnovas JA. 2003. A spatial information technology approach for the mapping and quantification of gully erosion. *Catena* 50 (2-4): 293-308.

Merritt WS, Letcher RA, and Jakeman AJ. 2003. A review of erosion and sediment transport models. *Environmental Modelling & Software* 18 (8-9): 761-799.

Metternicht GI. 1996. Detecting and monitoring land degradation features and processes in the Cochabamba valleys, Bolivia - A synergistic approach. Ph.D. Thesis, University of Ghent, Ghent, Belgium: 389 pp.

Meyer WB, and Turner BL. 1992. Human population growth and global land-use/cover change. *Annual Review of Ecology and Systematics* 23 (1): 39-61.

Morgan RPC. 2005. Soil erosion and conservation. Blackwell Publishing, Malden, MA: 304 pp.

Nachtergaele J, and Poesen J. 1999. Assessment of soil losses by ephemeral gully erosion using high-altitude (stereo) aerial photographs. *Earth Surface Processes and Landforms* 24 (8): 693-706.

Nearing MA, Govers G, and Norton LD. 1999. Variability in soil erosion data from replicated plots. *Soil Science Society of America Journal* 63 (6): 1829-1835.

Pickup G, and Nelson J. 1984. Use of Landsat radiance parameters to distinguish soil erosion, stability, and deposition in arid Central Australia. *Remote Sensing of Environment* 16 (3): 195-209.

Pimentel D, Harvey C, Resosudarmo P, Sinclair K, Kurz D, McNair M, Crist S, Shpritz L, Fitton L, Saffouri R, and Blair R. 1995. Environmental and economic costs of soil erosion and conservation benefits. *Science* 267: 1117-1123.

Reusing M, Schneider T, and Ammer U. 2000. Modelling soil loss rates in the Ethiopian Highlands by integration of high resolution MOMS-02/D2-stereo-data in a GIS. *International Journal of Remote Sensing* 21 (9): 1885-1896.

Saha AK, Gupta RP, and Arora MK. 2002. GIS-based Landslide Hazard Zonation in the Bhagirathi (Ganga) Valley, Himalayas. *International Journal of Remote Sensing* 23 (2): 357-369.

Schoorl JM, Sonneveld MPW, and Veldkamp A. 2000. Three-dimensional landscape process modelling: the effect of DEM resolution. *Earth Surface Processes and Landforms* 25 (9): 1025-1034.

Sekhar KR, and Rao BV. 2002. Evaluation of sediment yield by using remote sensing and GIS: a case study from the Phuland Vagu watershed, Nizamabad District (AP), India. *International Journal of Remote Sensing* 23 (20): 4499-4509.

Sonneveld BGJS. 2003. Formalizing expert judgements in land degradation assessment: a case study from Kenya. *Land Degradation & Development* 14 (4): 347-261.

Stroosnijder L. 2005. Measurement of erosion: is it possible? *Catena* 64 (2-3): 162-173.

Toutin T. 2001. Review article: Elevation modelling from satellite visible and infrared (VIR) data. *International Journal of Remote Sensing* 22 (6): 1097-1125.

Toutin T, and Gray L. 2000. State-of-the-art of elevation extraction from satellite SAR data. *ISPRS Journal of Photogrammetry and Remote Sensing* 55 (1): 13-33.

Tricart J, and KiewietdeJonge C. 1992. Ecogeography and Rural Management - a Contribution to the International Geosphere-Biosphere Programme. Longman Group, Harlow, UK: 267 pp.

UNEP. 2005. One Planet Many People: Atlas of Our Changing Environment. United Nations Environment Programme: 332 pp.

United Nations. 2002. World Summit on Sustainable Development: Plan of Implementation. United Nations, New York, USA.

Vigiak O, Okoba BO, Sterk G, and Groenenberg S. 2005. Modelling catchment-scale erosion patterns in the East African highlands. *Earth Surface Processes and Landforms* 30 (2): 183-196.

Wischmeier WH, and Smith DD. 1978. Predicting rainfall-erosion losses: A guide to conservation planning. Agricultural Handbook No. 537. US Department of Agriculture.

Woodcock CE, and Strahler AH. 1987. The factor of scale in remote sensing. *Remote Sensing of Environment* 21 (3): 311-332.

Zinck JA, López J, Metternicht GI, Shrestha DP, and Vázquez-Selem L. 2001. Mapping and modelling mass movements and gullies in mountainous areas using remote sensing and GIS techniques. *International Journal of Applied Earth Observation and Geoinformation* 3 (1): 43-53.

Chapter 2

SATELLITE REMOTE SENSING FOR
WATER EROSION ASSESSMENT:
A REVIEW

Vrieling A

2. Satellite remote sensing for water erosion assessment: a review

Abstract

Water erosion creates negative impacts on agricultural production, infrastructure, and water quality across the world. Regional-scale water erosion assessment is important, but limited by data availability and quality. Satellite remote sensing can contribute through providing spatial data to such assessments. During the past 30 years many studies have been published that did this to a greater or lesser extent. The objective of this paper is to review methodologies applied for water erosion assessment using satellite remote sensing. First, studies on erosion detection are treated. This comprises the detection of erosion features and eroded areas, as well as the assessment of off-site impacts such as sediment deposition and water quality of inland lakes. Second, the assessment of erosion controlling factors is evaluated. Four types of factors are discussed: topography, soil properties, vegetation cover, and management practices. Then, erosion mapping techniques are described that integrate products derived from satellite remote sensing with additional data sources. These techniques include erosion models and qualitative methods. Finally, validation methods used to assess the accuracy of maps produced with satellite data are discussed. It is concluded that a general lack of validation data is a main concern. Validation is of utmost importance to achieve regional operational monitoring systems, and close collaboration between the remote sensing community and field-based erosion scientists is therefore required.

2.1   Introduction

Soil erosion by water is the most important land degradation problem worldwide (Eswaran et al., 2001). Although some authors question its impact on global food security (Crosson, 1997; Lomborg, 2001) soil erosion creates strong environmental impacts and high economic costs by its effect on agricultural production, infrastructure and water quality (Lal, 1998; Pimentel et al., 1995). Furthermore, erosion results in emission of soil organic carbon to the atmosphere in the form of CO_2 and CH_4, causing impact on global warming (Lal, 2004). Global warming in turn is expected to increase erosion rates (Nearing et al., 2004). A proper assessment of erosion problems is greatly dependent on their spatial, economic, environmental, and cultural context (Warren, 2002).

Water erosion is controlled by climatic characteristics, topography, soil properties, vegetation, and land management. Detachment of soil material is caused by raindrop impact and drag force of running water. Detached particles are transported by overland flow (sheet- or interrill erosion) and concentrated flow (rill erosion) and deposited when flow velocity decreases (Lal, 2001). Gullies can develop as enlarged rills, but their genesis is generally more complex, involving sub-surface flows and side-wall processes (Bocco, 1991).

To control water erosion, biophysical measures need to be implemented at the field, hillslope or watershed scale. However, allocation of scarce conservation resources and development of policies and regulations require erosion assessment at the regional scale. An important limitation for this task is data availability and quality (Van Rompaey and Govers, 2002). Remote sensing provides homogeneous data over large regions with a regular revisit capability, and can therefore greatly contribute to regional erosion assessment (King and Delpont, 1993; Siakeu and Oguchi, 2000).

Traditionally, remote sensing has been used for soil erosion research through aerial photo interpretation both for detecting erosion features (e.g. Bergsma, 1974; Jones and Keech, 1966) and obtaining model input data (e.g. Morgan and Napela, 1982; Stephens et al., 1985). Starting in 1972 with the launch of Landsat-1, satellite imagery has become increasingly available to the scientific community.

During the past 30 years many studies have been published that fully or partially applied satellite imagery for soil erosion assessment in many different ways. The objective of this paper is to provide an overview of methodologies applied for water erosion assessment using satellite remote sensing. It focuses on erosion processes related to surface run-off and gullying. Although important sensor development has taken place during the past years using airborne systems, which are of interest to erosion research (e.g. laser altimetry, hyperspectral remote sensing), this paper focuses only on satellite-based applications. Mainly peer-reviewed journal articles are treated, with a few exceptions. The review addresses (1) erosion detection, (2) the assessment of erosion controlling factors, and (3) data integration for erosion mapping.

2.2   Satellites and sensors applied in erosion research

A large number of earth observation satellites has orbited, and is orbiting our planet to provide frequent imagery of its surface. From these satellites, many can potentially provide useful information for assessing erosion, although less have actually been used for this purpose. This section provides a brief overview of the spaceborne sensors applied in erosion studies. More recent satellites (e.g. SPOT-5, CBERS) and future satellites (e.g. ALOS, SMOS) that are of potential interest, are not discussed here. The sensors can be divided in those measuring reflection of sunlight in the visible and infrared part of the electromagnetic spectrum and thermal infrared radiance (optical systems), and those actively transmitting microwave pulses and recording the received signal (imaging radars).

Optical satellite systems have most frequently been applied in erosion research. The parts of the electromagnetic spectrum covered by these sensors include the visible and near-infrared (VNIR) ranging from 0.4 to 1.3 μm, the shortwave infrared (SWIR) between 1.3 and 3.0 μm, and the thermal infrared (TIR) from 3.0 to 15.0 μm. Table 2.1 summarises sensor characteristics of the systems used. Landsat is still among the widest used satellites, partly because it has the longest time series of data of currently available satellites. The first

Table 2.1   *Overview of optical satellite sensors applied in erosion research*

Satellite	Sensor	Operation time	Spatial resolution	# Spectral bands	Spectral domain
Landsat-1,2,3	MSS	1972-1983	80 m	4	VNIR
Landsat-4,5	TM	1982-1999	30 m	6	VNIR, SWIR
			120 m	1	TIR
Landsat-7	ETM	1999-present	15 m	1	VNIR
			30 m	6	VNIR, SWIR
			60 m	1	TIR
SPOT-1,2,3	HRV	1986-present	10 m	1	VNIR
			20 m	3	VNIR
SPOT-4	HRVIR	1998-present	10 m	1	VIS
			20 m	4	VNIR, SWIR
IRS-1A,1B	LISS-1	1988-1999	72.5 m	4	VNIR
	LISS-2		36.25 m	4	VNIR
IRS-1C,1D	PAN	1995-present	5.8 m	1	VNIR
	LISS-3		23.5 m	3	VNIR
			70 m	1	SWIR
Terra	ASTER	1999-present	15 m	3	VNIR
			30 m	6	SWIR
			90 m	5	TIR
NOAA/TIROS	AVHRR	1978-present	1.1 km	5	VNIR, SWIR, TIR
IKONOS	Panchromatic	1999-present	1.0 m	1	VNIR
	Multispectral		4.0 m	4	VNIR
QuickBird	Panchromatic	2001-present	0.61 m	1	VNIR
	Multispectral		2.44 m	4	VNIR

satellites of the Landsat family were equipped with the Multispectral Scanner (MSS), having four bands at 80-m resolution. Later Landsat satellites had the Thematic Mapper (TM) and the Enhanced TM (ETM) sensors onboard with improved resolution and more spectral bands. The SPOT (Système Pour l'Observation de la Terre) series of satellites started acquiring data in 1986 with the HRV-sensor (High Resolution Visible). The HRV-sensor has a 10-m panchromatic mode and a three-band 20-m resolution multispectral mode. SPOT-4 flew the HRVIR-sensor (High Resolution Visible Infrared) on which a SWIR band was added. The Indian Remote Sensing Satellites (IRS) 1A and 1B both have two sensors called LISS-1 and LISS-2 (Linear Imaging and Self-Scanning Sensor), which are identical except for a two times higher spatial resolution on LISS-2. IRS 1C and 1D also have an identical payload being a 5.8-m resolution panchromatic camera (PAN) and a 23.5-m resolution multispectral sensor called LISS-3. ASTER (Advanced Spaceborne Thermal Emission and Reflection Radiometer) is one of the sensors onboard the Terra satellite. It has 14 spectral bands of which several are situated in the SWIR and TIR regions. One near-infrared (NIR) band looks both nadir and backward creating stereo-view from a single pass. IKONOS and QuickBird

are both high-resolution satellites, with a spatial resolution in panchromatic mode of 0.61 and 1.00-m respectively, and 2.44 and 4.00-m in multispectral mode. AVHRR (Advanced Very High Resolution Radiometer) has five bands in 1.1-km resolution and has been flown on many platforms, including TIROS-N (Television Infrared Observation System) and several NOAA-satellites (National Oceanic and Atmospheric Administration).

The start of spaceborne imaging radar instruments was in 1978 with the SAR (synthetic aperture radar) onboard SEASAT, operating in L-band (23.5-cm wavelength) during 105 days only. For erosion studies, only five SAR sensors have been applied, which were flown on ERS-1 and 2, JERS-1, RADARSAT-1, and ENVISAT respectively. In 1991 ERS-1 was launched with onboard the Active Microwave Instrument (AMI) operating in C-band (5.7-cm wavelength). The SAR image mode of AMI acquired data at 30-m resolution. ERS-2 flies the same instrument and has been operational from 1995 till present. JERS-1 (Japanese Earth Resources Satellite) flew an 18-m resolution L-band SAR (23.5-cm wavelength), recording data from 1992 to 1998. RADARSAT-1 has acquired C-band SAR data since 1995 and has the possibility of using a variety of incidence angles (between 20 and 49°) and different resolutions (between 10 and 100-m). The Advanced SAR (ASAR) onboard ENVISAT, launched in 2002, also has the possibility of using several incidence angles (between 15 and 45°). Besides, its C-band SAR can transmit and receive radar pulses both in horizontal and vertical polarization, which refers to the plane in which the electromagnetic wave is propagating. Spatial resolutions of ASAR are approximately 30-m, 150-m, or 1 km, depending on the mode used.

Furthermore, a number of short-duration Space Shuttle flights have flown earth-observation instruments. Only two of them have been used for erosion studies, being MOMS-2, and SIR-C/X-SAR. MOMS-2 (Modular Optoelectronic Multispectral Scanner) is an optical sensor that was flown in 1993. It has four multispectral bands in the VNIR range at 13.5-m resolution, a panchromatic band having 4.5-m resolution, and two panchromatic stereo bands (backward and forward looking) at 13.5-m resolution. SIR-C/X-SAR is a joint instrument consisting of SIR-C (Shuttle Imaging Radar-C) and X-SAR, which was flown two times in 1994. SIR-C provided multi-polarization L- and C-band SAR imagery and X-SAR simultaneously X-band (3.1-cm wavelength) mono-polarized SAR imagery with approximately 30-m resolution.

2.3   Erosion detection

Satellite data can be applied to directly detect erosion or to detect erosion consequences. Direct detection has been achieved through identification of individual large erosion features, discrimination of eroded areas, and assessment of erosion intensity based on empirical relations. Detectable effects include the damage occurred due to major erosion events, and the sedimentation of reservoirs.

2.3.1 Detection of erosion features and eroded areas

Although the mapping of erosion features is an important application of aerial photography, the limited spatial extent of the features often inhibits its detection using satellite imagery. Spatial resolutions such as offered by Landsat and SPOT imagery can at best be applied for identification of individual large and medium sized gullies (Langran, 1983; Millington and Townshend, 1984) and do not allow gully growth analysis with sequential imagery (Bocco and Valenzuela, 1993). For large gullies in Central Brazil, Vrieling and Rodrigues (2004) found that optical ASTER imagery provided better description of gully shape than ENVISAT ASAR data, when compared to a QuickBird image. With the current availability of high-resolution satellites such as IKONOS and QuickBird, options for detecting and monitoring individual small-scale features have increased, although not yet reported in literature.

Instead of detecting individual erosion features, satellite data have been effectively applied for assessing eroded areas. Extensive areas suffering gully erosion (i.e. badlands) have been mapped with visual interpretation techniques on optical image composites of different sensors (e.g. Bocco et al., 1991; Dwivedi et al., 1997b; Kumar et al., 1996). In some cases erosion classes could be separated based on vegetation cover derived as well from visual interpretation (Dwivedi and Ramana, 2003; Sujatha et al., 2000) or vegetation and topographic characteristics derived from additional data sources (Yuliang and Yun, 2002). The delineation of eroded areas on multi-temporal images allowed an assessment of its increase (Fadul et al., 1999; Sujatha et al., 2000). Karale et al. (1988) performed a bi-temporal comparison using aerial photos and Landsat TM imagery. Although a clear increase of eroded lands was found, aerial pictures allowed for a better differentiation of ravine types than satellite imagery.

An alternative for visual interpretation techniques is the automatic extraction of eroded lands from satellite imagery. Serveney and Prat (2003) applied an unsupervised classification algorithm to multispectral SPOT HRV data to distinguish four stages of erosion. Floras and Sgouras (1999) used the maximum likelihood classifier after principal component analysis of Landsat TM imagery to separate one erosion class. Bocco and Valenzuela (1988) applied the same classifier for multispectral Landsat TM and SPOT HRV images to discern several erosion and vegetation classes. They found that the higher-resolution SPOT data performed better in classifying eroded areas, but that the larger number of spectral bands of Landsat TM resulted in a better classification of land cover and land use. Dwivedi et al. (1997a) also found that SPOT HRV was better in classifying eroded lands than Landsat TM and MSS, but they did not use all TM bands for classification. Metternicht and Zinck (1998) performed a maximum likelihood classification on Landsat TM, and on the combination of Landsat TM with JERS-1 SAR data. They achieved highest classification accuracy using the combination of both images.

Besides classification techniques, direct correlation between erosion and spectral reflectance values sometimes permits the detection of erosion and the mapping of its intensity. Price (1993) found high correlation between reflectance values of single Landsat

TM bands, especially band 4 (NIR), and erosion rates for pinyon-juniper woodlands. Erosion rates were determined from the distance between the ground level and a string that was stretched between the base of two adjacent tree trunks, assuming a stable surface level at the trunks. For arid rangelands in Australia, Pickup and Nelson (1984) successfully distinguished eroding, stable, and depositional areas using the data space defined by the 4/6 and 5/6 band ratios of Landsat MSS imagery (corresponding to green/NIR and red/NIR respectively). They stressed that the method is dependent on the relation between erosion status and vegetation cover, and is not suitable for humid climates. Pickup and Chewings (1988) used the same approach in combination with autocorrelation functions to predict changes in patterns of erosion and deposition. Beaulieu and Gaonac'h (2002) describe a more complex method involving Fourier scaling and multifractal analysis of Landsat TM and ERS-1 SAR imagery, which allowed for separating eroding surfaces in Ethiopia.

Changes of surface states can supply direct information on erosion occurrence. A great variety of methods for change detection from satellite imagery exists (Coppin et al., 2004). Studies that relate changes merely to soil properties will be described in Section 2.4.2. Albedo differences between different Landsat MSS passes allowed identification of soil degradation and erosion areas in arid and semi-arid environments of the USA (Frank, 1984a, b; Robinove et al., 1981). Dhakal et al. (2002) showed that the methods of spectral image differencing, principal component analysis, and spectral change vector analysis on bi-temporal Landsat TM imagery all resulted in a proper detection of erosion and flooded areas resulting from an extreme rainfall event, when compared to a field survey of affected and non-affected areas.

Repeat-pass SAR interferometry is a special change detection technique (Massonnet and Feigl, 1998; Rosen et al., 2000). It uses the amplitude and phase information of two SAR scenes having a very similar viewing geometry and a certain time lag. Although digital elevation model (DEM) extraction and slight deformation measurements are among the application areas, derived interferometric coherence imagery has most potential for erosion detection. Coherence between two radar signals is high when the land surface characteristics are very similar on both recording dates. Random surface changes as caused by erosion result in temporal decorrelation. Spatial decorrelation effects due to differences in satellite paths can be partly accounted for using the ratio between two coherence images (Lee and Liu, 2001). However, vegetation and soil moisture changes are also a major cause of decorrelation (e.g. Vrieling and Rodrigues, 2004; Wegmüller et al., 2000), which confines erosion detection with coherence imagery to (semi-)arid environments. In Mediterranean sites, ratio coherence imagery derived from ERS SAR data has been effectively applied to detect erosion (Lee and Liu, 2001; Liu et al., 2001; Liu et al., 2004). For an extreme glacier flooding event in Iceland, Smith et al. (2000) applied interferometric decorrelation to assess unstable areas that were related to erosion and deposition. Wegmüller et al. (2000) separated erosion classes in the Death Valley (USA) using coherence imagery in combination with backscatter values. A relation was found between erosion activity and degree of coherence. In spite of erosion detection possibilities, most authors stressed the need to integrate coherence imagery with

additional spatial data, like optical imagery, because of the multiple causes of temporal decorrelation.

For extreme events, the extraction of multi-temporal DEMs using SAR interferometry offers possibilities to assess erosion and deposition volumes, as demonstrated by Smith et al. (2000). They created DEMs from pre-flood and post-flood interferometric ERS tandem pairs, and by subtraction they were able to assess volumes of erosion and deposition. Because of height accuracy DEM subtraction is limited to areas that experience at least 4-m net erosion or deposition.

2.3.2 Detection of erosion consequences

Erosion is a process that transports soil particles. At downstream locations, both the transport and the deposition of soil material often cause undesired effects. Izenberg et al. (1996) determined the loss of agricultural land due to the extreme flooding of the Missouri River in 1993 with Landsat TM and SPOT HRV imagery. Thickness of deposited sand could be assessed with SIR-C L-band, as field data revealed a correlation between the sediment thickness and vegetation on deposition areas. Khan and Islam (2003) used multi-temporal Landsat data to investigate the dynamics of the Brahmaputra-Jamuna River, which is greatly influenced by the heavy sediment load originating from erosion in the Himalayas. However, most studies that have applied satellite imagery to assess erosion consequences focus on reservoirs and lakes, where sediments create important economic and ecological impacts.

Sedimentation volumes have been estimated for Indian reservoirs using multi-temporal IRS LISS-2 and LISS-3 imagery (Goel and Jain, 1996; Goel et al., 2002; Jain et al., 2002). Images were selected of a year with maximum variation in the reservoir water level. For different image dates, water-spread areas at varying depths were extracted using simple classification algorithms. Reservoir capacity was then calculated with geometric equations and compared with the original capacity to determine sedimentation volumes. A drawback of the approach is that capacities can only be determined in the water fluctuation zone. Comparison with a hydrographic survey showed a slight overestimation of sedimentation rates, which was attributed to confusion between water and land pixels at the reservoir periphery (Jain et al., 2002).

Erosion influences the water quality of downstream lakes and reservoirs. The suspended sediment concentration is the most important water quality parameter for erosion studies (Ritchie and Schiebe, 2000). Reflectance from surface water in the visible and infra-red domain is positively influenced by suspended sediments (Ritchie et al., 1976). Many studies found significant relationships between *in situ* determined suspended sediment concentration of inland water bodies and atmospherically corrected spectral reflectance derived from satellite remote sensing data, such as Landsat (e.g. Carpenter and Carpenter, 1983; Harrington-Jr. et al., 1992; Nellis et al., 1998), IRS LISS-1 (e.g. Choubey, 1998), and multispectral SPOT HRV (e.g. Chacontorres et al., 1992). The optimal wavelength to determine these relations depends on the sediment concentration (Curran and Novo, 1988;

Ritchie and Cooper, 1991), but often used spectral bands are between 500 and 800 nm (within VNIR range). Because sediment characteristics, like texture and colour, influence the water reflection (Han and Rundquist, 1996; Ritchie et al., 1989), developed empirical relationships are not easily transferable to other regions where erosion entrains different sediment types. To increase transferability, Schiebe et al. (1992) developed a theoretically-derived exponential equation for a wide range of sediment concentrations, which also attempted to account for chlorophyll and algal influences. However, until present a universal equation does not exist, and most models of suspended sediment are site-specific (Liu et al., 2003). Detailed reviews of remote sensing for water quality assessment, including suspended sediments, are provided by Dekker et al. (1995), Ritchie and Schiebe (2000) and Liu et al. (2003). A combination of suspended sediment equations and a remote sensing based identification of water bodies across the landscape, was proposed by Ritchie et al. (1987) to assess areas with high soil erosion rates, and concentrate soil conservation efforts. However, practical applications of this approach have not been found in literature.

2.4 Erosion controlling factors

Most remote sensing studies of soil erosion concentrated on the assessment of erosion controlling factors. Especially soil and vegetation attributes have often been determined with satellite data, and to a lesser extent topography and management. Here, only studies that determined these attributes in relation to erosion processes are treated. The climate factor is not discussed, as no satellite applications were found in literature for assessing rainfall characteristics in erosion studies. Rainfall gauges are generally used for this purpose, although Mannaerts and Saavedra (2003) propose the use of large-scale precipitation data derived from the Tropical Rainfall Measuring Mission (TRMM), which is the first satellite system with a precipitation radar.

2.4.1 Topography

To study the effect of topography on erosion, landforms have been discriminated on the basis of visual interpretation of e.g. Landsat image composites (Khan et al., 2001; Mitchell, 1981). However, current spatial erosion models nearly always require DEM input for the assessment of slope characteristics. Traditionally such DEMs have been obtained from contour lines on topographic maps, or less frequently from stereo aerial photography. Nowadays, various options exist to extract good quality DEMs (vertical accuracy < 20-m) from satellite data, such as stereo optical imagery provided by SPOT and ASTER (Toutin and Cheng, 2003) or SAR imagery (Toutin and Gray, 2000). SAR interferometric processing of the Shuttle Radar Topography Mission (SRTM) data, provided readily available DEMs for land areas between 60 degrees northern and 57 degrees southern latitude (Rabus et al., 2003).

Few researchers have applied DEMs derived from satellite data for erosion studies. Khawlie et al. (2002) calculated slope gradient from an ERS SAR interferometric DEM. Also ERS SAR interferograms, an interferometric product obtained before the DEM construction step, have been used directly for slope extraction (Liu et al., 2000). SPOT HRV derived DEMs were used to aid visual interpretation of erosion features (Bishop and Shroder-Jr., 2001) and to extract slope and topographic curvatures (Haboudane et al., 2002). Stereo-data of MOMS-2 allowed DEM extraction and subsequent calculation of slope length and gradient (Reusing et al., 2000). Applications of ASTER and SRTM derived DEMs for erosion studies have not been found yet in peer-reviewed literature, although it is probable that this already happens at the institution level.

2.4.2 Soil

Soils differ in their resistance to erosion, which is a function of a range of soil properties such as texture, structure, soil moisture, roughness, and organic matter content. The susceptibility of soil to erosion agents is generally referred to as soil erodibility (Lal, 2001). Soil classifications are often used to account for spatial differences in erodibility. Important factors on the basis of which soils can be classified include soil properties, climate, vegetation, topography, and lithology. These factors can be potentially mapped with satellite remote sensing (McBratney et al., 2003). Especially optical satellite imagery has been used for soil mapping, mainly through visual delineation of soil patterns (Dwivedi, 2001). To use visual interpretation techniques, detailed knowledge on the relationship between observable terrain characteristics and the occurrence of soil units is required. Such knowledge can be formalized in clear criteria, like those used for the creation of the Soils and Terrain digital databases SOTER (Van Engelen and Wen, 1995; Van Lynden and Mantel, 2001). Soil classification by visual interpretation of optical satellite imagery has been used to assess differences in soil erodibility (Reusing et al., 2000; Sharma and Singh, 1995). The relation between soil classes and erodibility was determined using equations of Wischmeier and Smith (1978).

Wang et al. (2003) used the same equations to determine erodibility in the field. The obtained erodibility values were extrapolated to the whole sampling region using two geostatistical methods, collocated co-kriging and joint sequential co-simulation. Within these methods, Landsat TM band 7 allowed for reproducing the spatial variability of the erodibility. The success of this mapping must be contributed to the existence of a clear link between natural vegetation and soil types in the studied area. When this link is clearly present, spatial variability of erodibility will probably be better represented than when assigning erodibility values to a soil classification.

Topsoil characteristics influence the soil surface colour, and thus spectral reflectance curves. Significant relationships were found between soil colours defined by the Munsell system and optical satellite imagery (Escadafal, 1993; Singh et al., 2004). Various soil properties affect the soil's spectral reflectance, such as soil texture, organic matter content,

moisture content, iron oxides and soil minerals (Barnes and Baker, 2000; Dwivedi, 2001; Escadafal, 1994). This can be a limitation for the study of one particular property, but surface states may be classified when one or more topsoil properties affect its spectral reflectance. These surface states can then be related to run-off and erosion potential using field measurements (Gardner and Duffy, 1985). Surface state conditions that are important for erosion are surface crusting and the uncovering of subsoil. Crusted soil can sometimes have distinct spectral properties as compared to uncrusted soil, due to an increase in clay particles at the soil surface, and a decrease of surface roughness (Ben-Dor et al., 2003; Escel et al., 2004), but this is largely dependent on the crust type and soil type. Satellite applications using this relation for erosion assessment are limited to analysis of crust dynamics of bare soil surfaces for Northern France with multi-temporal SPOT HRV imagery (King et al., 1989; Mathieu et al., 1997). Apart from crusting, the gradual uncovering of subsoil by erosion also results in detectable spectral changes. When these changes are well known, optical satellite data allows spatial and temporal assessment of erosion status (Latz et al., 1984; Pelletier and Griffin, 1985, see also Section 2.3.1).

A difficulty in measuring topsoil reflectance with satellite data is the disturbing influence of vegetation, which greatly limits satellite-based soil studies for temperate and humid areas, unless agricultural practices leave the soil bare periodically. To separate the soil from the vegetation signal, a common used technique in (semi-) arid environments is linear spectral unmixing (Adams et al., 1986; Smith et al., 1990). In this technique, spectral reflectance signatures are modelled as a linear combination of a few prototype spectra, called endmembers. It is assumed that the spectral variation in remote sensing images is caused by mixtures of a limited number of surface materials, which have sufficient spectral contrast, allowing their separability. As long as the number of endmembers does not exceed the number of spectral bands minus one, a unique solution is obtained for the relative endmember abundance per pixel. Disturbing influences for soil assessment as caused by vegetation and shade can thus be accounted for (Adams et al., 1989; Hill, 1993). Knowing the regional soil types and their respective climax and degradation forms in combination with their spectral characteristics, spectral unmixing allows erosion assessment (Hill et al., 1995a). When the top layer of the soil is removed by erosion, the volume of organic matter and iron oxides decreases, and gradually rock becomes visible at the surface (De Jong et al., 1999). Hence, spectral unmixing has been used for erosion status mapping with Landsat TM imagery (e.g. De Jong et al., 1999; Haboudane et al., 2002; Hill and Schütt, 2000; Metternicht and Fermont, 1998). Changes in erosion status were analyzed with multi-temporal imagery for a site in Greece and showed an increase of erosion between 1985 and 1990 (Hill et al., 1995a; Hill et al., 1995b).

Soil properties that can be assessed with SAR systems are surface roughness, soil moisture, and texture (Ulaby et al., 1978; Ulaby et al., 1979). Although many studies addressed the soil moisture assessment by SAR, satellite-based assessment is still very complicated (Walker et al., 2004). Even at locations with bare soil, there is a confusing influence of surface roughness conditions and soil moisture on radar backscatter (Davidson et

al., 2000) and the two effects cannot be separated without additional information (Colpitts, 1998). Nevertheless, several authors claimed success in representing spatial and temporal soil moisture variability when good land use information is available (e.g. Löw et al., 2004; Quesney et al., 2000). For erosion studies, few authors have used SAR to assess roughness and moisture properties. To identify run-off risks in vineyards in southern France, Remond et al. (1999) identified the periodic and stable surface roughness of agricultural areas with multi-temporal ERS-1 imagery. Baghdadi et al. (2002) classified surface roughness to determine run-off potential of bare soils in northern France. They found that RADARSAT-1 imagery with a high incidence angle (47º) performed better for roughness classification than images with incidence angles of 39º (RADARSAT-1) and 23º (ERS-1).

2.4.3 Vegetation

Vegetation cover provides protection of the soil against erosion processes. To account for vegetation in erosion assessments, a cover and management factor (C-factor) has often been used. The C-factor is defined as the ratio of soil loss from land cropped under specified conditions to the corresponding clean-tilled continuous fallow (Wischmeier and Smith, 1978). In many regions of the world, vegetation cover shows a high temporal dynamics. Long-term dynamics relate to e.g. land use conversions or gradual depletion of resources. Short-term dynamics are caused by rainfall characteristics, and by human activities such as crop harvesting or burning practices. Many satellite remote sensing studies of soil erosion focus on the assessment of vegetation cover. These studies need to account somehow for the temporal variation, and consequently image timing is highly important, although not always sufficiently highlighted. Depending on the purpose of the study, sometimes a mono-temporal assessment can be sufficient. However, especially for physically-based models (see Section 2.5.1) careful matching of satellite imagery with rainy periods and crop development is required, which demands a time series of remote sensing images to account for seasonal variability (e.g. Cyr et al., 1995).

Land use classification is often used to map vegetation types that differ in their effectiveness to protect the soil. After classification, a qualitative ranking of vegetation types is made, or C-factors are assigned from reported values in literature (e.g. Morgan, 1995; Wischmeier and Smith, 1978). In most cases seasonal crop dynamics are accounted for within the classification, because an average annual C-factor is assigned. For erosion studies, land use classification has been performed with optical satellite systems through visual interpretation of image composites (e.g. Khan et al., 2001; Mati et al., 2000; Sharma and Singh, 1995) or automated classification approaches. The most common ones are unsupervised classification, in which pixels are grouped according to their relative spectral similarity (e.g. Feoli et al., 2002; Jakubauskas et al., 1992) and supervised classification, where pixels are allocated to predefined classes that are generally established based on ground-truth data (e.g. Jürgens and Fander, 1993; Millward and Mersey, 1999; Pelletier, 1985). The mentioned classification techniques can also be combined. Folly et al. (1996)

performed a visual interpretation of a Landsat TM composite to classify main cover types. Subsequently a fine-tuning within each class was achieved with a supervised classification. Several authors applied hybrid unsupervised-supervised approaches (e.g. Bhuyan et al., 2002; Fraser et al., 1995; Vaidyanathan et al., 2002). Due to seasonal changes of some vegetation classes, classification of multi-temporal imagery can improve the classification accuracy (Müschen et al., 2001). Details on the accuracy assessment of land use classifications are given by Foody (2002). Although SAR systems allow land use classification (e.g. Brisco and Brown, 1998) and other classification approaches exist such as neural networks (e.g. Miller et al., 1995), no studies were found in literature that relate this to erosion assessment.

To decrease the influence of classification errors and account for within-class variability, direct linear regression has been performed between image bands or ratios and C-values determined in the field. For agricultural lands in New Brunswick, Canada, good relationships were obtained between C-values and band ratios of NIR to red reflection (Cihlar, 1987; Stephens and Cihlar, 1982). In a mixed savannah-woodland landscape in Texas, Gertner et al. (2002) found a high correlation between Landsat TM band ratio 3/4 (red over NIR) and vegetation attributes. They mapped C-factors with the technique of joint sequential co-simulation, in which the band ratio accounted for the spatial variability of vegetation attributes (secondary variable), while field data provided the attribute values (primary variable). In the same study area, Wang et al. (2002) used Landsat image ratio (TM3 + TM7 / TM4), which gave higher correlation with directly calculated C-values from the field. Wang et al. (2003) applied Landsat TM band 7 as a secondary variable, because they jointly mapped erodibility and C-values, for which band 7 gave optimal correlation. While comparing different C-factor mapping techniques for this area, joint sequential co-simulation with a Landsat TM image outperformed classification, regression of C-values against image ratios, collocated co-kriging, and co-simulation without a Landsat TM image (Wang et al., 2003; Wang et al., 2002).

Vegetation indices are a specific class of spectral band ratios. A wide range of such indices exists. Often they exploit the fact that green vegetation has high reflectance in the NIR and low reflectance in the red part of the spectrum. A common index is the normalized difference vegetation index (NDVI), which is defined as the NIR reflection minus red reflection divided by the sum of the two (Tucker, 1979). NDVI has been used directly as an indication of the protective cover of vegetation (Gay et al., 2002; Jain and Goel, 2002; Liu et al., 2000; Thiam, 2003) or was related to vegetation cover with regression analysis (Bhuyan et al., 2002; Symeonakis and Drake, 2004; Zhang, 1999). De Jong (1994b) concluded that the relationship between Landsat derived spectral indices and vegetation attributes was quite poor for Mediterranean France, but he still applied the NDVI for C-factor estimation in later works (De Jong et al., 1999; De Jong and Riezebos, 1997). Such poor relationships can also partly be explained by the methodological difficulties in precisely assessing the proportional vegetation cover in the field (Hill et al., 1995a; Zhou et al., 1998). Due to seasonal variability it is often highly important for which date a vegetation index is calculated, and for most

environments a carefully chosen time series of satellite images is required to reliably estimate the vegetative soil protection (e.g. De Jong et al., 1999).

Main problems with indices like the NDVI are the effect of soil reflectance (Escadafal, 1994, Section 2.4.2) and the sensitivity to the vitality of the vegetation (De Jong, 1994b; Frederiksen, 1993). To account for soil reflectance, several soil adjusted vegetation indices have been developed, like the transformed soil adjusted vegetation index TSAVI (Baret and Guyot, 1991). Cyr et al. (1995) showed that TSAVI performed better for the assessment of low vegetation covers than NDVI. Negative TSAVI values have been related to potentially degraded areas (Flügel et al., 2003; Hochschild et al., 2003). However, soil adjusted indices have difficulty in accounting for spatially variable soil types (Hill et al., 1994a). The main vegetation vitality effects are during early growth stages, when thin vegetation covers are often over-estimated by vegetation indices due to intense chlorophyll activity, and during vegetation senescence when vegetation indices usually decrease even when the cover remains the same (Cyr et al., 1995). For erosion processes, vegetation condition is of minor importance however, as senescent vegetation offers the same protection to the soil as vigorous vegetation. To improve the detection of dry vegetation, Bonn et al. (1997) proposed to combine SWIR and NIR reflection in a soil adjusted crop residue index (SACRI). Spectroradiometer studies support the use of SWIR reflection for separating crop residue from soils (e.g. Daughtry et al., 2004; Nagler et al., 2000). French et al. (2000) showed that senescent vegetation can be distinguished from bare soil using TIR emissivity in combination with NDVI, which is currently possible with the ASTER sensor on the Terra satellite. Bhuyan et al. (2002) avoided vegetation indices for separating wheat-stubble areas, but related ground data on crop residue to classes obtained by unsupervised clustering instead.

Linear spectral unmixing is an alternative technique for assessing the vegetation cover (see Section 2.4.2). This technique is mainly used in (semi)-arid environments, where it has the advantage that different soil characteristics within a scene can be accounted for. Using the green vegetation spectrum as an endmember, spectral unmixing permits an estimation of percentage green cover (e.g. De Jong et al., 1999; Haboudane et al., 2002; Hill, 1993). In this way, Zhang et al. (2002) determined green vegetation cover at different spatial scales using aerial photographs, Landsat TM and AVHRR imagery. Ma et al. (2003) related the derived vegetation cover from unmixing Landsat data to the C-factor using a log-linear relation. To account for distinct spectral properties of vegetation types, Paringit and Nadaoka (2003) automatically retrieved the vegetation endmember from a field-survey based land use map before applying the unmixing procedure, assuming no mixing of vegetation types per pixel. Hill et al. (1995a; 1995b) proposed that possible endmembers can include non-photosynthetic vegetation, like senescent vegetation or leaf litter. Bonn et al. (1997) stated that for such vegetation, SWIR spectral bands are required, and thus Landsat TM is more appropriate than SPOT (HRV) satellites. Asner and Heidebrecht (2002) effectively assessed non-photosynthetic vegetation cover with spectral unmixing. To assess the protection effect to erosion of crop residues, Biard and Baret (1997) proposed the algorithm CRIM (crop residue

index multiband) which is based on spectral unmixing of soil and residue spectra. Using field radiometric measurements, they achieved better estimates for residue cover with CRIM than with the vegetation index SACRI. As the crop residue spectrum tends towards the soil spectrum with progressive aging, the residue fraction can best be determined soon after harvest. Using Landsat data, CRIM also performed better than indices like SACRI in assessing maize and wheat residue fractions on clayey and silty soils in Quebec (Arsenault and Bonn, 2005).

2.4.4 Conservation practices and tillage

Especially in agricultural areas, conservation practices such as contouring, strip cropping, or terracing, reduce soil losses. The effectiveness of such practices is often analyzed with a support practice factor (P-factor), defined as the ratio of soil loss with the practice applied and up- and downslope cultivation (Wischmeier and Smith, 1978). P-values have been assigned to land use classes that were derived from a classification of remote sensing imagery, using literature values (Lee, 2004) or expert opinion (Bhuyan et al., 2002) for practices that commonly occur for the land use class in the studied area. Interpretation of aerial photographs allows the detection of many conservation measures, but with coarse resolution Landsat MSS data this becomes problematic (Langran, 1983). Nevertheless, Pelletier and Griffin (1985) managed to successfully detect several conservation measures with Landsat MSS and TM imagery. Still, there have been few studies on the detection of conservation practices with satellite remote sensing.

An exception to this is the detection of tillage practices with satellite imagery. Tillage practices differ in their effect on surface roughness and amount of crop residues, which forms the basis of their detection (see also Section 2.4.2 and 2.4.3). Image timing is very important, because tillage operations are performed during a specific time of the year. DeGloria et al. (1986) performed visual interpretation of 5-year Landsat MSS data to monitor land under conventional and conservation tillage practices in California. Various authors used logistic regression techniques to separate tillage practices in Landsat imagery (Bricklemyer et al., 2002; Gowda et al., 2001; Van Deventer et al., 1997). Although several band combinations were used in the different studies, all authors included TM band 5 (SWIR), which has been related to crop residue (Section 2.4.3).

In temperate regions, cloud cover restricts acquisitions of optical imagery at the time of tillage. Therefore, SAR data has been used for assessing tillage, mainly because the radar return is dependent on surface roughness. To assess the effect of autumn tillage on erosion in Norway, ERS-1 SAR imagery allowed a good separation of grain stubble and ploughed fields, whereas SPOT HRV imagery performed worse (Leek and Solberg, 1995; Solberg, 1992). Using RADARSAT imagery, McNairn et al. (1998) separated classes with different erosion potential based on the effect of residue cover and tillage operations on radar return. They stress that multi-temporal or multi-polarization SAR imagery is required for effective class separation. As radar return depends on other factors than those affected by tillage, such

as soil moisture and vegetation density, assessment of tillage practices is not always straightforward. For example, effects of tillage row direction on radar backscatter have found to be as significant as the differences between tillage implements for grain stubble fields (Brisco et al., 1991). Moran et al. (2002) demonstrated that integration of optical and SAR imagery provides more information on tillage and other surface characteristics than the separate analysis of both data sources.

2.5 Data integration for erosion mapping

Many rationales exist for the mapping of soil erosion. A first step in erosion mapping is the definition of clear objectives on the type of assessment, the extent of the region, the spatial integration level, and temporal aspects. A general used level of spatial integration is a pixel, but also hydrological catchments may be used. Temporal aspects refer to the assessment of either past, actual, or predicted erosion, to events versus long-term averages, and to the mono- versus multi-temporal assessment.

Remote sensing data assist erosion mapping through direct erosion detection (Section 2.3) or through the use of erosion controlling factors (Section 2.4). With detection, multiple explanations may exist for certain image characteristics, which could be accounted for with additional data sources. Using erosion controlling factors, a framework for integrating the different factors is required to map erosion. In many cases, only one factor (e.g. vegetation) is assessed with satellite imagery, and other factors are derived from additional data. The choice for a specific integration method depends highly on the mapping objectives. A common way of integrating erosion controlling factors is through the use of erosion models, although other more qualitative approaches exist. Such qualitative approaches may include erosion detection results within the framework. To assess the accuracy of the produced maps, validation with independent data is required, which can be obtained from field measurements, surveys, and high-resolution imagery.

2.5.1 Erosion models

A large number of erosion models exists, which can be divided in empirical models and physically-based models (Morgan, 1995). Empirical models have a statistical basis, whereas physically-based models intend to describe the acting processes on a storm event basis. Nevertheless, many models contain both empirical and physically-based components. A recent review of several current erosion models is provided by Merritt et al. (2003). Satellite imagery has the potential to provide regional spatial data for several input parameters of erosion models (e.g. King and Delpont, 1993; Pelletier, 1985). However, most published studies merely use optical satellite data to assess the vegetation component (see Section 2.4.3). Additional spatial data is generally extracted from rainfall gauges, readily available

soil maps and DEMs, topographic maps, aerial photographs, and field measurements. Conservation practices are sometimes considered, but usually assumed not present.

The most widely used model is the Universal Soil Loss Equation (USLE), which is an empirical model assessing long term averages of sheet and rill erosion, based on plot data collected in eastern USA (Wischmeier and Smith, 1978). The USLE and adapted versions (RUSLE: Renard et al., 1997; MUSLE: Smith et al., 1984) have been applied to various spatial scales and region sizes in different environments worldwide. USLE applications in which satellite imagery accounted for the vegetation component have been performed for a small hydrological catchment of about 2.5 km^2 in size (Jürgens and Fander, 1993), areas between 10 to 100 km^2 (Fenton, 1982; Fraser et al., 1995; Lee, 2004; Millward and Mersey, 1999; Reusing et al., 2000), between 100 and 500 km^2 (Anys et al., 1994; Baban and Yusof, 2001; Bonn et al., 1997; Cihlar, 1987), large watersheds of more than 10,000 km^2 (Cerri et al., 2001; Ma et al., 2003; Mati et al., 2000), the country scale for Morocco (Gay et al., 2002) and to the European scale (CORINE, 1992; Van der Knijff et al., 2000). Most of these studies have not sufficiently realized that in different environments empirical relationships of the USLE may not be valid. Besides, the model is developed for evaluating sheet and rill erosion on short slopes. In larger regions also other erosion processes and deposition occur, which are not included in the USLE. Furthermore the data applied in these studies generally have a low spatial resolution (30-m to 1-km), which greatly affects soil loss estimates (e.g. Schoorl et al., 2000). Ideally, the spatial scale of a model is in balance with the various erosion processes that occur in a specific region (Favis-Mortlock et al., 1996). These considerations also concern the application of other models, as many studies fail to provide a clear rationale why a specific model is selected.

The only model which was developed with the intention to be used with satellite data is the Soil Erosion Model for Mediterranean regions SEMMED (SEMMED: De Jong, 1994a). It is based on the Morgan, Morgan and Finney model (Morgan et al., 1984), but modifications were made to model the erosion process in a spatially distributed approach and to enable the input from satellite imagery and DEMs. SEMMED uses optical imagery to assess the crop cover factor (same as USLE C-factor) and the rainfall interception factor of vegetation at different moments. Multi-temporal Landsat TM imagery and additional data sources allowed the application of SEMMED to the Ardèche Province in France (De Jong and Riezebos, 1997), to a small watershed (12 km^2) in the same area, and to a 4200-km^2 watershed in Sicily, Italy (De Jong et al., 1999). Although the model yields quantitative values, De Jong and Riezebos (1997) recommend to use model outcomes in a qualitative sense, thus to assess the spatial erosion pattern.

Other models that have been used in combination with satellite data include the Thornes model (Thornes, 1985), the Agricultural Nonpoint Source Pollution model (AGNPS: Young et al., 1989), and the Areal Nonpoint Source Watershed Environment Response Simulation model (ANSWERS: Beasley et al., 1980). The Thornes model was applied with satellite-derived vegetation cover information at the continental scale for assessing annual erosion rates, both in a multi-scale approach with remote sensing data of different resolutions

(Zhang et al., 2002), and in a multi-temporal approach using AVHRR NDVI data (Symeonakis and Drake, 2004). The AGNPS model was used for predicting soil loss from several watersheds (33-1223 km^2) within Kansas State (USA) employing a land use map derived from satellite data (Bhuyan et al., 2003; Bhuyan et al., 2002). ANSWERS allowed for the prediction of soil loss at the outlet of three watersheds (320-1020 km^2) in the arid zone of northwest India (Sharma and Singh, 1995). Landsat TM data was used here to assess landform, drainage, soil, land use, and land cover. Paringit and Nadaoka (2003) compiled their own physical model from existing equations using a Landsat image to derive vegetation parameters. A combination of models was used by Flügel et al. (2003) for a 4400-km^2 catchment in South Africa. They first delineated terrain units having homogeneous process dynamics with aerial photography and a Landsat TM image. Depending on the relative importance of sheet and rill erosion versus gully erosion, the RUSLE and a gully erosion model were applied to estimate sediment yields.

2.5.2 Qualitative methods

Drawbacks of erosion models are the fixed data requirement, and the fact that models are developed for a certain region, scale, and specific processes. Often erosion rates are not required, but merely an indication of the spatial distribution of erosion, e.g. for conservation prioritization. Therefore, qualitative erosion mapping approaches have been developed, which are adapted to regional characteristics and data availability. Resulting maps usually depict classes ranging from very low to very high erosion or erosion risk. There is not a standard method for qualitative data integration, and consequently many different methods exist. However, common features are the classification of considered erosion controlling factors in discrete classes and the application of a decision rule to combine the classes. Factor selection and decision rules are generally based on expert judgment, or on the author's personal knowledge of the regional erosion processes.

The most basic qualitative approach is to assign weights to spatial units expressing the erosion intensity. This way, Khan et al. (2001) assigned a weighting to visually delineated units from a Landsat TM image. Multiplication with a sediment delivery ratio allowed the contribution of each watershed to sedimentation at a reservoir downstream. Instead of directly assigning weights to units, separate weights can be assigned to different erosion controlling factors according to their importance in the occurring erosion processes. Erosion risk has subsequently been determined from factor weights by summation (Jain and Goel, 2002; Shrimali et al., 2001), averaging (Vrieling et al., 2002), and using hierarchical decision rules to combine the weights (Haboudane et al., 2002). Simple if-then decision rules were applied by Hill et al. (1994b) to combine soil status and vegetation cover information layers derived from spectral unmixing of Landsat TM data. The resulting index is related to erosion occurrence. Multi-temporal comparison of this index derived from images acquired in the same season but during different years would allow the assessment of further erosion, stability, or recovery (Hill et al., 1995b).

For semi-arid Spain, Liu et al. (2000; 2004) used multi-temporal SAR interferometric decorrelation images to detect candidate pixels for erosion. Areas vulnerable to rapid erosion were determined by applying fuzzy logic and multi-criteria evaluation to Landsat-derived lithology and vegetation information, and slope calculated from a SAR interferogram. Where the candidate pixels and vulnerable areas coincided, rapid erosion was expected. However, erosion on agricultural land cannot be accounted for with this approach. For a semi-arid part of Bolivia, Metternicht (1996) applied fuzzy logic to determine the degree of membership of a particular pixel to considered factors, including slope, landscape position, vegetation cover, rock fragments, reddish soil, and whitish soil, derived from a DEM, a geopedologic map, and spectral unmixing of Landsat TM data. The membership functions were translated to five classes from very low to very high expressing the erosion hazard. If-then decision rules subsequently combined the ranges for the different factors.

2.5.3 Validation

To evaluate the performance of a specific erosion mapping method and its predictive value, validation of resulting maps with independent data is required. Validation implies an assessment of the accuracy of the representation of spatial erosion patterns, and of erosion rates in the case of quantitative results. Obtaining spatial validation data for assessing the accuracy of erosion maps is a complicated task. Two major issues play a role: first, the considerable investment of time and money required to understand, assess and possibly quantify the local erosion processes; and second the difficulty of extrapolating local observations to larger areas (Stroosnijder, 2003). For example, a common measurement technique for quantification purposes is the collection of runoff and sediments from bounded plots. However, plot size has a considerable impact on measured sediment concentrations (Chaplot and Le Bissonnais, 2000) and results from plot replications can show high variation, which stresses the need for long-term measurements (Nearing et al., 1999). Several good summaries of field techniques for erosion assessment and measuring exist (e.g. Ciesiolka and Rose, 1998; Hudson, 1993; Loughran, 1989; Morgan, 1995). Here we will focus on techniques applied for validation in remote sensing studies of erosion.

From the reviewed literature, it is striking that many studies have not or only slightly addressed the issue of validation. Some merely related the acquired range of quantitative erosion rates to measured or predicted values from literature, and were satisfied when values correlated (e.g. De Jong, 1994a; Reusing et al., 2000; Zhang et al., 2002). However, reported values of erosion rates should be treated carefully, as was pointed out by Boardman (1998). De Jong and Riezebos (1997) performed an internal validation of the SEMMED model, using a Monte Carlo approach to compute the effect of various sources of uncertainty on the model outcome. They found a large uncertainty in soil loss predictions, although the error contribution of remotely sensed vegetation parameters was relatively small.

Erosion measurements were seldom used for validating satellite-based erosion assessments, which is partly due to the high time and labour requirement to perform these

measurements. Techniques that have been used include soil loss measurements from bounded plots (Mati et al., 2000); runoff measurement and sampling to determine sediment concentrations at the outlet of a watershed (Sharma and Singh, 1995); the assessment of sediment concentrations at the outlet using optical turbidity sensors (Paringit and Nadaoka, 2003); and the evaluation of sediment accumulation in a reservoir through successive bathymetry campaigns (Bonn et al., 1997).

The common output of satellite-based erosion assessment is a spatial map, which ideally requires validation at several locations. The above-mentioned measurements cannot be easily repeated at many locations. Spatial validation may however be done with Cesium-137 measurements that were used by Bonn et al. (1997) to determine areas of erosion and deposition. More common though are erosion surveys, in which rill dimensions are measured (Cerri et al., 2001; Mathieu et al., 1997), or which are limited to a visual field estimation of erosion risk based on observed features and erosion factors that depend on the study region (e.g. Dwivedi et al., 1997b; Metternicht and Zinck, 1998; Millward and Mersey, 1999).

Besides erosion measurements and surveys, interpretation of high-resolution remote sensing imagery can also be used for validating erosion maps. Aerial photographs have been used to locate evidence of erosion or deposition, and this information provided good correlation with a data space defined by two Landsat MSS band ratios (Pickup and Chewings, 1988; Pickup and Nelson, 1984). Current availability of high-resolution satellites provides similar possibilities as aerial photography in detecting erosion features and thus providing validation data. Panchromatic QuickBird imagery was used to evaluate the potential of detecting and delineating large gullies with optical and SAR satellite imagery (Vrieling and Rodrigues, 2004).

2.6   Conclusions and recommendations

This review has shown that satellite remote sensing can contribute to erosion assessment in many ways. The effectivity of most methodologies presented largely depends on site characteristics. For semi-arid areas, many interesting techniques such as SAR interferometry and spectral unmixing of optical data were applied to assess erosion status. However, these techniques will only work under specific conditions and cannot be transferred easily to more humid environments. In these environments, satellite applications were mostly limited to the assessment of vegetation class and cover. Recent and future satellite missions will continuously provide new possibilities for erosion research and assist in filling current gaps. Some of the major observation-related gaps are (1) the automatic detection of individual erosion features like gullies or medium-sized rills; (2) the accurate assessment of senescent vegetation cover in different environments; (3) the spatial and temporal evaluation of rainfall characteristics; (4) precise mapping of soil properties and soil moisture in a wide range of environments.

Due to the complexity of erosion processes, regional differences, and scale dependency, it cannot be expected that a standardized operational erosion assessment system using satellite data will develop in the near future. Furthermore the required erosion assessment type depends largely on the regional context and the intended use. Therefore no recommendations can be made for one single technique or a set of methods in erosion assessment. Instead, it is recommended for any erosion study that intends to use satellite data, to first thoroughly evaluate what are the observables that may be derived from different types of satellite imagery for the region and the scale required. For most cases, empirical relations will have to be developed, and thus field data on the variable to be observed is needed. Promising methods that deserve special attention and require additional testing include: (1) SAR interferometric decorrelation for erosion detection; (2) evaluation of differential suspended sediment across water bodies in a landscape; (3) the use of geostatistics for soil erodibility or C-factor mapping; and (4) spectral unmixing of optical data to assess soil and vegetation status.

Satellite-derived vegetation information has been the most important input for erosion mapping approaches. For simple empirical models generally one well-timed image is sufficient, but for process-based models multi-temporal imagery is often needed to account for seasonal variability of vegetation cover. Qualitative erosion mapping methods are more flexible than models and can easily incorporate other satellite-derived information. For erosion mapping and monitoring, it is recommended to use qualitative approaches in the case that no model is available that was developed or tested in the region under study. Unless merely a quick identification of erosion risk is envisaged, a proper validation of presented results is always required, which currently is not or poorly done in many studies. Validation is essential for identifying methods that allow accurate mapping and monitoring of erosion. Long-term erosion field measurements and detailed field surveys are indispensable for this purpose, although costly and time-consuming. Close collaboration between the remote sensing community and field-based erosion scientists is therefore required, and accordingly forms the key towards achieving regional operational erosion monitoring systems.

References

Adams JB, Smith MO, and Gillespie AR. 1989. Simple models for complex natural surfaces: a strategy for the hyperspectral era of remote sensing, Proceedings of IGARSS'89. IEEE, Vancouver, Canada: pp. 16-21.

Adams JB, Smith MO, and Johnsen PE. 1986. Spectral mixture modeling: a new analysis of rock and soil types at the Viking Lander-1 site. *Journal of Geophysical Research - Solid Earth and Planets* 91 (B8): 8098-8112.

Anys H, Bonn F, and Merzouk A. 1994. Remote sensing and GIS based mapping and modeling of water erosion and sediment yield in a semi-arid watershed of Morocco. *Geocarto International* 9 (1): 31-40.

Arsenault E, and Bonn F. 2005. Evaluation of soil erosion protective cover by crop residues using vegetation indices and spectral mixture analysis of multispectral and hyperspectral data. *Catena* 62 (2-3): 157-172.

Asner GP, and Heidebrecht KB. 2002. Spectral unmixing of vegetation, soil and dry carbon cover in arid regions: comparing multispectral and hyperspectral observations. *International Journal of Remote Sensing* 23 (19): 3939-3958.

Baban SMJ, and Yusof KW. 2001. Modelling soil erosion in tropical environments using remote sensing and geographical information systems. *Hydrological Sciences Journal* 46 (2): 191-198.

Baghdadi N, King C, Bourguignon A, and Remond A. 2002. Potential of ERS and Radarsat data for surface roughness monitoring over bare agricultural fields: application to catchments in Northern France. *International Journal of Remote Sensing* 23 (17): 3427-3442.

Baret F, and Guyot G. 1991. Potentials and limits of vegetation indices for LAI an APAR assessment. *Remote Sensing of Environment* 35 (2-3): 161-173.

Barnes EM, and Baker MG. 2000. Multispectral data for mapping soil texture: possibilities and limitations. *Applied Engineering in Agriculture* 16 (6): 731-741.

Beasley DB, Huggins LF, and Monke EJ. 1980. ANSWERS: A model for watershed planning. *Transactions of the American Society of Agricultural Engineers* 23 (4): 938-944.

Beaulieu A, and Gaonac'h H. 2002. Scaling of differentially eroded surfaces in the drainage network of the Ethiopian Plateau. *Remote Sensing of Environment* 82 (1): 111-122.

Ben-Dor E, Goldshleger N, Benyamini Y, Agassi M, and Blumberg DG. 2003. The spectral reflectance properties of soil structural crusts in the 1.2- to 2.5-μm spectral region. *Soil Science Society of America Journal* 67 (1): 289-299.

Bergsma E. 1974. Soil erosion sequences on aerial photographs. *ITC Journal* 3: 342-376.

Bhuyan SJ, Koelliker JK, Marzen LJ, and Harrington-Jr. JA. 2003. An integrated approach for water quality assessment of a Kansas watershed. *Environmental Modelling & Software* 18 (5): 473-484.

Bhuyan SJ, Marzen LJ, Koelliker JK, Harrington-Jr. JA, and Barnes PL. 2002. Assessment of runoff and sediment yield using remote sensing, GIS, and AGNPS. *Journal of Soil and Water Conservation* 57 (6): 351-364.

Biard F, and Baret F. 1997. Crop residue estimation using multiband reflectance. *Remote Sensing of Environment* 59 (3): 530-536.

Bishop MP, and Shroder-Jr. JF. 2001. Remote sensing and geomorphometric assessment of topographic complexity and erosion dynamics in the Nanga Parbat massif. *In*: Khan MA, Treloar PJ, Searle MP, and Jan MQ (Editors), Tectonics of the Nanga Parbat Syntaxis and the Western Himalaya. Special Publication 170. Geological Society, London, UK: pp. 181-200.

Boardman J. 1998. An average soil erosion rate for Europe: Myth or reality? *Journal of Soil and Water Conservation* 53 (1): 46-50.

Bocco G. 1991. Gully erosion: processes and models. *Progress in Physical Geography* 15 (4): 392-406.

Bocco G, Palacio JL, and Valenzuela CR. 1991. Gully erosion modelling using GIS and geomorphological knowledge. *ITC Journal* 1991 (3): 253-261.

Bocco G, and Valenzuela CR. 1988. Integration of GIS and image processing in soil erosion studies using ILWIS. *ITC Journal* 1988 (4): 309-319.

Bocco G, and Valenzuela CR. 1993. Integrating satellite remote sensing and Geographic Information Systems technologies in gully erosion research. *Remote Sensing Reviews* 7: 233-240.

Bonn F, Mégier J, and Ait Fora A. 1997. Remote sensing assisted spatialization of soil erosion models with a GIS for land degradation quantification: Expectations, errors and beyond... *In*: Spiteri A (Editor), Remote Sensing '96: integrated applications for risk assessment and disaster prevention for the Mediterranean. Balkema, Rotterdam: pp. 191-198.

Bricklemyer RS, Lawrence RL, and Miller PR. 2002. Documenting no-till and conventional till practices using Landsat ETM+ imagery and logistic regression. *Journal of Soil and Water Conservation* 57 (5): 267-271.

Brisco B, and Brown RJ. 1998. Agricultural applications with radar. *In*: Henderson FM, and Lewis AJ (Editors), Principles and Applications of Imaging Radar - Manual of Remote Sensing. John Wiley & Sons, Inc., New York (NY), USA: pp. 381-406.

Brisco B, Brown RJ, Snider B, Sofko GJ, Koehler JA, and Wacker AG. 1991. Tillage effects on the radar backscattering coefficient of grain stubble fields. *International Journal of Remote Sensing* 12 (11): 2283-2298.

Carpenter DS, and Carpenter SM. 1983. Monitoring inland water quality using Landsat data. *Remote Sensing of Environment* 13 (4): 345-352.

Cerri CEP, Demattê JAM, Ballester MVR, Martinelli LA, Victoria RL, and Roose E. 2001. GIS erosion risk assessment of the Piracicaba River basin, southeastern Brazil. *Mapping Sciences and Remote Sensing* 38 (3): 157-171.

Chacontorres A, Ross LG, Beveridge MCM, and Watson AI. 1992. The application of SPOT multispectral imagery for the assessment of water-quality in Lake Patzcuaro, Mexico. *International Journal of Remote Sensing* 13 (4): 587-603.

Chaplot V, and Le Bissonnais Y. 2000. Field measurements of interrill erosion under different slopes and plot sizes. *Earth Surface Processes and Landforms* 25 (2): 145-153.

Choubey VK. 1998. Laboratory experiment, field and remotely sensed data analysis for the assessment of suspended solids concentration and secchi depth of the reservoir surface water. *International Journal of Remote Sensing* 19 (17): 3349-3360.

Ciesiolka CAA, and Rose CW. 1998. The measurement of soil erosion. *In*: Penning de Vries FWT, Agus F, and Kerr J (Editors), Soil erosion at multiple scales: principles and methods for assessing causes and impacts. CABI Publishing, Oxon, UK: pp. 287-301.

Cihlar J. 1987. A methodology for mapping and monitoring cropland soil erosion. *Canadian Journal of Soil Science* 67: 433-444.

Colpitts BG. 1998. The integral equation model and surface roughness signatures in soil moisture and tillage type determination. *IEEE Transactions on Geoscience and Remote Sensing* 36 (3): 833-837.

Coppin P, Jonckheere I, Nackaerts K, Muys B, and Lambin E. 2004. Digital change detection methods in ecosystem monitoring: a review. *International Journal of Remote Sensing* 25 (9): 1565-1596.

CORINE. 1992. Soil Erosion Risk and Important Land Resources in the Southern Regions of the European Community. EUR 13233. Office for Offical Publications of the European Communities, Luxembourg: 97 pp.

Crosson P. 1997. "Will erosion threaten agricultural productivity?" *Environment* 39 (8): 4-12.

Curran PJ, and Novo EMM. 1988. The relationship between suspended sediment concentration and remotely sensed spectral radiance: a review. *Journal of Coastal Research* 4 (3): 351-368.

Cyr L, Bonn F, and Pesant A. 1995. Vegetation indices derived from remote sensing for an estimation of soil protection against water erosion. *Ecological Modelling* 79 (1-3): 277-285.

Daughtry CST, Hunt Jr. ER, and McMurtrey III JE. 2004. Assessing crop residue cover using shortwave infrared reflectance. *Remote Sensing of Environment* 90 (1): 126-134.

Davidson MWJ, Le Toan T, Mattia F, Satalino G, Manninen T, and Borgeaud M. 2000. On the characterization of agricultural soil roughness for radar remote sensing studies. *IEEE Transactions on Geoscience and Remote Sensing* 38 (2): 630-640.

De Jong SM. 1994a. Applications of reflective remote sensing for land degradation studies in a Mediterranean Environment. Ph.D. Thesis, Utrecht University, The Netherlands: 237 pp.

De Jong SM. 1994b. Derivation of vegetative variables from a Landsat TM image for modelling soil erosion. *Earth Surface Processes and Landforms* 19 (2): 165-178.

De Jong SM, Paracchini ML, Bertolo F, Folving S, Megier J, and De Roo APJ. 1999. Regional assessment of soil erosion using the distributed model SEMMED and remotely sensed data. *Catena* 37 (3-4): 291-308.

De Jong SM, and Riezebos HT. 1997. SEMMED: a distributed approach to soil erosion modelling. *In*: Spiteri A (Editor), Remote Sensing '96: integrated applications for risk assessment and disaster prevention for the Mediterranean. Balkema, Rotterdam: pp. 199-204.

DeGloria SD, Wall SL, Benson AS, and Whiting ML. 1986. Monitoring conservation tillage practices using Landsat multispectral data. *Journal of Soil and Water Conservation* 41 (3): 187-190.

Dekker AG, Malthus TJ, and Hoogenboom HJ. 1995. The remote sensing of inland water quality. *In*: Danson FM, and Plummer SE (Editors), Advances in environmental remote sensing. John Wiley and Sons, Chichester: pp. 123-142.

Dhakal AS, Amada T, Aniya M, and Sharma RR. 2002. Detection of areas associated with flood and erosion caused by a heavy rainfall using multitemporal Landsat TM data. *Photogrammetric Engineering and Remote Sensing* 68 (3): 233-239.

Dwivedi RS. 2001. Soil resources mapping: a remote sensing perspective. *Remote Sensing Reviews* 20: 89-122.

Dwivedi RS, Kumar AB, and Tewari KN. 1997a. The utility of multi-sensor data for mapping eroded lands. *International Journal of Remote Sensing* 18 (11): 2303-2318.

Dwivedi RS, and Ramana KV. 2003. The delineation of reclamative groups of ravines in the Indo-Gangetic alluvial plains using IRS-1D LISS-III data. *International Journal of Remote Sensing* 24 (22): 4347-4355.

Dwivedi RS, Sankar TR, Venkaratnam L, Karale RL, Gawande SP, Rao KVS, Senchaudhary S, Bhaumik KR, and Mukharjee KK. 1997b. The inventory and monitoring of eroded lands using remote sensing data. *International Journal of Remote Sensing* 18 (1): 107-119.

Escadafal R. 1993. Remote sensing of soil color: principles and applications. *Remote Sensing Reviews* 7: 261-279.

Escadafal R. 1994. Soil spectral properties and their relationships with environmental parameters: examples from arid regions. *In*: Hill J, and Mégier J (Editors), Imaging Spectrometry - a Tool for Environmental Observations. Kluwer Academic Publishers, Dordrecht, The Netherlands: pp. 71-87.

Escel G, Levy GJ, and Singer MJ. 2004. Spectral reflectance properties of crusted soils under solar illumination. *Soil Science Society of America Journal* 68 (6): 1982-1991.

Eswaran H, Lal R, and Reich PF. 2001. Land degradation: an overview. *In*: Bridges EM, Hannam ID, Oldeman LR, Penning de Vries FWT, Scherr SJ, and Sombatpanit S (Editors), Response to land degradation. Science Publishers Inc., Enfield, NH, USA: pp. 20-35.

Fadul HM, Salih AA, Ali IA, and Inanaga S. 1999. Use of remote sensing to map gully erosion along the Atbara River, Sudan. *International Journal of Applied Earth Observation and Geoinformation* 1 (3-4): 175-180.

Favis-Mortlock DT, Quinton JN, and Dickinson WT. 1996. The GCTE validation of soil erosion models for global change studies. *Journal of Soil and Water Conservation* 51 (5): 397-403.

Fenton TE. 1982. Estimating soil erosion by remote sensing techniques. *In*: Johannsen CJ, and Sanders JL (Editors), Remote sensing for resource management. Soil Conservation Society of America, Ankeny, Iowa: pp. 217-231.

Feoli E, Vuerich LG, and Zerihun W. 2002. Evaluation of environmental degradation in northern Ethiopia using GIS to integrate vegetation, geomorphological, erosion, and socio-economic factors. *Agriculture, Ecosystems and Environment* 91 (1-3): 313-325.

Floras SA, and Sgouras ID. 1999. Use of geoinformation techniques in identifying and mapping areas of erosion in a hilly landscape of central Greece. *International Journal of Applied Earth Observation and Geoinformation* 1 (1): 68-77.

Flügel WA, Märker M, Moretti S, Rodolfi G, and Sidorchuk A. 2003. Integrating geographical information systems, remote sensing, ground truthing and modelling approaches for regional erosion classification of semi-arid catchments in South Africa. *Hydrological Processes* 17 (5): 929-942.

Folly A, Bronsveld MC, and Clavaux M. 1996. A knowledge-based approach for C-factor mapping in Spain using Landsat TM and GIS. *International Journal of Remote Sensing* 17 (12): 2401-2415.

Foody GM. 2002. Status of land cover classification accuracy assessment. *Remote Sensing of Environment* 80 (1): 185-201.

Frank TD. 1984a. Assessing change in surficial character of a semiarid environment with Landsat residual image. *Photogrammetric Engineering and Remote Sensing* 50 (4): 471-480.

Frank TD. 1984b. The effect of change in vegetation cover and erosion patterns on albedo and texture of Landsat images in a semiarid environment. *Annals of the Association of American Geographers* 74 (3): 393-407.

Fraser RH, Warren MV, and Barten PK. 1995. Comparative evaluation of land cover data sources for soil erosion prediction. *Water Resources Bulletin* 31 (6): 991-1000.

Frederiksen P. 1993. Mapping and monitoring of soil degradation in semi-arid areas - satellite image methodology. In: Adriansen HK, and Rasmussen K (Editors), Proceedings from the seminar on satellite remote sensing of environment and agriculture in developing countries. Institute of Geography, University of Copenhagen, Copenhagen, Denmark: pp. 49-52.

French AN, Schmugge TJ, and Kustas WP. 2000. Discrimination of senescent vegetation using thermal emissivity contrast. *Remote Sensing of Environment* 74 (2): 249-254.

Gardner TW, and Duffy WD. 1985. Infiltration parameters of Landsat classification of erosion-prone landscapes in the San Juan Basin, New Mexico. *Journal of Soil and Water Conservation* 40 (4): 370-374.

Gay M, Cheret V, and Denux JP. 2002. Apport de la télédétection dans l'identification du risque d'érosion. *La Houille Blanche* 2002 (1): 81-86.

Gertner G, Wang G, Fang S, and Anderson AB. 2002. Mapping and uncertainty of predictions based on multiple primary variable from joint co-simulation with Landsat TM image and polynomial regression. *Remote Sensing of Environment* 83 (3): 498-510.

Goel MK, and Jain SK. 1996. Evaluation of reservoir sedimentation using multi-temporal IRS-1A LISS-II data. *Asian-Pacific Remote Sensing and GIS Journal* 8 (2): 39-43.

Goel MK, Jain SK, and Agarwal PK. 2002. Assessment of sediment deposition rate in Bargi Reservoir using digital image processing. *Hydrological Sciences Journal* 47 (Special Issue: Towards Integrated Water Resources Management for Sustainable Development): S81-S92.

Gowda PH, Dalzell BJ, Mulla DJ, and Kollman F. 2001. Mapping tillage practices with landsat thematic mapper based logistic regression models. *Journal of Soil and Water Conservation* 56 (2): 91-96.

Haboudane D, Bonn F, Royer A, Sommer S, and Mehl W. 2002. Land degradation and erosion risk mapping by fusion of spectrally-based information and digital geomorphometric attributes. *International Journal of Remote Sensing* 23 (18): 3795-3820.

Han L, and Rundquist DC. 1996. Spectral characterization of suspended sediments generated from two texture classes of clay soil. *International Journal of Remote Sensing* 17 (3): 643-649.

Harrington-Jr. JA, Schiebe FR, and Nix JF. 1992. Remote sensing of Lake Chicot, Arkansas: monitoring suspended sediments, turbidity, and Secchi depth with Landsat MSS data. *Remote Sensing of Environment* 39 (1): 15-27.

Hill J. 1993. Monitoring land degradation and soil erosion in Mediterranean environments. *ITC Journal* 1993 (4): 323-331.

Hill J, Mégier J, and Mehl W. 1995a. Land degradation, soil erosion and desertification monitoring in Mediterranean ecosystems. *Remote Sensing Reviews* 12: 107-130.

Hill J, Mehl W, and Altherr M. 1994a. Land degradation and soil erosion mapping in a Mediterranean ecosystem. *In*: Hill J, and Mégier J (Editors), Imaging Spectrometry - a Tool for Environmental Observations. Kluwer Academic Publishers, Dordrecht, The Netherlands: pp. 237-260.

Hill J, Mehl W, Smith MO, and Mégier J. 1994b. Mediterranean ecosystem monitoring with earth observation satellites. *In*: Vaughan R (Editor), Remote Sensing - from research to operational applications in the new Europe: Proceedings of the 13th EARSeL Symposium. Springer-Verlag, Budapest, Hungary: pp. 131-141.

Hill J, and Schütt B. 2000. Mapping complex patterns of erosion and stability in dry mediterranean ecosystems. *Remote Sensing of Environment* 74 (3): 557-569.

Hill J, Sommer S, Mehl W, and Mégier J. 1995b. Towards a satellite-observatory for mapping and monitoring the degradation of Mediterranean ecosystems. *In*: Askne J (Editor), Sensors and environmental application of remote sensing. Balkema, Rotterdam: pp. 53-61.

Hochschild V, Märker M, Rodolfi G, and Staudenrausch H. 2003. Delineation of erosion classes in semi-arid southern African grasslands using vegetation indices from optical remote sensing data. *Hydrological Processes* 17 (5): 917-928.

Hudson NW. 1993. Field measurement of soil erosion and runoff. FAO Soils Bulletin, 68. Food and Agriculture Organization, Rome, Italy.

Izenberg NR, Arvidson RE, Brackett RA, Saatchi SS, Osburn GR, and Dohrenwend J. 1996. Erosional and depositional patterns associated with the 1993 Missouri River floods inferred from SIR-C and TOPSAR radar data. *Journal of Geophysical Research* 101 (E10): 23149-23167.

Jain SK, and Goel MK. 2002. Assessing the vulnerability to soil erosion of the Ukai Dam catchments using remote sensing and GIS. *Hydrological Sciences Journal* 47 (1): 31-40.

Jain SK, Singh P, and Seth SM. 2002. Assessment of sedimentation in Bhakra Reservoir in the western Himalayan region using remotely sensed data. *Hydrological Sciences Journal* 47 (2): 203-212.

Jakubauskas ME, Whistler JL, Dillworth ME, and Martinko EA. 1992. Classifying remotely sensed data for use in an agricultural nonpoint-source pollution model. *Journal of Soil and Water Conservation* 47 (2): 179-183.

Jones RGB, and Keech MA. 1966. Identifying and assessing problem areas in soil erosion surveys using aerial photographs. *Photogrammetric Record* 5 (27): 189-97.

Jürgens C, and Fander M. 1993. Soil erosion assessment and simulation by means of SGEOS and ancillary digital data. *International Journal of Remote Sensing* 14 (15): 2847-2855.

Karale RL, Saini KM, and Narula KK. 1988. Mapping and monitoring of ravines using remotely sensed data. *Journal of Soil and Water Conservation in India* 32 (1-2): 75-82.

Khan MA, Gupta VP, and Moharana PC. 2001. Watershed prioritization using remote sensing and geographical information system: a case study from Guhiya, India. *Journal of Arid Environments* 49 (3): 465-475.

Khan NI, and Islam A. 2003. Quantification of erosion patterns in the Brahmaputra-Jamuna River using geographical information system and remote sensing techniques. *Hydrological Processes* 17 (5): 959-966.

Khawlie M, Awad M, Shaban A, Kheir RB, and Abdallah C. 2002. Remote sensing for environmental protection of the eastern Mediterranean rugged mountaineous areas, Lebanon. *ISPRS Journal of Photogrammetry and Remote Sensing* 57 (1-2): 13-23.

King C, and Delpont G. 1993. Spatial assessment of erosion: contribution of remote sensing, a review. *Remote Sensing Reviews* 7: 223-232.

King C, Maucorps J, Aumonier F, Renaux B, and Lenotre N. 1989. Détection d'indices d'érosion par SPOT dans les sols limoneux du Nord-Pas de Calais - une étude multidate. *Bulletin de la Société Française de Photogrammétrie et de Télédétection (SFPT)* 114 (2): 10-13.

Kumar AB, Dwivedi RS, and Tiwari KN. 1996. The effects of image scale on delineation of eroded lands using remote sensing data. *International Journal of Remote Sensing* 17 (11): 2135-2143.

Lal R. 1998. Soil erosion impact on agronomic productivity and environment quality. *Critical Reviews in Plant Sciences* 17 (4): 319-464.

Lal R. 2001. Soil degradation by erosion. *Land Degradation & Development* 12 (6): 519-39.

Lal R. 2004. Soil carbon sequestration impacts on global climate change and food security. *Science* 304 (5677): 1623-1627.

Langran KJ. 1983. Potential for monitoring soil erosion features and soil erosion modelling components from remotely sensed data, Proceedings of IGARSS'83. IEEE, San Francisco, California: pp. 2.1-2.4.

Latz K, Weismiller RA, Scoyoc GEV, and Baumgardner MF. 1984. Characteristic variations in spectral reflectance of selected eroded alfisols. *Soil Science Society of America Journal* 48 (5): 1130-1134.

Lee H, and Liu JG. 2001. Analysis of topographic decorrelation in SAR interferometry using ratio coherence imagery. *IEEE Transactions on Geoscience and Remote Sensing* 39 (2): 223-232.

Lee S. 2004. Soil erosion assessment and its verification using the Universal Soil Loss Equation and Geographic Information System: a case study at Boun, Korea. *Environmental Geology* 45 (4): 457-465.

Leek R, and Solberg R. 1995. Using remote sensing for monitoring of autumn tillage in Norway. *International Journal of Remote Sensing* 16 (3): 447-466.

Liu JG, Black A, Lee H, Hanaizumi H, and Moore JM. 2001. Land surface change detection in a desert area in Algeria using multi-temporal ERS SAR coherence images. *International Journal of Remote Sensing* 22 (13): 2463-2477.

Liu JG, Hilton F, Mason P, and Lee H. 2000. A RS/GIS study of rapid erosion in SE Spain using ERS SAR multi-temporal interferometric coherence imagery. *In*: Owe M, Zilioli E, and D'Urso G (Editors), Remote Sensing for Agriculture, Ecosystems, and Hydrology II. Proceedings of SPIE Vol. 4171. SPIE International, Barcelona, Spain: pp. 367-375.

Liu JG, Mason P, Hilton F, and Lee H. 2004. Detection of rapid erosion in SE Spain: A GIS approach based on ERS SAR coherence imagery. *Photogrammetric Engineering and Remote Sensing* 70 (10): 1179-1185.

Liu Y, Islam MA, and Gao J. 2003. Quantification of shallow water quality parameters by means of remote sensing. *Progress in Physical Geography* 27 (1): 24-43.

Lomborg B. 2001. The skeptical environmentalist: measuring the real state of the world. Cambridge University Press, Cambridge, UK.

Loughran RJ. 1989. The measurement of soil erosion. *Progress in Physical Geography* 13 (2): 216-233.

Löw A, Waske B, Ludwig R, and Mauser W. 2004. Derivation of hydrological parameters from ENVISAT ASAR wide swath data, Proceedings of IGARSS'04. IEEE, Anchorage, Alaska.

Ma JW, Xue Y, Ma CF, and Wang ZG. 2003. A data fusion approach for soil erosion monitoring in the Upper Yangtze River Basin of China based on Universal Soil Loss Equation (USLE) model. *International Journal of Remote Sensing* 24 (23): 4777-4789.

Mannaerts CM, and Saavedra CP. 2003. Regional scale erosion modelling and monitoring using remotely sensed data: some spatial data scale issues. In: Gabriels D, and Cornelis W (Editors), Proceedings of the International Symposium on 25 Years of Assessment of Erosion. Ghent University, Ghent, Belgium: pp. 433-440.

Massonnet D, and Feigl KL. 1998. Radar interferometry and its application to changes in the earth's surface. *Reviews of Geophysics* 36 (4): 441-500.

Mathieu R, King C, and Bissonnais YL. 1997. Contribution of multi-temporal SPOT data to the mapping of a soil erosion index: the case of the loamy plateaux of northern France. *Soil Technology* 10 (2): 99-110.

Mati BM, Morgan RPC, Gichuki FN, Quinton JN, Brewer TR, and Liniger HP. 2000. Assessment of erosion hazard with the USLE and GIS: a case study of the Upper Ewaso Ng'iro North basin of Kenya. *International Journal of Applied Earth Observation and Geoinformation* 2 (2): 78-86.

McBratney AB, Santos MLM, and Minasny B. 2003. On digital soil mapping. *Geoderma* 117 (1-2): 3-52.

McNairn H, Wood D, Gwyn QHJ, Brown RJ, and Charbonneau F. 1998. Mapping tillage and crop residue management practices with RADARSAT. *Canadian Journal of Remote Sensing* 24 (1): 28-35.

Merritt WS, Letcher RA, and Jakeman AJ. 2003. A review of erosion and sediment transport models. *Environmental Modelling & Software* 18 (8-9): 761-799.

Metternicht GI. 1996. Detecting and monitoring land degradation features and processes in the Cochabamba valleys, Bolivia - A synergistic approach. Ph.D. Thesis, University of Ghent, Ghent, Belgium: 389 pp.

Metternicht GI, and Fermont A. 1998. Estimating erosion surface features by linear mixture modeling. *Remote Sensing of Environment* 64 (3): 254-265.

Metternicht GI, and Zinck JA. 1998. Evaluating the information content of JERS-1 SAR and Landsat TM data for discrimination of soil erosion features. *ISPRS Journal of Photogrammetry and Remote Sensing* 53 (3): 143-153.

Miller DM, Kaminsky EJ, and Rana S. 1995. Neural-network classification of remote-sensing data. *Computers & Geosciences* 21 (3): 377-386.

Millington AC, and Townshend JRG. 1984. Remote sensing applications in African erosion and sedimentation studies. *In*: Walling DE, Foster SSD, and Wurzel P (Editors), Challenges in African Hydrology and Water Resources: Proceedings of the Harare symposium. IAHS Publication No. 144. IAHS Press: pp. 373-384.

Millward AA, and Mersey JE. 1999. Adapting the RUSLE to model soil erosion potential in a mountaineous tropical watershed. *Catena* 38 (2): 109-129.

Mitchell CW. 1981. Soil degradation mapping from Landsat imagery in North Africa and the Middle East. *In*: Allan JA, and Bradshaw M (Editors), Remote Sensing in Geological and Terrain Studies. Remote Sensing Society, London, UK: pp. 49-68.

Moran MS, Hymer DC, Qi J, and Kerr Y. 2002. Comparison of ERS-2 SAR and Landsat TM imagery for monitoring agricultural crop and soil conditions. *Remote Sensing of Environment* 79 (2-3): 243-252.

Morgan KM, and Napela R. 1982. Application of aerial photographic and computer analysis to the USLE for areawide erosion studies. *Journal of Soil and Water Conservation* 37 (6): 347-350.

Morgan RPC. 1995. Soil erosion and conservation. Longman Group, Essex, UK: 198 pp.

Morgan RPC, Morgan DDV, and Finney JJ. 1984. A predictive model for the assessment of erosion risk. *Journal of Agricultural Engineering Research* 30 (3): 245-253.

Müschen B, Flügel WA, Hochschild V, Steinnocher K, and Quiel F. 2001. Spectral and spatial classification methods in the ARSGISIP project. *Physics and Chemistry of the Earth, Part B: Hydrology, Oceans and Atmosphere* 26 (7-8): 613-616.

Nagler PL, Daughtry CST, and Goward SN. 2000. Plant litter and soil reflectance. *Remote Sensing of Environment* 71 (2): 207-215.

Nearing MA, Govers G, and Norton LD. 1999. Variability in soil erosion data from replicated plots. *Soil Science Society of America Journal* 63 (6): 1829-1835.

Nearing MA, Pruski FF, and O'Neal MR. 2004. Expected climate change impacts on soil erosion rates: a review. *Journal of Soil and Water Conservation* 59 (1): 43-50.

Nellis MD, Harrington-Jr. JA, and Wu J. 1998. Remote sensing of temporal and spatial variations in pool size, suspended sediment, turbidity, and Secchi depth in Tuttle Creek Reservoir, Kansas: 1993. *Geomorphology* 21 (3-4): 281-293.

Paringit EC, and Nadaoka K. 2003. Sediment yield modelling for small agricultural catchments: land-cover parameterization based on remote sensing data analysis. *Hydrological Processes* 17 (9): 1845-1866.

Pelletier RE. 1985. Evaluating nonpoint pollution using remotely sensed data in soil erosion models. *Journal of Soil and Water Conservation* 40 (4): 332-335.

Pelletier RE, and Griffin RH. 1985. Remote sensing techniques for the detection of soil erosion and the identification of soil conservation practices, Proceedings of IGARSS'85. IEEE, University of Massachusetts, Amherst, Massachusetts: pp. 40-45.

Pickup G, and Chewings VH. 1988. Forecasting patterns of soil erosion in arid lands from Landsat MSS data. *International Journal of Remote Sensing* 9 (1): 69-84.

Pickup G, and Nelson J. 1984. Use of Landsat radiance parameters to distinguish soil erosion, stability, and deposition in arid Central Australia. *Remote Sensing of Environment* 16 (3): 195-209.

Pimentel D, Harvey C, Resosudarmo P, Sinclair K, Kurz D, McNair M, Crist S, Shpritz L, Fitton L, Saffouri R, and Blair R. 1995. Environmental and economic costs of soil erosion and conservation benefits. *Science* 267: 1117-1123.

Price KP. 1993. Detection of soil erosion within pinyon-juniper woodlands using Thematic Mapper (TM) data. *Remote Sensing of Environment* 45 (3): 233-248.

Quesney S, Le Hégarat-Mascle S, Taconet O, Vidal-Madjar D, Wigneron JP, Loumagne C, and Normand M. 2000. Estimation of watershed soil moisture index from ERS/SAR data. *Remote Sensing of Environment* 72 (3): 290-303.

Rabus B, Eineder M, A. R, and Bamler R. 2003. The shuttle radar topography mission: a new class of digital elevation models acquired by spaceborne radar. *ISPRS Journal of Photogrammetry and Remote Sensing* 57 (4): 241-262.

Remond A, Beaudoin A, and King C. 1999. SAR imagery to estimate roughness parameters when modelling runoff risk. *International Journal of Remote Sensing* 20 (13): 2613-2625.

Renard KG, Foster GR, Weesies GA, McCool DK, and Yoder DC. 1997. Predicting soil erosion by water: A guide to conservation planning with the Revised Universal Soil Loss Equation. Agricultural Handbook No. 703. US Department of Agriculture: 404 pp.

Reusing M, Schneider T, and Ammer U. 2000. Modelling soil loss rates in the Ethiopian Highlands by integration of high resolution MOMS-02/D2-stereo-data in a GIS. *International Journal of Remote Sensing* 21 (9): 1885-1896.

Ritchie JC, and Cooper CM. 1991. An algorithm for estimating surface suspended sediment concentrations with Landsat MSS digital data. *Water Resources Bulletin* 27 (3): 373-379.

Ritchie JC, Cooper CM, and Yongqing J. 1987. Using Landsat Multispectral Scanner data to estimate suspended sediments in Moon Lake, Mississippi. *Remote Sensing of Environment* 23 (1): 65-81.

Ritchie JC, and Schiebe FR. 2000. Water quality. *In*: Schultz GA, and Engman ET (Editors), Remote Sensing in Hydrology and Water Management. Springer-Verlag, Berlin, Germany: pp. 287-303, 351-352.

Ritchie JC, Schiebe FR, and Cooper CM. 1989. Remote sensing of off-site downstream effects of erosion in freshwater lakes and reservoirs. *Lake and Reservoir Management* 5 (1): 95-100.

Ritchie JC, Schiebe FR, and McHenry JR. 1976. Remote sensing of suspended sediment in surface water. *Photogrammetric Engineering and Remote Sensing* 42 (12): 1539-1545.

Robinove CJ, Chavez PS, Gehring D, and Holmgren R. 1981. Arid land monitoring using Landsat albedo difference images. *Remote Sensing of Environment* 11 (2): 133-156.

Rosen PA, Hensley S, Joughin IR, Li FK, Madsen SN, Rodríguez E, and Goldstein RM. 2000. Synthetic aperture radar interferometry. *Proceedings of the IEEE* 88 (3): 333-382.

Schiebe FR, Harrington-Jr. JA, and Ritchie JC. 1992. Remote sensing of suspended sediments: the Lake Chicot, Arkansas project. *International Journal of Remote Sensing* 13 (8): 1487-1509.

Schoorl JM, Sonneveld MPW, and Veldkamp A. 2000. Three-dimensional landscape process modelling: the effect of DEM resolution. *Earth Surface Processes and Landforms* 25 (9): 1025-1034.

Servenay A, and Prat C. 2003. Erosion extension of indurated volcanic soils of Mexico by aerial photographs and remote sensing analysis. *Geoderma* 117 (3-4): 367-375.

Sharma KD, and Singh S. 1995. Satellite remote sensing for soil erosion modelling using the ANSWERS model. *Hydrological Sciences Journal* 40 (2): 259-272.

Shrimali SS, Aggarwal SP, and Samra JS. 2001. Prioritizing erosion-prone areas in hills using remote sensing and GIS - a case study of the Sukhna Lake catchment, Northern India. *International Journal of Applied Earth Observation and Geoinformation* 3 (1): 54-60.

Siakeu J, and Oguchi T. 2000. Soil erosion analysis and modelling: a review. *Transactions of the Japanese Geomorphological Union* 21 (4): 413-429.

Singh D, Herlin I, Berroir JP, Silva EF, and Meirelles MS. 2004. An approach to correlate NDVI with soil colour for erosion process using NOAA/AVHRR data. *Advances in Space Research* 33 (3): 328-332.

Smith LC, Alsdorf DE, Magilligan FJ, Gomez B, Mertes LAK, Smith ND, and Garvin JD. 2000. Estimation of erosion, deposition, and net volumetric change caused by the 1996 Skeiðarársandur jökulhlaup, Iceland, from synthetic aperture radar interferometry. *Water Resources Research* 36 (6): 1583-1594.

Smith MO, Ustin SL, Adams JB, and Gillespie AR. 1990. Vegetation in deserts: I. A regional measure of abundance from multispectral images. *Remote Sensing of Environment* 31 (1): 1-26.

Smith SJ, Williams JR, Menzel RG, and Coleman GA. 1984. Prediction of sediment yield from Southern Plains grasslands with the Modified Universal Soil Loss Equation. *Journal of Range Management* 37 (4): 295-297.

Solberg R. 1992. Monitoring soil erosion in agricultural fields by ERS-1 SAR, Proceedings of IGARSS'92. IEEE, Houston, Texas: pp. 1356-1359.

Stephens PR, and Cihlar J. 1982. Mapping erosion in New Zealand and Canada. *In*: Johannsen CJ, and Sanders JL (Editors), Remote sensing for resource management. Soil Conservation Society of America, Ankeny, Iowa: pp. 232-242.

Stephens PR, MacMillan JK, Daigle JL, and Cihlar J. 1985. Estimating universal soil loss equation factor values with aerial photography. *Journal of Soil and Water Conservation* 40 (3): 293-296.

Stroosnijder L. 2003. Measurement of erosion: is it possible? In: Gabriels D, and Cornelis W (Editors), Proceedings of the International Symposium on 25 Years of Assessment of Erosion. Ghent University, Ghent, Belgium: pp. 53-59.

Sujatha G, Dwivedi RS, Sreenivas K, and Venkataratnam L. 2000. Mapping and monitoring of degraded lands in part of Jaunpur district of Uttar Pradesh using temporal spaceborne multispectral data. *International Journal of Remote Sensing* 21 (3): 519-531.

Symeonakis E, and Drake N. 2004. Monitoring desertification and land degradation over sub-Saharan Africa. *International Journal of Remote Sensing* 25 (3): 573-592.

Thiam AK. 2003. The causes and spatial pattern of land degradation risk in southern Mauritania using multitemporal AVHRR-NDVI imagery and field data. *Land Degradation & Development* 14 (1): 133-142.

Thornes JB. 1985. The ecology of erosion. *Geography* 70: 222-234.

Toutin T, and Cheng P. 2003. Comparison of automated digital elevation model extraction results using along-track ASTER and across-track SPOT stereo images. *Optical engineering* 41 (9): 2102-2106.

Toutin T, and Gray L. 2000. State-of-the-art of elevation extraction from satellite SAR data. *ISPRS Journal of Photogrammetry and Remote Sensing* 55 (1): 13-33.

Tucker CJ. 1979. Red and photographic infrared linear combinations for monitoring vegetation. *Remote Sensing of Environment* 8 (2): 127-150.

Ulaby FT, Batlivala PP, and Dobson MC. 1978. Microwave backscatter dependence on surface roughness, soil moisture and soil texture: Part 1 - Bare soil. *IEEE Transactions on Geoscience and Remote Sensing* 16 (4): 286-295.

Ulaby FT, Bradley GA, and Dobson MC. 1979. Microwave backscatter dependence on surface roughness, soil moisture and soil texture: Part 2 - Vegetation covered soil. *IEEE Transactions on Geoscience and Remote Sensing* 17 (2): 33-40.

Vaidyanathan NS, Sharma G, Sinha R, and Dikshit O. 2002. Mapping of erosion intensity in the Garhwal Himalaya. *International Journal of Remote Sensing* 23 (20): 4125-4129.

Van der Knijff JM, Jones RJA, and Montanarella L. 2000. Soil erosion risk assessment in Europe, EUR 19044 EN. European Soil Bureau: 34 pp.

Van Deventer AP, Ward AD, Gowda PH, and Lyon JG. 1997. Using Thematic Mapper data to identify contrasting soil plains and tillage practices. *Photogrammetric Engineering and Remote Sensing* 63 (1): 87-93.

Van Engelen V, and Wen TT. 1995. Global and national Soils and Terrain Digital Databases (SOTER): procedures manual. World soil resources reports, 74 Rev. 1. FAO, Rome, Italy: 125 pp.

Van Lynden GWJ, and Mantel S. 2001. The role of GIS and remote sensing in land degradation assessment and conservation mapping: some user experiences and expectations. *International Journal of Applied Earth Observation and Geoinformation* 3 (1): 61-68.

Van Rompaey AJJ, and Govers G. 2002. Data quality and model complexity for regional scale soil erosion prediction. *Geomorphology* 16 (7): 663-680.

Vrieling A, and Rodrigues SC. 2004. Erosion assessment in the Brazilian Cerrados using multi-temporal SAR imagery, Proceedings of the 2004 Envisat & ERS Symposium. SP-572. ESA, Salzburg, Austria.

Vrieling A, Sterk G, and Beaulieu N. 2002. Erosion risk mapping: a methodological case study in the Colombian Eastern Plains. *Journal of Soil and Water Conservation* 57 (3): 158-163.

Walker JP, Houser PR, and Willgoose GR. 2004. Active microwave remote sensing for soil moisture measurement: a field evaluation using ERS-2. *Hydrological Processes* 18 (11): 1975-1997.

Wang G, Gertner G, Fang S, and Anderson AB. 2003. Mapping multiple variables for predicting soil loss by geostatistical methods with TM images and a slope map. *Photogrammetric Engineering and Remote Sensing* 69 (8): 889-898.

Wang G, Wente S, Gertner GZ, and Anderson A. 2002. Improvement in mapping vegetation cover factor for the universal soil loss equation by geostatistical methods with Landsat Thematic Mapper images. *International Journal of Remote Sensing* 23 (18): 3649-3667.

Warren A. 2002. Land degradation is contextual. *Land Degradation & Development* 13 (6): 449-459.

Wegmüller U, Strozzi T, Farr T, and Werner CL. 2000. Arid land surface characterization with repeat-pass SAR interferometry. *IEEE Transactions on Geoscience and Remote Sensing* 38 (2): 776-781.

Wischmeier WH, and Smith DD. 1978. Predicting rainfall-erosion losses: A guide to conservation planning. Agricultural Handbook No. 537. US Department of Agriculture.

Young RA, Onstad CA, Bosch DD, and Anderson W. 1989. AGNPS: a nonpoint-source pollution model for evaluating agricultural watersheds. *Journal of Soil and Water Conservation* 44 (2): 168-173.

Yuliang Q, and Yun Q. 2002. Fast soil erosion investigation and dynamic analysis in the Loess Plateau of China by using information composite technique. *Advances in Space Research* 29 (1): 85-88.

Zhang X. 1999. Soil erosion modelling at the global scale using remote sensing and GIS. Ph.D. Thesis, University of London, London, UK.

Zhang X, Drake N, and Wainwright J. 2002. Scaling land surface parameters for global-scale soil erosion estimation. *Water Resources Research* 38 (9): 19(1)-19(9).

Zhou Q, Robson M, and Pilesjö P. 1998. On the ground estimation of vegetation cover in Australian rangelands. *International Journal of Remote Sensing* 19 (9): 1815-1820.

Chapter 3

AUTOMATIC IDENTIFICATION OF
EROSION GULLIES WITH ASTER IMAGERY
IN THE BRAZILIAN CERRADOS

Vrieling A, Rodrigues SC, Bartholomeus H, and Sterk G

3. Automatic identification of erosion gullies with ASTER imagery in the Brazilian Cerrados

Abstract

Gully erosion is a serious problem at many locations worldwide, but little is known about its importance at large spatial scales. The remote sensing contribution for the spatial assessment of gullies has thus far been confined to visual image interpretation. This study was conducted to determine whether automatic classification of optical ASTER imagery could accurately discern permanent erosion gullies in the Brazilian Cerrados. A maximum likelihood classifier (MLC) was trained with two classes, gullies and non-gullies, and applied to images of March (wet season) and August (dry season). Moreover, a bi-temporal classification was performed by labelling a pixel as gully when both for the March and August image it was classified as such. Validation was done with a gully map obtained from a panchromatic QuickBird image and field data. For mono-temporal classification, the March image performed much better than the August image, because spectral differences are more pronounced during the wet season. Based on spatial analysis of output maps, the bi-temporal classification performed best in identifying gullies, as user's accuracy was above 90%, while two of 17 actual gullies were not detected and two small locations were erroneously identified as gully. The combination of ASTER bands 1, 2, 3, and 4 gave highest accuracies. It is concluded that accurate automatic identification of permanent gullies is possible with optical satellite data. Because the Cerrados occupy a vast area, it is expected that the approach presented could be applied to larger areas with similar characteristics.

3.1   Introduction

Erosion gullies are important sources of sediments in reservoirs, while they reduce agricultural land and form a threat to infrastructures like roads. Gully initiation is usually triggered by land use changes (Valentin et al., 2005), thus reducing infiltration and increasing runoff which accumulates in narrow channels and consequently incises the soil profile. When incisions are shallow, ploughing operations may remove them (ephemeral gullies), but when incisions are deeper, gullies become permanent features in the landscape. Although many studies have addressed gully erosion, little is known about its importance at larger spatial scales (Poesen et al., 2003).

The major contribution of remote sensing to gully erosion assessment has been the visual interpretation of aerial photography. Gully limits are delineated from aerial photographs and gully retreat rates are assessed using multi-temporal comparison (e.g. Daba et al., 2003; Vandekerckhove et al., 2003). However, the size of the regions studied is generally small. Satellite imagery can be used to evaluate the importance of gully erosion at

larger spatial scales. Mostly this has been done through classification of large areas suffering from gully erosion, called badlands (Vrieling, 2006).

Identification of individual gullies with satellite data has also been suggested (e.g. Langran, 1983), but accurate identification was judged impossible without additional data or expert knowledge (Bocco and Valenzuela, 1993). This can be attributed to the spectral heterogeneity of the gullies themselves (including natural vegetation, bare soil, shadows) as well as the heterogeneity of their environment (King et al., 2005; Zinck et al., 2001). However, it remains questionable whether this necessarily prohibits automatic gully retrieval in all environments and for all gully types. In different environments worldwide, permanent erosion gullies of large spatial sizes (>10m wide) and considerable depth (>5m) occur (Bocco, 1991; Poesen et al., 2003). Such gullies may possess distinct spectral characteristics due to e.g. exposed subsoil and bedrock, shadows from gully walls, and a permanently moist gully bottom.

Automatic identification of erosion gullies may contribute to the understanding of why and where gully erosion occurs. Furthermore, an automatic method may provide fast insight in the importance of gully erosion and the consequent loss of productive land for large regions. This study was conducted to evaluate whether automatic classification of ASTER imagery can accurately identify permanent erosion gullies within the Brazilian Cerrados.

3.2   Materials and methods

3.2.1 Study area

The Brazilian Cerrados are a natural savannah ecosystem originally consisting of grassland, shrubland, and woodland, occupying nearly 23% of Brazil (Furley, 1999). During the past 35 years the ecosystem experienced strong impacts from the expansion of agriculture, cattle raising and forestry. It was estimated that approximately 40% of the Cerrados has currently been converted to human land uses (Ferreira and Huete, 2004). A major negative environmental impact of these land conversions has been soil erosion including the development of large erosion gullies (Rodrigues, 2002).

The study area is located near the city of Uberlândia in Minas Gerais (Fig. 3.1). It has a humid tropical climate with rainfall occurring from November to April. Topography is slightly undulating with slope angles of 0-15%. Soils are deep (up to 25 m) and consist predominantly of loamy sand. Large erosion gullies occur in the area (Fig. 3.2), with gully depths ranging from 4 to 25 m, thus reaching the bedrock. Several gullies initiated more than 50 years ago, but are still active. They most likely initiated due to increased drainage by road construction, parcelling of properties by ditches, and land conversions. The current vegetation cover is dominated by pastures, often with scattered trees and shrubs. Most pastures are degraded and their vegetation cover can be minimal including bare patches. Furthermore shrubland, woodland, and gallery forest is present in the area. A 16-km^2 area
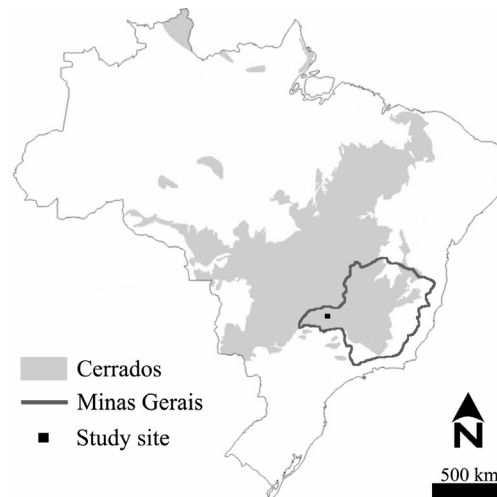
Figure 3.1   Location of the study site in Brazil (map source: EMBRAPA)

was selected for method development, and an adjoining 36-km^2 area for independent validation (Fig. 3.3). Both areas have similar characteristics in terms of land cover types and contain several large gullies.

3.2.2 Data and pre-processing

ASTER (Advanced Spaceborne Thermal Emission and Reflection Radiometer) imagery from the Terra-satellite was selected for this study, because of the good spatial resolution – 15 m in the three visible and near infrared (VNIR) bands – in combination with considerable spectral information, including six 30-m resolution bands in the shortwave infrared (SWIR). Moreover, the reasonable image swath (60 km) may allow gully identification over wide

Figure 3.2   Example of a large erosion gully within the study area (picture taken in July 2002, dry season)
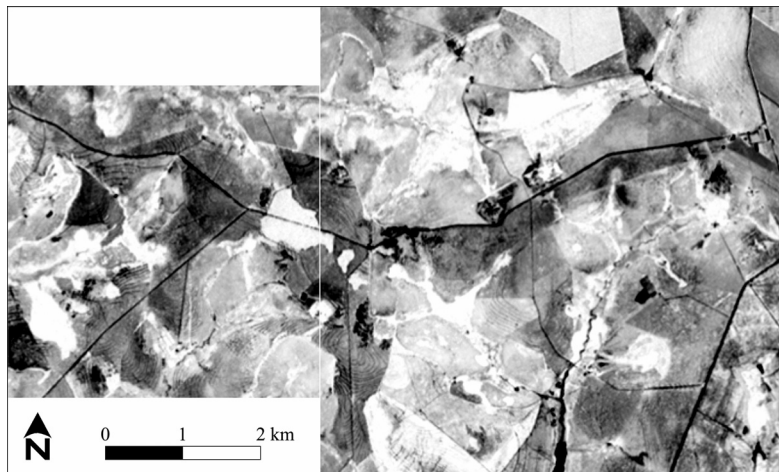
*Figure 3.3   Study area divided in a 16-km^2 training area (left quadrant) and a 36-km^2
validation area (right quadrant). The figure shows the NDVI of the ASTER March
image, linearly scaled between 0.40 (black) and 0.90 (white).*

regions, as opposed to high-resolution (about 1-m) data. Table 3.1 summarizes the
characteristics of the ASTER spectral bands. The five ASTER thermal infrared bands were
not used in this study. Surface reflectance products of VNIR and SWIR (AST_07: Thome et
al., 1999) were acquired for the wet season (4 March 2003) and the dry season (11 August
2003). The two ASTER scenes were geocoded using a panchromatic orthorectified
QuickBird image acquired on 4 August 2003. A first-order polynomial model was applied
and cubic convolution resampling to a 12.5-m pixel size was performed for all bands,
resulting in a positional accuracy of less than 10 m.

Reference data on gully location and extent were obtained during fieldwork
performed in January 2004, and from the QuickBird image. Potential gullies were identified
on the QuickBird image for the 16-km^2 and 36-km^2 areas, and their existence was
subsequently confirmed in the field using a GPS. Limits of actual gullies were then

Table 3.1   Characteristics of ASTER VNIR and SWIR spectral bands

Spectral domain	Resolution	Spectral band	Spectral range (μm)
VNIR	15 m	1	0.52 - 0.60
		2	0.63 - 0.69
		3	0.76 - 0.86
SWIR	30 m	4	1.600 - 1.700
		5	2.145 - 2.185
		6	2.185 - 2.225
		7	2.235 - 2.285
		8	2.295 - 2.365
		9	2.360 - 2.430

delineated by means of visual interpretation of the QuickBird image. Besides, representative samples of other land cover classes were determined with the same procedure, including: bare soil, pasture, degraded pasture, shrubland, woodland, and gallery forest. These land cover classes were merely used for analysing their spectral signatures in comparison to the gullies' spectral signature, as to understand why gullies may be detected in the study area. Because of potential human activities, a check of both ASTER images was performed to ascertain that the land cover classes actually existed at the selected locations both in March and in August 2003.

3.2.3 Gully identification

Identifying gullies from satellite imagery is a form of feature extraction. A variety of methods exist for extracting features from multi-spectral images. Here we used the supervised classification approach of the maximum likelihood classifier (MLC), based on only two classes: gullies and non-gullies. This method was chosen, because:

- the training procedure accounts for spectral variability within the gully class and for the background variability,
- there is no need for extensive training, because only two classes are used,
- there is no need to set subjective thresholds,
- results can be reproduced for different scenes, unlike unsupervised classification methods whose results depend on specific scene characteristics,
- it is difficult or impossible to assign one representative signature or pixel for the gully class, which is required for methods like linear spectral unmixing (Adams et al., 1986) and spectral angle mapping (Kruse et al., 1993).

The statistics for the MLC classes were derived from the 16-km^2 (4 by 4 km) area. In this area seven gullies are present. The gully training set consisted of a subset of ASTER pixels located fully within the gully limits digitized from the QuickBird image. The non-gully training set is a big class consisting of all pixels fully outside these limits. For both classes, the probability density function $P(X|w_i)$ which gives the probability that a pixel belongs to class w_i is calculated using:

$$P(X \mid w_i) = \frac{1}{(2\pi)^{n/2}|V_i|^{1/2}} \exp\left[-1/2(X - M_i)^T V_i^{-1}(X - M_i)\right] \qquad (3.1)$$

where X is the pixel's data vector in all spectral bands, n is the number of spectral bands, M_i is the mean vector for class w_i, and V_i is the variance-covariance matrix for class w_i (Jensen, 2004). A pixel is classified as gully when the probability for that pixel being a gully is higher than the probability of belonging to the non-gully class.

The MLC was applied separately to the March-image and the August-image, resulting in two maps showing classified gully pixels in the 36-km^2 (6 by 6 km) validation area. A sieve filter was applied to remove small isolated pixel groups smaller than three pixels. Subsequently, using the logical *AND* the two maps were combined creating the March-August (MA) classification. For the MA classification, a pixel is therefore labelled as a gully if for both the March and the August scene it was classified as gully.

This procedure was repeated for several spectral band combinations with the aim of improving classification results. The rationale for testing other band combinations is that highest feature separability (and thus classification accuracy) does not necessarily result from the maximum number of bands (e.g. Metternicht and Zinck, 1997). For nine spectral bands, 511 possible band combinations exist. Because it is impracticable to test all 511 combinations, band selection was performed to obtain a subset of potentially good band combinations. These potentially good combinations were assessed separately for the individual March and August scenes, using statistics calculated from the 16-km^2 calibration area. The following common band selection methods were applied for this purpose:

- The correlation-variance (CV) method. Correlation between all different pairs of spectral bands and the variance of each individual band is calculated. For the two highest-correlating bands, the one with the lowest variance is removed from the selection. This is repeated until the desired number of bands remains.
- The Jeffries-Matusita (JM) distance calculated between the gully and the non-gully training set (Jensen, 2004). For the desired number of bands, the band combination with the highest JM-distance is selected.
- The Transformed Divergence (TD) calculated between the gully and the non-gully training set (Jensen, 2004). For the desired number of bands, the band combination with the highest TD is selected.

If for example the desired number of bands is set at four, six potentially good band combinations may be found, i.e. three selection methods (CV, JM, and TD) applied to two scenes (March and August). In practice however, different methods may select the same band combination, or the same method may select the same band combination for both images. A specific band combination selected for one scene (e.g. March) was also applied to the other scene (August) and combined to create the MA gully map for that band combination. The number of bands used in this study ranges from three to nine.

3.2.4 Validation

The gully classifications were validated using the reference gullies obtained from the QuickBird image in the 36-km^2 area. The digitized gullies were converted to the same 12.5-m raster format as the ASTER scenes. The total number of gullies was 17 covering an area of about 46 ha (1.27% of the validation area). The accuracy of each classification was

determined using merely the gully class, because the number of non-gully pixels was very large compared to the number of gully pixels. Inclusion of non-gully pixels would therefore excessively influence common accuracy measures like the overall accuracy or the kappa statistic (Congalton, 1991). Instead, a good gully classification should meet two criteria:

1. Most of the actual gully pixels in the reference data are also classified as being gully. This implies a high producer's accuracy (A_p).
2. As few as possible actual non-gully pixels are classified as gully. This means that the user's accuracy (A_u) is high for the gully class.

Both criteria are considered important. To obtain the best result for the combination of both criteria, here we propose to use the average accuracy (A_a) as an additional measure. A_a is defined as the average of A_u and A_p and is not intended to represent the overall accuracy of the classification, but is merely used to determine which of the band combinations results in the optimal classification. The accuracy measures used can thus be expressed as:

$$A_u = \frac{G_c}{G_t} \tag{3.2}$$

$$A_p = \frac{G_c}{G_r} \tag{3.3}$$

$$A_a = \frac{A_u + A_p}{2} \tag{3.4}$$

where G_c is the number of pixels correctly classified as gully, G_t is the total number of pixels classified as gully, and G_r is the number of gully pixels in the reference data.

Besides the area-based accuracy assessment, resulting maps with the highest accuracies were visually compared to the reference map to understand which actual gullies are detected and which locations are erroneously assigned to the gully class.

3.3   Results and discussion

3.3.1 Spectral signatures

Fig. 3.4 shows average spectral signatures for gullies and three other land cover classes that are found to be most similar to gullies, including bare soil, degraded pasture, and shrubland. The relatively high reflectance for band 9 is probably caused by instrument problems (Rowan and Mars, 2003), but because the effect is similar for different land uses, MLC results will not be affected.
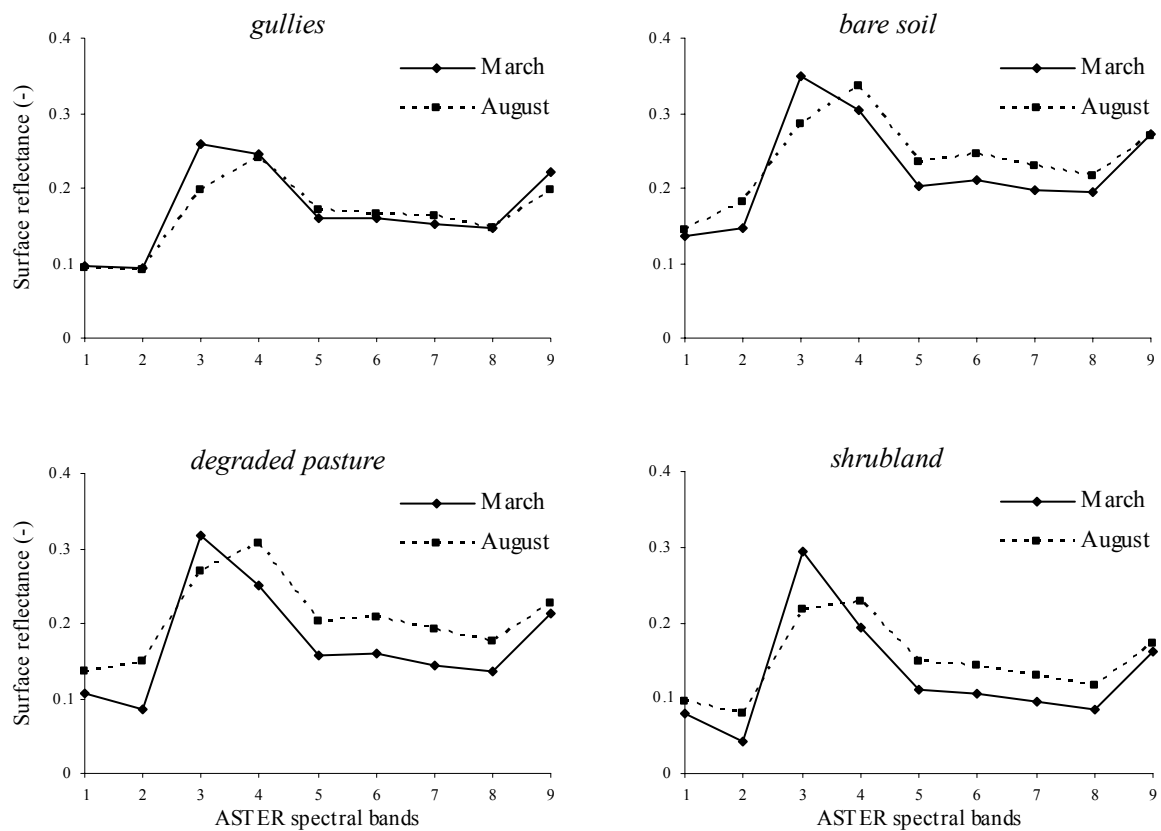
Figure 3.4   Spectral signatures of gullies, bare soil, degraded pasture, and shrubland for ASTER scenes of March and August 2003

From Fig. 3.4, it can be observed that the overall reflectance of gullies is generally low compared to normal bare soil. Knowing that an important fraction of the gullies is also bare soil, the low reflectance can be attributed to several factors: a higher moisture content (Baumgardner et al., 1985), a higher iron content in the subsoil (EMBRAPA, 1982; Stoner and Baumgardner, 1981), and presence of a shadow component caused by the gully depth and the irregular surface (Metternicht and Zinck, 1998). The wet-season (March) signature of degraded pasture is to some extent similar to the gullies signature, but pasture has a higher NIR reflectance (band 3) due to the vegetation. Shrubland also has a higher NIR reflectance and moreover lower red and SWIR reflectances, but during the dry season (August) its signature is rather similar to gullies. In general the differences between gullies and the other land cover classes are more pronounced in March.

Furthermore the spectral graphs show that gully reflectance is more constant over time as compared to other land cover classes. This should probably be attributed to:

1. the general moist conditions of the gully bottom, also during the dry season;
2. the steep gully walls, and active sidewall erosion processes during the wet season, impeding normal vegetation development.

This does however not imply that vegetation development does not occur in gullies during the wet season, which is shown by the higher NIR reflectance in March.

Identification of gullies with ASTER imagery seems to be feasible following the comparison of spectral signatures. The March-image (wet-season) is most promising for mono-temporal identification, because spectral differences are more pronounced. Bi-temporal identification using both images may however be more valuable to limit misclassifications, by exploiting the fact that gullies generally have a more stable spectral signature through time than its surroundings.

3.3.2 Gully identification results

Gully identification was performed with the MLC for 25 different spectral band combinations. Table 3.2 shows the band combinations used and the method(s) that selected each specific combination (CV, JM, and TD). Band 3 is the only spectral band present in all combinations, mostly likely because the gully reflectance for this spectral range is generally lower than the reflectance of all other land use types, which is not the case for the other spectral bands (Fig. 3.4). For each combination, a March, an August, and a MA gully map were constructed. Comparison with the reference gully map, generated from the QuickBird image and field data, yielded the accuracies A_u, A_p, and A_a (Table 3.2). A clear relation between the method selecting a specific band combination and the accuracy does not exist. E.g. for March the highest A_u and A_a for a six-band combination is a combination selected by JM and TD using the August image. Nevertheless, these band selection methods generated a reasonable and workable subset of promising spectral band combinations for detecting gullies in the study area. From Table 3.2 statements on whether CV, JM, or TD is better for spectral band selection cannot be made, but this was not a purpose of this study.

Table 3.2 demonstrates that A_u and A_a are considerably higher for the March image as compared to the August image, which supports the observation made in Section 3.3.1 that spectral differences are more pronounced in March. The higher A_p for the August image indicates that more actual gully pixels are correctly classified, but following the low A_u it shows that this is mostly a consequence of the fact that a much larger area is also erroneously classified as gully. As stated in Section 3.2.4, a good classification has both a low fraction of non-gullied area classified as gullies (high A_u) and a large area of the actual gullies classified as such (high A_p). The average accuracy A_a is used to define this optimum. A_a is highest (0.75) for the March image using the band combination '1,2,3,4'. For this classification, 64% of the actual gully pixels are classified as gully, whereas in 87% of the cases a classified gully pixel is actually part of a gully. For the best August classification (using bands '1-4,6,7,8') these values are 64% and 60% respectively.

The bi-temporal MA classification can by its definition not have a higher A_p than the individual classifications, because a gully pixel is only a gully pixel when this is the case for both the March and August classification. Nevertheless, the A_u increases due to this condition and reaches values of above 90%. Although the highest A_a for MA (0.74 for band combination

Table 3.2   *Selected ASTER band combinations and corresponding accuracy values: M=March image; A=August image; MA=March and August combined. Band selection methods are: CV=Correlation/variance method; JM=Jeffries-Matusita distance; TD=Transformed Divergence distance. Grey cells indicate the highest accuracy level for the specific column (taking into account also the third decimal).*

Spectral bands			User's accuracy (A_u)			Producer's accuracy (A_p)			Average accuracy (A_a)		
#	combination	selected by:	M	A	MA	M	A	MA	M	A	MA
9	1-9	-	0.79	**0.63**	**0.94**	0.53	0.60	0.43	0.66	0.61	0.68
8	1-4,6-9	*CV/JM/TD* A/M	0.85	0.60	0.93	0.53	0.63	0.44	0.69	0.61	0.68
7	1-4,6,7,8	*JM* A	0.88	0.60	0.93	0.57	0.64	0.48	0.72	**0.62**	0.70
	1-4,6,7,9	*JM/TD* M, *CV* A	0.87	0.52	0.93	0.55	0.64	0.46	0.71	0.58	0.69
	1-4,6,8,9	*CV* M	0.86	0.57	0.92	0.55	0.64	0.47	0.70	0.60	0.69
	1,3,4,6-9	*TD* A	0.89	0.55	0.93	0.51	0.65	0.45	0.70	0.60	0.69
6	1,2,3,4,6,7	*JM* M	0.85	0.54	0.93	0.60	0.66	0.51	0.72	0.60	0.72
	1,2,3,4,6,9	*CV* A/M	0.83	0.30	0.92	0.62	0.67	0.52	0.72	0.48	0.72
	1,2,3,4,7,9	*TD* M	0.80	0.43	0.93	0.57	0.66	0.48	0.68	0.55	0.71
	1,3,4,6,7,8	*JM/TD* A	0.89	0.54	0.93	0.57	0.67	0.50	0.73	0.60	0.72
5	1,2,3,4,6	*CV* A	0.90	0.27	0.92	0.51	0.58	0.43	0.71	0.43	0.67
	1,2,3,4,9	*CV* M	0.89	0.29	0.92	0.50	0.60	0.41	0.69	0.44	0.66
	1,2,3,6,7	*JM* M	**0.90**	0.47	0.93	0.54	0.60	0.43	0.72	0.53	0.68
	1,3,4,6,8	*JM/TD* A	0.89	0.55	0.93	0.52	0.62	0.45	0.71	0.58	0.69
	1,3,4,7,9	*TD* M	0.88	0.37	0.93	0.48	0.63	0.42	0.68	0.50	0.67
4	1,2,3,4	*CV* M	0.87	0.26	0.92	**0.64**	0.67	**0.55**	**0.75**	0.47	**0.74**
	1,3,4,7	*TD* M	0.87	0.35	0.93	0.55	0.68	0.50	0.71	0.52	0.71
	2,3,4,6	*CV* A	0.83	0.20	0.90	0.61	0.66	0.51	0.72	0.43	0.71
	2,3,6,7	*JM* M	0.83	0.28	0.90	0.63	0.67	0.53	0.73	0.48	0.72
	3,4,6,8	*JM/TD* A	0.83	0.49	0.91	0.60	0.67	0.53	0.72	0.58	0.72
3	1,3,4	*CV* M	0.72	0.15	0.84	0.63	0.67	0.55	0.68	0.41	0.69
	2,3,4	*CV* A	0.76	0.19	0.84	0.63	0.67	0.54	0.70	0.43	0.69
	2,3,7	*TD* M	0.85	0.15	0.92	0.61	0.63	0.50	0.73	0.39	0.71
	3,6,7	*JM* M	0.85	0.25	0.90	0.61	**0.69**	0.52	0.73	0.47	0.71
	3,6,8	*JM/TD* A	0.83	0.38	0.90	0.61	0.68	0.53	0.72	0.53	0.72

'1,2,3,4') is slightly lower than for the best March classification, A_u is 92% in this case, implying that only 8% of the pixels are erroneously labelled as gullies, whereas still 55% of all gully pixels are classified as such. Therefore, depending on the purpose of gully identification, the combination of classifications from different image acquisition dates can be useful because the reliability of a pixel being correctly assigned to the gully class increases. This may be important e.g. when using the gully map acquired for deriving empirical relationships between gully occurrence and controlling factors derived from additional spatial data sources.

Band combination '1,2,3,4' gives best results both for mono-temporal and bi-temporal gully identification. This indicates that optimal identification can be obtained using spectral data from the visible, NIR, and SWIR domain. Fig. 3.4 shows that the average spectral signature of gullies is distinct in this domain, especially during March. Band 1 and 2 have a similar reflectance, as well as band 3 and 4. For bi-temporal identification, the August scene is mostly used to reduce false identifications, as August by itself does not allow accurate extraction of gullies. The most important characteristics allowing gully identification therefore seem to be the limited vegetation (low ratio band 1/2 and band 3/2) and the differences of the subsoil as mentioned in Section 3.3.1 (moisture, iron, and shadows) causing a lower reflectance as bare soil. An additional effect which may play a role is the higher spatial resolution of bands 1, 2, and 3, resulting in less spectral mixing than for the other bands. Information in bands 5 to 9 seems to be redundant and does not increase the separability of gullies from their environment.

Besides analysing how many pixels are correctly classified, it is of interest to determine spatially which pixels and gullies are detected. Fig. 3.5 shows the gully maps corresponding with the highest A_a's of the March, the August, and the MA classifications, and furthermore the reference gully map (Fig. 3.5a). It is clear from Fig. 3.5c that the A_u of the August map is much lower, because many non-gully areas are erroneously classified. The March map (Fig. 3.5b) is a lot better: 16 out of 17 actual gullies are detected (only missing gully #16), however also 14 non-existing small gullies are identified. The MA gully map (Fig. 3.5d) is a combination of Fig. 3.5b with an August classification based on the band combination '1,2,3,4' (not presented in figure). Comparing the MA map to the March map, the number of actual gullies identified reduces from 16 to 15 (gully #1 and #16 are not present in the MA map) which is a slight reduction, but more importantly the number of non-existing small gullies detected is reduced to only two. From field observations it is known that these two locations are sedimentation areas just upstream of a large reservoir. Soil material from the gullies is detached and transported by active gully erosion, and subsequently deposited at these locations that are generally moist, resulting in a similar spectral behaviour. The spatial analysis shows that the MA map outperforms the March map in terms of number of gullies correctly classified, because only two locations are wrongly identified as gullies and most of the actual gullies are detected.

Despite the good performance of the MA map, several gully parts and entire gullies remain unidentified. A good example is gully #16, which is absent in all classifications. The reasons are first that this gully is narrow (< 15m) complicating identification due to mixed pixels, and second that abundant trees grow in and around it. Therefore, the gully has low activity, implying that further erosion of the gully is minimal, and thus the distinct characteristic of exposed bare subsoil is not dominant and moreover concealed by tree crowns. The presence of many trees in and around parts of other gullies is also the chief reason for not classifying these gully parts (e.g. gully #10, #14, #15), judging from overlaying the detected gullies with the QuickBird image. In this respect it can be expected that A_p and consequently A_a increase when focussing solely on gully parts with active
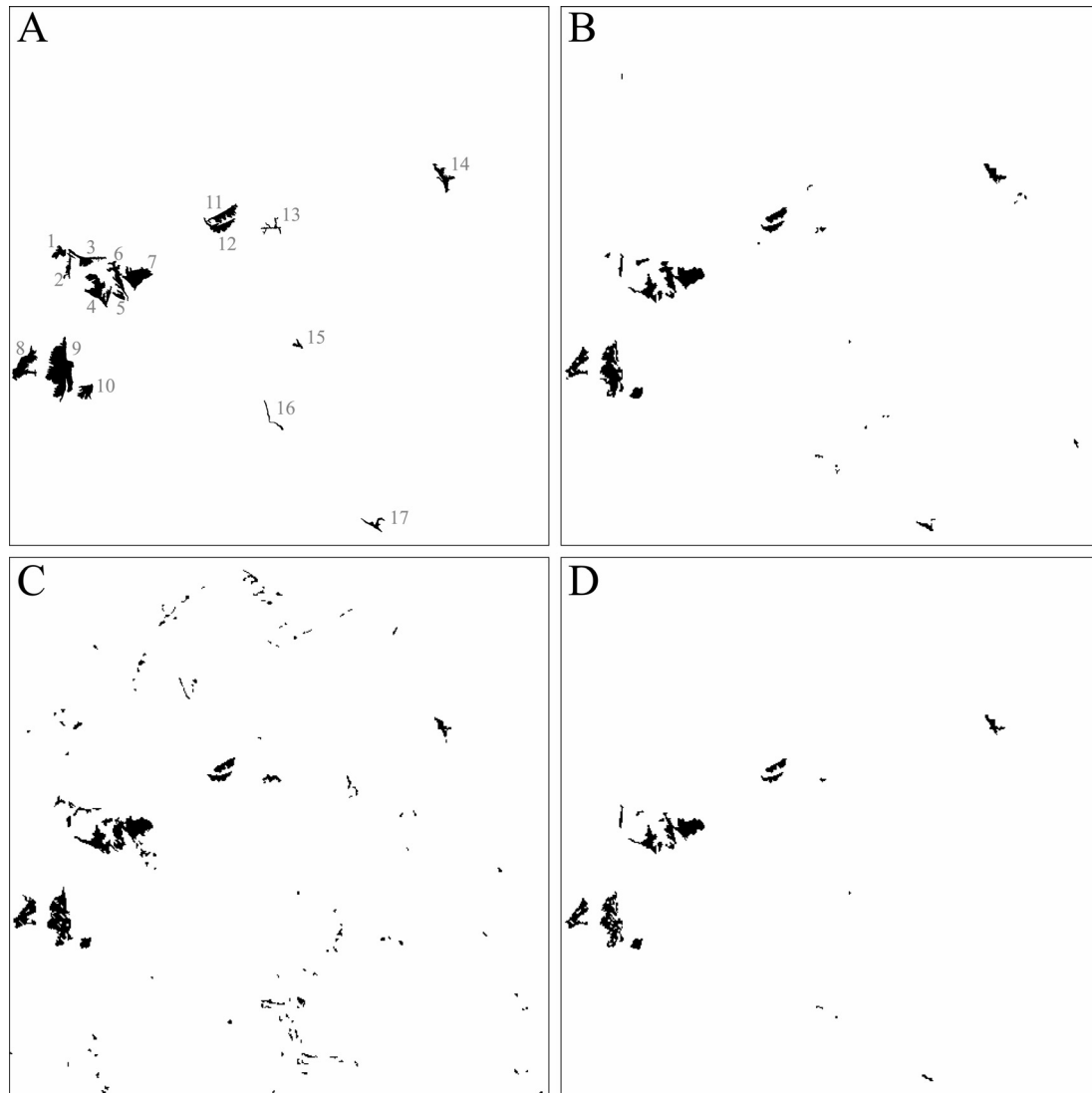
Figure 3.5   *Gully detection with ASTER imagery in 36-km² validation area. (A) Reference data acquired from QuickBird image and field data, gully numbers refer to the text; (B) detected gullies from March image, bands 1-4; (C) detected gullies from August image, bands 1-9; (D) detected gullies from combined March and August, bands 1-4.*

erosion. However, the activity of gully parts cannot be objectively determined based merely on one QuickBird image, and does moreover depend on the time scale. Therefore, in this study no distinction was made between more or less active gully parts for the accuracy assessment.

The areal extent affected by gullies is underestimated as a result of the failure to identify certain gullies and gully parts, as mentioned above. The reference data show that 1.27% of the validation area is covered by gullies, versus 0.95% for the March classification, and 0.76% for the MA classification. Probably here also gully activity plays a role, and the estimation may improve if it were done only for the active parts.

3.3.3 General discussion

A two-class MLC proved to be a good method for extracting erosion gullies in the study area. Usually a MLC is applied for land use classification where each pixel in the image should belong to a specific land use class. Here, MLC is applied for extracting one specific class from an image by training the classifier with a gully class and a very general class of any pixel falling outside the gully boundaries. Subsequent analysis showed that the training set for the latter class could also be replaced by all pixels in the scene, thus including gully pixels as well. This way an average scene class is formed and compared with the gully spectral statistics. The results appeared to be practically the same due to the very small number of pixels in the gully class, as compared to the non-gully class. The only training involved would then be the definition of a set of known gully pixels. No references were found in literature for this special application of the MLC.

The methodology may be adapted to enhance specific gully spectral and temporal characteristics prior to classification. One option for this relates to the statement made in Section 3.3.1 that the gully reflectance is more constant over time as compared to other land cover types. For each band, the difference in reflectance between March and August could be calculated and used in the classification procedure. Another option is to calculate spectral indices and use those in the classification. Potential indices include the normalized difference vegetation index (NDVI), the Infrared Index (II: Hardisky et al., 1983) or the ferric index (Madeira et al., 1997). NDVI and II would be substantially lower for gullies than for most other land cover types, whereas the ferric index would be higher. Here, we chose not to make any enhancements prior to classification to maintain a simple and straightforward analysis procedure. Moreover, classification without further enhancements provided good results.

The gully identification methodology of this study may be applied to imagery acquired by different satellites. Landsat TM, ETM+, and SPOT-5 for example have the same spectral bands as the best-performing set of spectral bands selected here (ASTER bands 1-4). For lower spatial resolutions (Landsat) more spectral mixing problems will occur, whereas SPOT-5 data may result in better gully identification due to its higher resolution. Very-high resolution data (IKONOS, QuickBird) has limited spectral information and little spatial coverage, and is therefore considered inappropriate for large-scale automatic gully identification.

Fusion of synthetic aperture radar (SAR) and optical data can in some cases enhance classification accuracies. For example Metternicht and Zinck (1998) achieved higher accuracies for classifying badlands and other eroded areas in the Bolivian Andes when combining JERS-1 L-band data (23 cm wavelength) with Landsat TM, as compared to Landsat TM alone. For the study area, fusion with ENVISAT Advanced SAR (ASAR) C-band (5.6 cm wavelength) was tested, but did not provide better classification results. This can be attributed to the side-looking nature of radar systems, and the steep gully walls causing in some instances radar shadows (no signal received) and at other occasions a very high return signal due to double bounce mechanisms, depending on the gully orientation.

Furthermore the radar backscatter of gullies changes substantially during time and much confusion with other features in the environment exists (Vrieling and Rodrigues, 2004).

Assessing gully retreat rates from ASTER-derived gully maps will be difficult, if not impossible, knowing that the method presented does not allow identification of all gully parts. Moreover, reported gully retreat rates in the area do not exceed 5 m year^{-1} (Baccaro, 1999), which is less than the ASTER resolution. Even if ASTER imagery would be available for longer time-series (> 10 years), the gully identification method does not provide a very accurate delineation of gully boundaries. Only major changes (>100 m) and the establishment of new gullies may therefore potentially be identified.

A major question remaining is how information on gully identification may contribute to the understanding of where and why gully erosion occurs, as stated in the introduction. Where gully erosion occurs, can be assessed by overlaying the identified gullies with additional information sources like DEMs, lithology and land use maps, etc. (e.g. Bocco and Valenzuela, 1993). For this region one of the conclusions would then be that most gullies are situated near the drainage divides and are generally encountered in the vicinity of roads. Statistical analysis for larger areas using a variety of spatial information layers can result in significant correlations between gully occurrence and controlling factors, which provides insight in why gully erosion takes place at these locations. Models of gully erosion can thus be created (Poesen et al., 2003) that could also assist in predicting what may happen if land use changes. Potentially such models may then be linked to spatially-explicit land use change models (Veldkamp and Lambin, 2001), and thus allow predictions on effects of global warming or human disturbances on gully erosion.

Before gully erosion models can be created using ASTER-based gully identification, the methodology should be applied to larger regions (more than 1000-km^2). An important issue is therefore up-scaling, i.e. can the method be applied to larger regions within the Cerrados? A clear answer to this question cannot be given at this stage. Nevertheless, the Cerrados have a very large spatial extent of around two million km^2. Although substantial differences exist between regions (e.g. differences in rainfall amounts, land use, lithology, and gully types), vast areas of the Cerrados are to a greater or lesser extent similar to the study site and comparable large gullies can be found at many locations (Motta et al., 2002). In any case, this study showed that despite the heterogeneity of gullies and their surroundings (King et al., 2005; Zinck et al., 2001), permanent gullies within the Cerrados may possess sufficient spectral homogeneity to allow their accurate automatic detection with optical satellite data.

3.4   Conclusions

Automatic identification of gullies with satellite data is possible for certain areas in the Cerrados. This study showed that a simple MLC with ASTER data using only two classes was effective for discriminating gullies in a 36-km^2 area. The only training required is the

identification of a number of known gully areas. Wet-season imagery gave the best performance for mono-temporal classification. However, when combining a wet-season with a dry-season classification into a single map, user's accuracy increased to above 90%, while only at two locations small non-existing gullies were identified and two of 17 actual gullies were not detected. Based on a combination of area-based and spatial validation, it is concluded that bi-temporal classification is the best approach for extracting gullies within the Brazilian Cerrados. The spectral band combination used has a strong effect on the results. Highest overall accuracies in this study were obtained with ASTER bands 1, 2, 3, and 4, both for the mono-temporal (wet-season) and bi-temporal classification. Therefore, this combination of visible, NIR, and middle infrared bands is recommended for future gully identification studies. Although limitations exist for gully change detection, there are clear opportunities for applying the method presented to larger areas within the Cerrados. Resulting spatial maps of gully occurrence could then be integrated with additional spatial data, and thus advance the understanding of where and why gully erosion occurs.

References

Adams JB, Smith MO, and Johnsen PE. 1986. Spectral mixture modeling: a new analysis of rock and soil types at the Viking Lander-1 site. *Journal of Geophysical Research - Solid Earth and Planets* 91 (B8): 8098-8112.

Baccaro CAD. 1999. Processos erosivos no Domínio do Cerrado. *In*: Guerra AJT, da Silva AS, and Botelho RGM (Editors), Erosão e Conservação dos Solos. Bertrand Brasil, Rio de Janeiro, Brazil: pp. 195-227.

Baumgardner MF, Silva LF, Biehl LL, and Stoner ER. 1985. Reflectance Properties of Soils. *Advances in Agronomy* 38: 1-44.

Bocco G. 1991. Gully erosion: processes and models. *Progress in Physical Geography* 15 (4): 392-406.

Bocco G, and Valenzuela CR. 1993. Integrating satellite remote sensing and Geographic Information Systems technologies in gully erosion research. *Remote Sensing Reviews* 7: 233-240.

Congalton RG. 1991. A review of assessing the accuracy of classifications of remotely sensed data. *Remote Sensing of Environment* 37 (1): 35-46.

Daba S, Rieger W, and Strauss P. 2003. Assessment of gully erosion in eastern Ethiopia using photogrammetric techniques. *Catena* 50 (2-4): 273-291.

EMBRAPA. 1982. Levantamento de reconhecimento de média intensidade dos solos e avaliação da aptidão das terras do Triângulo Mineiro. EMBRAPA-SNLCS, Rio de Janeiro: 526 pp.

Ferreira LG, and Huete AR. 2004. Assessing the seasonal dynamics of the Brazilian Cerrado vegetation through the use of spectral vegetation indices. *International Journal of Remote Sensing* 25 (10): 1837-1860.

Furley PA. 1999. The nature and diversity of neotropical savanna vegetation with particular reference to the Brazilian cerrados. *Global Ecology and Biogeography* 8 (3-4): 223–241.

Hardisky MA, Klemas V, and Smart RM. 1983. The Influence of Soil-Salinity, Growth Form, and Leaf Moisture on the Spectral Radiance of Spartina-Alterniflora Canopies. *Photogrammetric Engineering and Remote Sensing* 49 (1): 77-83.

Jensen JR. 2004. Introductory digital image processing: a remote sensing perspective (3rd edition). Pearson Prentice Hall, Upper Saddle River, NJ, USA: 526 pp.

King C, Baghdadi N, Lecomte V, and Cerdan O. 2005. The application of remote-sensing data to monitoring and modelling of soil erosion. *Catena* 62 (2-3): 79-93.

Kruse FA, Lefkoff AB, Boardman JW, Heidebrecht KB, Shapiro AT, Barloon PJ, and Goetz AFH. 1993. The spectral image processing system (SIPS) - interactive visualization and analysis of imaging spectrometer data. *Remote Sensing of Environment* 44 (2-3): 145-163.

Langran KJ. 1983. Potential for monitoring soil erosion features and soil erosion modelling components from remotely sensed data, Proceedings of IGARSS'83. IEEE, San Francisco, California: pp. 2.1-2.4.

Madeira J, Bedidi A, Cervelle B, Pouget M, and Flay N. 1997. Visible spectrometric indices of hematite (Hm) and goethite (Gt) content in lateritic soils: the application of a Thematic Mapper (TM) image for soil-mapping in Brasilia, Brazil. *International Journal of Remote Sensing* 18 (13): 2835-2852.

Metternicht G, and Zinck JA. 1997. Spatial discrimination of salt- and sodium-affected soil surfaces. *International Journal of Remote Sensing* 18 (12): 2571-2586.

Metternicht GI, and Zinck JA. 1998. Evaluating the information content of JERS-1 SAR and Landsat TM data for discrimination of soil erosion features. *ISPRS Journal of Photogrammetry and Remote Sensing* 53 (3): 143-153.

Motta PEF, Curi N, and Franzmeier D. 2002. Relation of soils and geomorphic surfaces in the Brazilian Cerrado. *In*: Oliveira PS, and Marquis RJ (Editors), The Cerrados of Brazil: Ecology and Natural History of a Neotropical Savanna. Columbia University Press, New York: pp. 13-32.

Poesen J, Nachtergaele J, Verstraeten G, and Valentin C. 2003. Gully erosion and environmental change: importance and research needs. *Catena* 50 (2-4): 91-133.

Rodrigues SC. 2002. Impacts of human activity on landscapes in Central Brazil: a case study in the Araguari watershed. *Australian Geographical Studies* 40 (2): 167-178.

Rowan LC, and Mars JC. 2003. Lithologic mapping in the Mountain Pass, California area using Advanced Spaceborne Thermal Emission and Reflection Radiometer (ASTER) data. *Remote Sensing of Environment* 84 (3): 350-366.

Stoner ER, and Baumgardner MF. 1981. Characteristic Variations in Reflectance of Surface Soils. *Soil Science Society of America Journal* 45 (6): 1161-1165.

Thome K, Biggar S, and Takashima T. 1999. Algorithm Theoretical Basis Document for ASTER Level 2B1 - Surface Radiance and ASTER Level 2B5 - Surface Reflectance, University of Arizona, Tucson, Arizona: 45 pp.

Valentin C, Poesen J, and Li Y. 2005. Gully erosion: Impacts, factors and control. *Catena* 63 (2-3): 132-153.

Vandekerckhove L, Poesen J, and Govers G. 2003. Medium-term gully headcut retreat rates in Southeast Spain determined from aerial photographs and ground measurements. *Catena* 50 (2-4): 329-352.

Veldkamp A, and Lambin EF. 2001. Predicting land-use change. *Agriculture Ecosystems & Environment* 85 (1-3): 1-6.

Vrieling A. 2006. Satellite remote sensing for water erosion assessment: a review. *Catena* 65 (1): 2-18.

Vrieling A, and Rodrigues SC. 2004. Erosion assessment in the Brazilian Cerrados using multi-temporal SAR imagery, Proceedings of the 2004 Envisat & ERS Symposium. SP-572. ESA, Salzburg, Austria.

Zinck JA, López J, Metternicht GI, Shrestha DP, and Vázquez-Selem L. 2001. Mapping and modelling mass movements and gullies in mountainous areas using remote sensing and GIS techniques. *International Journal of Applied Earth Observation and Geoinformation* 3 (1): 43-53.

Chapter 4

EROSION RISK MAPPING:
A METHODOLOGICAL CASE STUDY IN THE
COLOMBIAN EASTERN PLAINS

Vrieling A, Sterk G, Beaulieu N

4. Erosion risk mapping: a methodological case study in the Colombian Eastern Plains

Abstract

Soil erosion caused by water is an increasing global problem. Land use and soil conservation planning for large areas requires erosion risk maps, which are typically created using erosion models. These models are often developed for different regions than where they are applied. This paper describes a new qualitative methodology for mapping soil erosion risks over large areas, called Qualitative Erosion Risk Mapping (QUERIM). It is a flexible method that uses decision trees to assign ratings to the erosion-controlling factors. Constructed using expert knowledge, these decision trees reflect the important characteristics influencing erosion risk within a specific region. Ratings for erosion-controlling factors are combined at every location to obtain potential and actual erosion risk maps. QUERIM was applied to the Puerto López municipality in the Colombian Eastern Plains. The obtained erosion risk maps showed agreement with field observations of erosion risk. However, more ground data should be gathered for a better evaluation of the method. It is concluded that a simple qualitative approach such as QUERIM can be more effective in erosion risk mapping than the use of models that were not developed for the region to which they are applied.

4.1   Introduction

Accelerated soil erosion caused by water is an increasing global problem that threatens sustainable agricultural production (Oldeman, 1994). Analyzing soil erosion risks is an important task, especially in vulnerable areas. Erosion risk maps of large areas are required to plan land use and soil conservation measures. Many mapping methods exist to fulfill this requirement (e.g. De Jong and Riezebos, 1992; Fu and Gulinck, 1994; Stocking and Elwell, 1973). Each method usually accounts for the following erosion-controlling factors: climatic characteristics, soil properties, topography, and land management (Morgan, 1986). These factors are often highly variable in space and time, which makes erosion risk mapping a complicated task.

Most erosion risk mapping methods use empirical or physically-based models. They all address the erosion-controlling factors differently. In general, these models have some important drawbacks. First, they require a large amount of detailed data. Often, these data are not available for large areas, especially in less-developed countries. Second, the models are most often developed for regions other than those to which they are applied, and for scales in which different processes and process-interactions may be important (Favis-Mortlock et al., 1996). Moreover, past studies reveal a low correlation between model outcome and observed soil loss (Favis-Mortlock, 1998; Jetten et al., 1999; Nearing, 1998; Rudra et al., 1998; Takken et al., 1999).

The most widely applied erosion model for erosion risk studies over large areas is the Universal Soil Loss Equation (USLE: Wischmeier and Smith, 1978). It is a statistically calibrated model that combines erosion-controlling factors based on runoff plot data collected in the United States. A point of criticism made by Tricart and KiewietdeJonge (1992) is that the USLE is a simple addition of parameters and thus excludes all interaction and feedback effects in the erosion process, which invalidates its universal use. They advocate a more qualitative approach in mapping erosion risks. While a quantitative approach is necessary for the design of hydraulic infrastructures such as reservoirs, a qualitative approach is usually suitable for land use and conservation planning purposes (Herweg, 1996).

Soil erosion risks can be divided into potential and actual risk. Potential erosion risk is defined here as the inherent risk of erosion irrespective of current land use or vegetation cover. Actual erosion risk relates to the risk of erosion under current vegetation and land management conditions.

The aim of this study was to define a methodological framework for qualitative mapping of erosion risks over large areas (several thousand square kilometres), using expert knowledge. It is hypothesized that a relatively simple qualitative approach is sufficient to indicate the spatial distribution of erosion risk. To illustrate the developed methodology, it was applied to the Puerto López municipality in the Eastern Plains of Colombia as part of a study that aimed at exploring simple methods that could be used for land use planning in Colombian municipalities (Beaulieu et al., 2000).

4.2 Methodological framework

Erosion studies can benefit from increased attention to the morphogenic-pedogenic balance (Tricart and KiewietdeJonge, 1992). Morphogenic processes form the landscape by gravitational or other tangential working forces. Erosion is a typical example of a morphogenic process. Pedogenic processes refer to the development of soil horizons parallel to the soil surface, including rock weathering. Morphogenesis generally proceeds downslope along a topographic gradient, whereas pedogenesis proceeds vertically into the soil profile. As the factors controlling the morphogenic-pedogenic balance vary in space, their study is a good starting point for determining the spatial distribution of erosion risks.

Tricart and KiewietdeJonge (1992) consider geology, soil, relief, vegetation, and climate as being the most important factors influencing the morphogenic-pedogenic balance. The Brazilian National Institute for Space Research (INPE) developed a method to rate these factors (Crepani et al., 1996). If at a certain location a specific factor is favourable to pedogenesis, which implies a low erosion risk for that factor, its value becomes 1.0. For example, if permanent vegetation with a high fractional vegetation cover (FVC) is present at a specific location, its vegetation factor becomes 1.0. If the factor is favourable to morphogenesis (high erosion risk), its value becomes 3.0. In the case of the vegetation factor,

this value would be assigned to bare soil. The values of the five factors are averaged at every location, resulting in an erosion risk map.

INPE's approach intends to analyze erosion risk within the whole of Brazil. Therefore, they use standard values or methods of calculation for each of the five factors across the entire country (Crepani et al., 1999). Although this is a valid approach for analysis on the national scale, it cannot account for regionally distinct processes and process-interactions, nor does it give insight into the characteristics that determine erosion risks within a particular area. A different methodology is needed for erosion risk evaluation on a regional scale, especially considering that erosion control and mitigation strategies are mostly regionally planned.

We propose a new methodology known as Qualitative Erosion Risk Mapping (QUERIM). QUERIM uses the same strategy as INPE in the scaling and averaging of the factors that influence the morphogenic-pedogenic balance. The factors are essentially the same, although the vegetation factor is renamed the management factor to account for human impact such as tillage and conservation measures. The main difference between INPE's approach and QUERIM is the way the factor values are derived. QUERIM divides the five factors into sub-factors, which reflect the physical parameters that affect the erosion processes in the region. These parameters can be derived from the available spatial data and are assigned a qualitative rating, which may be the same as the rating from the data classes. To extract a final numerical index for each factor, the occurring value combinations of the sub-factors are evaluated using decision trees that are a qualitative representation of the relationships between each of the sub-factors. The average of the geology, soil, relief, and climate factors at each location results in the potential erosion risk map, whereas the average of all five factors (including management) gives the actual risk map.

Two other aspects of the QUERIM method should be noted. First, sub-factors and decision trees can vary according to region. Second, the success of the method depends on the use of appropriate expert knowledge. Experts that have worked on soil erosion in the region under study form a valuable source of information. They often understand the regionally occurring erosion processes and they usually know the locally significant parameters controlling those processes. QUERIM uses the knowledge of these experts in the definition and selection of the sub-factors, which are subsequently extracted from the available data. The experts also help create the decision trees by assigning an appropriate numerical index to each factor according to the occurring combinations of sub-factor values. QUERIM translates expert knowledge into a formal structure that uses available spatial data to create erosion risk maps.

In principle, QUERIM can be applied to a zoned area, when the zones have the same characteristics and a high degree of internal uniformity. In this case, erosion-controlling factors have to be evaluated for each zone. But it can also be used in a raster environment to account for the high spatial variability of erosion risks. Then factors are analyzed per pixel. The choice also depends on the data availability. Either way, a geographic information system (GIS) is an indispensable tool for analysis of the spatial data.

4.3   Study area

QUERIM was applied to the Puerto López municipality, located in the department of Meta, Colombia (Fig. 4.1). It covers an area of 6907 km^2 and belongs to the Colombian Eastern Plains. The region has an average temperature of 27°C and an annual rainfall, most of which occurs in high intensity storms between April and November, of 2800 mm. On an annual basis, rainfall amount and characteristics are distributed evenly over the municipality. Terrain elevations vary from 180 to 300 m above mean sea level.

The area consists of low-lying alluvial plains where floods occur and a higher elevation that is called the *altillanura* (high plains). These high plains can be divided into non-dissected and dissected regions. They are underlain by coarse to medium sands with argillic horizons at varying depths and layers of gravel and petroferric rock that appear on the surface of hills. The alluvial plains are composed of younger material with finer sands, clay, and cemented gravel. Introduced and natural pastures form the main ground cover in the high plains, whereas forest vegetation can be found along the drainage network. Analysis of Landsat Thematic Mapper (TM) data shows that pastures constitute 50%, forest 20%, and transitional vegetation 25% of the area. The remainder consists mainly of agricultural crops, of which lowland rice is the most important.

Soils in the municipality generally have a low infiltration capacity, which results from low organic matter content, poor soil structure, and surface crusting. Rainfall with intensities of more than 20 mm h^{-1} causes Hortonian runoff and erosion (Amézquita and Londoño, 1997). Given the present rainfall regime, the area is at high risk for soil erosion, and a good vegetation cover is essential to prevent the soil from being eroded.
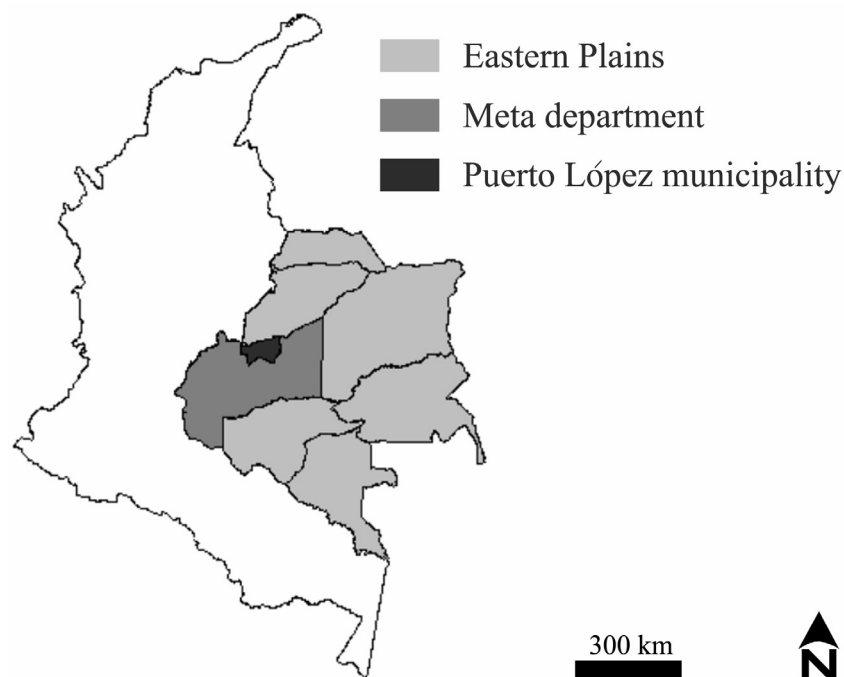

Figure 4.1   Location of study area in Colombia

4.4   Methods and materials

We used three available spatial data sources for the Puerto López municipality. The first is a soil survey done by the Colombian Geographical Institute (IGAC, 1978), which resulted in a soil map on a scale of 1:100,000. The study is well documented; for each cartographic unit the constituting soil profiles are described in terms of their physical and chemical properties. The second data source is a Digital Elevation Model (DEM) that was interpolated from contour lines and point elevation data. The third data source is a Landsat TM image from August 10, 1998. The soil survey data were converted into a 25-m grid format and the Landsat TM image was resampled to obtain the same 25-m grid as the DEM. This allowed a pixel-based evaluation of erosion risk within a GIS. In this study PCI Geomatics software was used, but any raster-based GIS package could be applied for this purpose.

In addition, ground data of land use and FVC were gathered using a Global Positioning System (GPS). Border coordinates of parcels or homogeneous vegetation areas were measured, resulting in a collection of polygons. For every polygon, land use and average FVC were determined. The average FVC was estimated visually.

Apart from vegetation data, the GPS was used to indicate areas with clear signs of erosion and that suffer from a very high erosion risk. Erosion risk verification data were taken at seven locations distributed over the study area. After construction of the risk maps, we observed signs of erosion and estimated topsoil, geology, topography, and vegetation characteristics.

We interviewed four soil experts who have worked in the region. Three of them have performed soil erosion studies within the Puerto López municipality or in its vicinity. The experts identified the sub-factors to select and extract from the available spatial data, as well as the relationships needed for the construction of decision trees.

4.5   Results and discussion

The selected sub-factors are shown in Table 4.1. Every sub-factor was given a qualitative rating that was subsequently used in the decision trees. Note that this value is not necessarily between 1.0 and 3.0. In this study, the climate factor was not used, as annual rainfall can be assumed homogeneous in the study area and therefore climate would not contribute to the spatial distribution of the erosion risk. The sub-factors for geology and soil were selected from the attributes contained in the soil survey by IGAC (1978). The geology sub-factor, alteration degree, was defined as the degree of physical and chemical change that occurs in rocks at the ground surface or close to it through atmospheric agents (SSSA, 1987). The relief attributes followed from the DEM. Slope gradient was calculated and dissection grade was visually interpreted. For the management factor, a maximum likelihood classification was performed, using the Landsat TM image and ground data on land use, to obtain a land use map. The overall accuracy of this map was 84 %. The FVC was determined for the total

Table 4.1 *Factors and sub-factors for Qualitative Erosion Risk Mapping (QUERIM) in Puertó Lopez, Colombia*

Factor	Sub-factor	Rating	Description	Criteria
Geology	Alteration degree	1	Strongly weathered	
		2	Moderately weathered	
		3	Slightly weathered	
Soils	Effective depth	1	Moderately deep	> 50 cm
		2	Superficial	25 - 50 cm
		3	Very superficial	10 - 25 cm
		4	Excessively superficial	0 - 10 cm
	Topsoil texture	1	Fine	
		2	Medium	
		3	Coarse	
	Organic matter content (topsoil)	1	Very high	> 6.0 %
		2	High	2.5 - 6.0 %
		3	Medium	1.5 - 2.5 %
		4	Low	1.0 - 1.5 %
		5	Very low	< 1.0 %
	Structure	1	Strong	
		2	Moderate	
		3	Weak	
		4	Structureless - massive	
Relief	Dissection grade	1	Not dissected	
		2	Slightly dissected	
		3	Moderately dissected	
		4	Very dissected	
	Slope gradient	1	Flat	0 - 3 %
		2	Slightly inclining	3 - 7 %
		3	Moderately inclining	7 - 12 %
		4	Strongly inclining	12 - 25 %
		5	Steep	25 - 50 %
		6	Very steep	>50 %
Management	Land use	1	Water	
		2	Tree and shrub vegetation	
		3	Natural pastures	
		4	Introduced pastures	
		5	Lowland rice	
		6	Bare and burned land	
	Fractional vegetation Cover (FVC)	1	High	80 – 100 %
		2	Moderately high	60 – 80 %
		3	Moderate	40 – 60 %
		4	Low	20 – 40 %
		5	Very low	0 – 20 %
		6	None	0 %

Table 4.2   Decision tree for soil factor*

Effective depth	Topsoil texture	Organic matter content	Structure	Soil Factor
1	1	4	3	1.4
1	2	2	3	1.3
1	2	3	1	1.3
1	2	3	2	1.4
1	2	4	2	1.5
1	2	4	4	2.3
2	2	1	2	1.7
2	2	2	2	1.9
2	2	4	1	2.2
2	2	5	3	2.4
2	3	3	2	2.3
2	3	5	4	2.8
3	1	1	3	2.0
3	2	3	2	2.5
3	2	3	3	2.6
3	2	4	3	2.7
4	3	5	4	3.0

* The decision tree shows the occurring value combinations of the specific sub-factors. These values correspond with Table 1. The last column shows the final factor rating as assigned by the local experts for each sub-factor combination.

area by relating the ground estimates to the normalized difference vegetation index (NDVI) extracted from the image. Neither erosion prevention measures nor practices of conservation tillage are present in the area, and therefore these factors were not included in this study.

A numerical index between 1.0 and 3.0 was assigned to each factor by the local experts through qualitative evaluation of the occurring combinations of sub-factor values, as shown in the decision trees (Tables 4.2, 4.3, and 4.4).The geology factor obtained the same rating as in Table 4.1. Table 4.2 shows the decision tree for the soil factor. The experts gave the four sub-factors nearly equal weight in determining erosion risk, although structure-less massive soils (structure rating = 4) considerably increased the risk. Table 4.3 shows the decision tree for the relief factor. Experts indicated that the slope gradient should receive the highest weight, but stressed the increased erosion risk in highly dissected terrain. Table 4.4 shows the decision tree for the management factor. Erosion risk is highest on the pastures (land use ratings = 3 and 4) that form a great part of the area, as well as on bare soils (mainly burned pastures; land use rating = 6). The FVC is the most determining sub-factor according to the experts.

A map was constructed for each factor, resulting in a numerical index for every pixel. The averages of the geology, soil, and relief factors per pixel produced the potential erosion risk map (Fig. 4.2), whereas the averages of the geology, soil, relief, and management factors resulted in the actual erosion risk map (Fig. 4.3). Table 4.5 reclassifies the values to obtain a more comprehendible legend.

Table 4.3   Decision tree for relief*

Dissection grade	Slope gradient	Relief factor
1	1	1.0
1	2	1.3
1	3	1.8
1	4	2.1
1	5	2.3
1	6	2.5
2	1	1.4
2	2	1.7
2	3	2.0
2	4	2.3
2	5	2.5
2	6	2.7
3	1	1.9
3	2	2.2
3	3	2.4
3	4	2.6
3	5	2.8
3	6	2.9
4	1	2.2
4	2	2.6
4	3	2.8
4	4	2.9
4	5	3.0
4	6	3.0

Table 4.4   Decision tree for management*

Land use	FVC	Management factor
1	6	1.0
2	1	1.0
2	2	1.2
3	1	1.3
3	2	1.5
3	3	1.9
3	4	2.3
3	5	2.7
4	1	1.4
4	2	1.6
4	3	2.0
4	4	2.4
4	5	2.8
5	3	1.8
6	6	3.0

*   The decision trees show the occurring value combinations of the specific sub-factors. These values correspond with Table 1. The last column shows the final factor rating as assigned by the local experts for each sub-factor combination.

The potential erosion risk map (Fig. 4.2) shows a high risk for the dissected high plains (centre and south) and the low-lying areas (western and northern boundary), which consist of young unstable alluvial sediments. A low risk is found on the non-dissected high plains (north). A similar attenuated pattern can be seen on the actual erosion risk map (Fig. 4.3). This attenuation does not hold for patches with bare soil or pastures with a very low FVC. As the geology, soil, and relief factors are much more stable over time than the management factor, recurrent satellite remote sensing imagery should be used for better monitoring of the actual erosion risk. This allows timely identification of management changes, such as pastures that have been burnt, resulting in a low FVC and therefore a high actual risk.

The erosion risk verification data showed a correspondence between areas in the field with advanced signs of erosion or high erosion risk, and areas on the map indicating a high erosion risk at all of the seven locations visited. At four locations advanced signs of sheet erosion and gully formation could be observed, whereas at the remaining three locations favourable conditions for erosion (steep slopes, bare soil, etc.) were present. In spite of this

Table 4.5   *Reclassification of erosion risk classes*

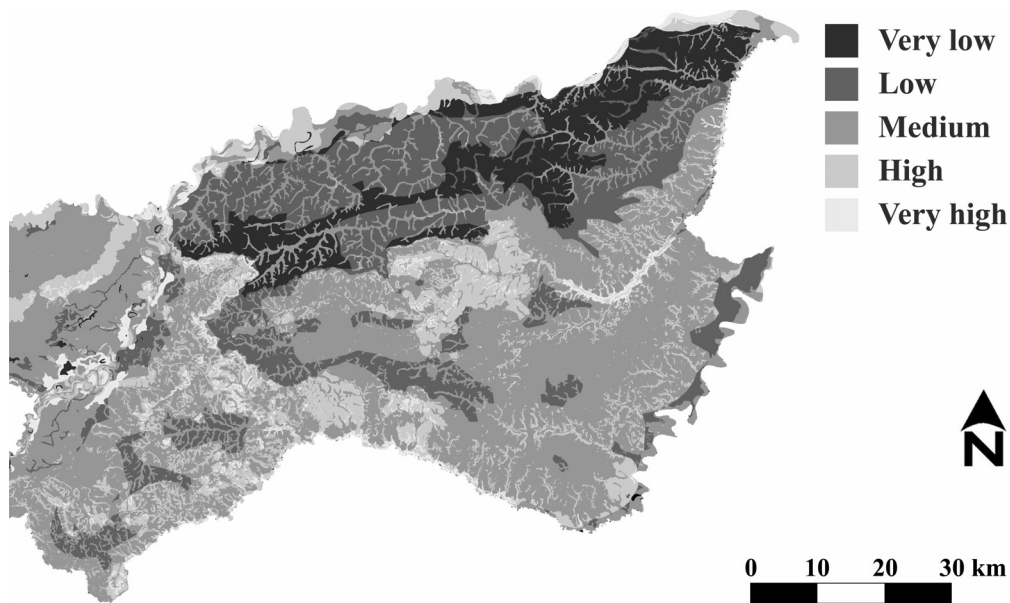| Rating	Erosion risk
1.0 - 1.3	very low
1.4 - 1.6	low
1.7 - 1.9	medium
2.0 - 2.2	high
2.3 - 3.0	very high

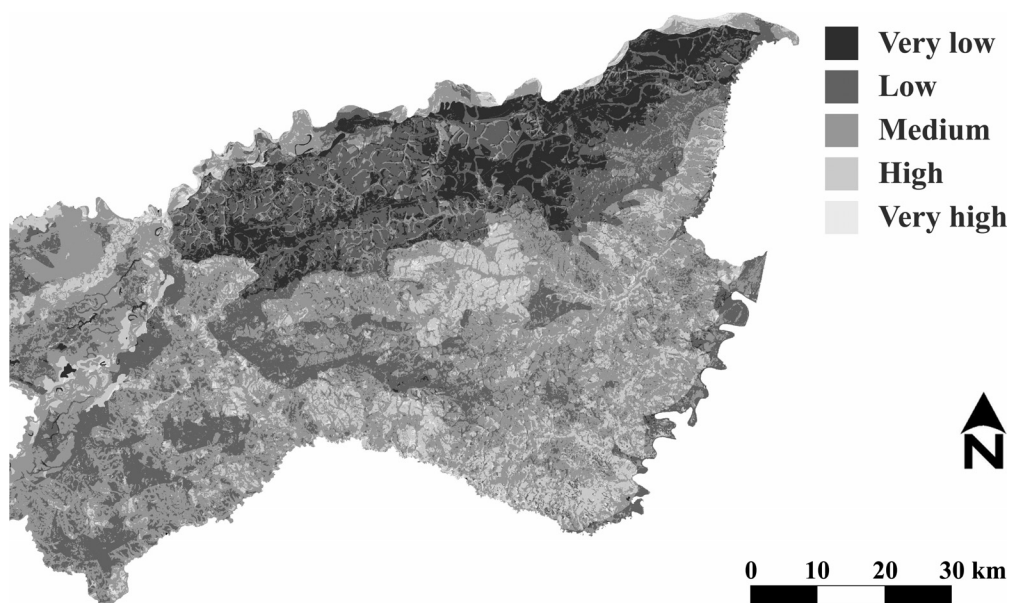*Figure 4.2*   *QUERIM potential erosion risk map of Puerto López municipality*

Figure 4.3   *QUERIM actual erosion risk map of Puerto López municipality*

correspondence between high erosion risk areas on the map and in the field, the study could benefit from a more thorough ground check. We suggest selecting several sites, not larger than 0.2 km^2, with clear differences in erosion risk on the maps. Within these sites the interrelations between the erosion-controlling factors can be identified through detailed field estimations of topsoil characteristics, geology, topography, and vegetation cover. Combined, these estimations can help predict site-specific erosion processes, which will result in a qualitative rating of the erosion risk.

It could be argued that QUERIM is a simple averaging of parameters, but the region-specific decision trees representing the interactions between sub-factors lend flexibility to the method. In the Puerto López study, the important controlling role of vegetation (management) becomes clear through the overall attenuated pattern of actual erosion risk as compared to potential erosion risk. If vegetation were removed, soil characteristics influencing the infiltration rate would become a key factor, as well as the stability of the underlying material (geology factor). Obviously, low infiltration rates would create more runoff and erosion in steep and highly dissected terrain.

The merit of applying QUERIM to the Puerto López municipality is that it has produced a map of areas under potential or actual erosion risk. This will encourage proper land use and conservation planning, mostly by identifying areas threatened by erosion if, for example, vegetation were removed or burnt, or fields taken under cultivation. Land use planning using QUERIM results will direct these activities to "safer" areas. Moreover, areas having high actual erosion risk will qualify for being re-planted. Implications for conservation planning principally relate to recommendations of tillage practices, on either present or future agricultural fields.

As a qualitative method, QUERIM cannot give quantitative estimates of erosion, other than through the up-scaling of erosion measurements that could be executed in the previously mentioned sites of 0.2 km^2. This may be a shortcoming for high-relief regions, if radical measures, such as terraces or dams, are to be constructed. QUERIM can indicate areas of interest within a larger region, but other quantitative methods such as the Water Erosion Prediction Project (WEPP: Flanagan and Nearing, 1995), may have to be used in these areas for final conservation planning.

4.6   Summary and conclusions

A simple qualitative approach that takes expert knowledge into account is a valuable tool for erosion risk mapping, especially when this mapping is conducted to focus soil conservation actions or to establish land use restrictions. Such an approach can be more effective than the use of quantitative models that were not developed for the region to which they are applied. QUERIM provides a methodological framework for mapping erosion risks over large areas. A ground check indicated that it is an appropriate method for mapping erosion risks in the Puerto López municipality. More detailed ground data is desirable for a better verification.

The flexibility of QUERIM has several advantages. First, although the erosion-controlling factors have to be accounted for, QUERIM has no fixed data requirement, such as necessary parameters. This makes the method applicable to a wide variety of regions for which studies are available that do not necessarily contain model parameters. Second, the choice of sub-factors and their combinations can be adapted by region, so locally-important processes and factors can be accounted for. Furthermore, QUERIM uses the knowledge of experts that have worked for a long time in the region under study. The absence of local expert input is a main shortcoming of present geographical data integration. Current models that integrate geographical data seldom serve the purpose for which they are used.

References

Amézquita CE, and Londoño H. 1997. La infiltración del agua en algunos suelos de los Llanos Orientales y sus implicaciones en su uso y manejo. *Revista Suelos Ecuatoriales* 27: 163-168.

Beaulieu N, Rubiano Y, Vrieling A, Rodriguez M, Jaramillo JE, Muñoz OJ, and Zakhia N. 2000. Use of geographic information systems (GIS) in land resource management in the Colombian Orinoco region. *In*: Kokubun M, Uchida S, and Tsurumi K (Editors), GIS applications for agro-environmental issues in developing regions. International Symposium Series No. 8. JIRCAS, Tsukuba, Japan.

Crepani E, de Medeiros JS, Guimarães de Azevedo L, Hernandez F. P, Galloti F. T, and Duarte V. 1996. Curso de Sensoriamento Remoto Aplicado ao Zoneamento Ecológico-Econômico. INPE, São José dos Campos, Brazil.

Crepani E, de Medeiros JS, Hernandez F. P, Galloti F. T, Duarte V, and Faria B. CC. 1999. Sensoriamento Remoto e Geoprocessamento Aplicados ao Zoneamento Ecológico-Econômico e ao Ordenamento Territorial. INPE, São José dos Campos, Brazil.

De Jong SM, and Riezebos HT. 1992. Assessment of erosion risk using multitemporal remote sensing data and an empirical erosion model, Proceedings of the 3rd European Conference on Geographic Information Systems (EGIS'92), Munich, Germany: pp. 893-900.

Favis-Mortlock DT. 1998. Evaluation of field-scale erosion models on the UK South Downs. *In*: Boardman J, and Favis-Mortlock DT (Editors), Modelling Soil Erosion by Water. NATO-ASI Series I-55. Springer-Verlag, Berlin, Germany: pp. 141-157.

Favis-Mortlock DT, Quinton JN, and Dickinson WT. 1996. The GCTE validation of soil erosion models for global change studies. *Journal of Soil and Water Conservation* 51 (5): 397-403.

Flanagan DC, and Nearing MA (Editors). 1995. USDA Water Erosion Prediction Project: Hillslope profile and watershed model documentation. NSERL Report No. 10. USDA-ARS National Soil Erosion Research Laboratory, West Lafayette, IN, USA.

Fu B, and Gulinck H. 1994. Land evaluation in an area of severe erosion: the Loess Plateau of China. *Land Degradation and Rehabilitation* 5 (1): 33-40.

Herweg K. 1996. Field Manual for Assessment of Current Erosion Damage. SCRP Ethiopia, and Centre for Development and Environment, University of Berne, Switzerland: 69 pp.

IGAC. 1978. Estudio General de Suelos de los Municipios de Cabuyaro, Fuento de Oro, Puerto López, San Carlos de Guaroa, y la Inspección de Barranca de Upia (Departamento del Meta). Instituto Geográfico Agustín Codazzi, Bogotá, Colombia.

Jetten V, De Roo A, and Favis-Mortlock D. 1999. Evaluation of field-scale and catchment-scale soil erosion models. *Catena* 37 (3-4): 521-541.

Morgan RPC. 1986. Soil erosion and conservation. Longman Group, Essex, England: 298 pp.

Nearing MA. 1998. Why soil erosion models over-predict small soil losses and under-predict large soil losses. *Catena* 32 (1): 15-22.

Oldeman LR. 1994. Global extent of soil degradation. *In*: Greenland DJ, and Szabolcs I (Editors), Soil Resilience and Sustainable Land Use. CAB International, Wallingford, UK: pp. 98-118.

Rudra RP, Dickinson WT, and Wall GJ. 1998. Problems regarding the use of soil erosion models. *In*: Boardman J, and Favis-Mortlock DT (Editors), Modelling Soil Erosion by Water. NATO-ASI Series I-55. Springer-Verlag, Berlin, Germany: pp. 175-189.

SSSA. 1987. Glossary of Soil Science Terms. Soil Science Society of America, Madison, WI, USA.

Stocking MA, and Elwell HA. 1973. Soil erosion hazard in Rhodesia. *Rhodesian Agricultural Journal* 70 (4): 193-210.

Takken I, Beuselinck L, Nachtergaele J, Govers G, Poesen J, and Degraer G. 1999. Spatial evaluation of a physically-based distributed erosion model (LISEM). *Catena* 37 (3-4): 431-447.

Tricart J, and KiewietdeJonge C. 1992. Ecogeography and Rural Management - a Contribution to the International Geosphere-Biosphere Programme. Longman Group, Harlow, UK: 267 pp.

Wischmeier WH, and Smith DD. 1978. Predicting rainfall-erosion losses: A guide to conservation planning. Agricultural Handbook No. 537. US Department of Agriculture.

Chapter 5

SPATIAL EVALUATION OF SOIL EROSION RISK
IN THE WEST USAMBARA MOUNTAINS,
TANZANIA

Vrieling A, Sterk G, and Vigiak O

5. Spatial evaluation of soil erosion risk in the West Usambara Mountains, Tanzania

Abstract

Effective soil and water conservation programmes require the concentration of resources on limited areas. For that purpose regional scale assessments of erosion risk are required. However, availability of good-quality spatial data for such assessments is often poor, especially in regions like sub-Saharan Africa. This study was conducted to evaluate the potential of analyzing regional erosion risk using a limited amount of readily available data. The analysis was executed for the 70-km2 Baga watershed in the West Usambara Mountains, Tanzania. Principal data sources were a Landsat image and an SRTM DEM. Two qualitative mapping methods resulting in five erosion risk classes were evaluated against field-based erosion risk estimates. The first method derived slope classes from the DEM and fractional vegetation cover (FVC) classes from the Landsat image and FVC field estimates. Data integration was achieved with a decision tree. The second method did not apply field data for the map construction, but combined five equally sized NDVI classes and five slope classes using the minimum-operator. Resulting maps showed a high and comparable accuracy, 80 % for Method 1, and 81 % for Method 2, when allowing a maximum difference of one class with field erosion risk estimates. Spatial patterns of erosion risk were well represented by both methods and high erosion risk areas can be properly identified within the Baga watershed. Due to the limited data requirement of Method 2, it has a high potential for quick identification of erosion risk in other areas of the East African Highlands.

5.1 Introduction

Soil erosion negatively affects sustainable agricultural production in sub-Saharan Africa (Lal, 1988). Governmental policies targeted at reducing soil erosion, thereby increasing production levels, are required when local land users lack the resources or knowledge for effective erosion control (Ananda and Herath, 2003). National programmes towards soil and water conservation have altered substantially during the past decades, moving from top-down conservation planning towards increased farmer participation (Pretty and Shah, 1997). Although proper farmer participation has proven to be more effective than top-down approaches in soil and water conservation adoption (Mbaga-Semgalawe and Folmer, 2000), participatory methods require substantial time and dedication of extension staff. Given the limited budgets of involved institutions, there is a need to focus resources and efforts on small areas (e.g. 50-500 ha). Once the implemented measures proved their effectiveness, these areas can have a demonstration effect on surrounding farmer groups or villages. The selection of such a focal area is therefore very important. Criteria for this selection generally

include social factors like local requests for support, but a very important criterion is the extent of erosion (Pretty et al., 1995).

As a consequence, information on erosion is required at different spatial scales. Both for the selection of a focal area, and for assisting the conservation planning procedures within a focal area, spatial information is needed on where erosion is occurring or is likely to occur in the near future. This can be either quantitative information (erosion rates) or qualitative information (e.g. high versus low erosion risk). There is not one single straightforward method for assessing erosion and its evaluation is highly dependent on the spatial scale and the purpose of the assessment (Warren, 2002). For limited spatial scales (<100 ha) field surveys can provide an accurate means of analyzing erosion damage (Herweg, 1996). For focal area selection however, other approaches should be applied that integrate available spatial data.

Current methods for spatial erosion assessment at the regional scale (50 - 10,000 km^2) include the application of erosion models and qualitative approaches. Many erosion models exist at present (Merritt et al., 2003). However, performance of these models outside the region where they were developed has generally been poor (e.g. Brazier et al., 2000) and the models require substantial calibration to have some predictive value (Jetten et al., 1999; Jetten et al., 2003). Furthermore, most models have been developed for small scales and cannot easily be applied to larger regions (Kirkby et al., 1996; Schoorl et al., 2000; Yair and Raz-Yassif, 2004). To overcome some of the drawbacks of erosion models, alternative approaches have been developed that aim at a qualitative mapping of erosion risk through the use of expert judgments (Sonneveld, 2003). This is possible through (1) spatial assessments by experts (e.g. Oldeman et al., 1991) or (2) through the identification of key factors and processes in a certain region (e.g. De la Rosa et al., 1999; Vrieling et al., 2002). In the second case, decision rules are defined to combine important factors that can be derived from available spatial data. For example, Vrieling et al. (2002) developed an erosion risk mapping methodology for the Colombian Eastern Plains, in which expert judgments determined the important erosion controlling factors in the study area and the rules to combine those factors.

Whether erosion models or qualitative approaches are used for assessing the erosion risk in an area and for focal area selection, spatial data are always required. Many erosion models have a high data demand, and can therefore only be applied in data-rich environments, or even after extensive collection of field data on model parameters. Such models have their major benefit in increasing the understanding of the erosion process for the region under study. However, to be useful for decision makers, erosion assessment methods must have limited data requirements (Renschler and Harbor, 2002). This becomes even more important in data-poor regions, such as sub-Saharan Africa. For example, soils data are often merely available at very coarse scales, which hampers its direct use in regional assessments (<10,000 km^2). Van Rompaey and Govers (2002) showed that simple methods provide a more accurate assessment of erosion than complex methods, for which the available data does not allow the estimation of required parameters with a minimum accuracy.

A positive development is the increasing availability of good quality spatial data with a near worldwide coverage. For a large part this can be contributed to the many earth observing space missions that have been conducted by national, international, and private agencies since the 1970s. A wide variety of satellite images and image-derived products, such as digital elevation models (DEMs), are currently available to the general public, often at low or no cost, although some image types are still expensive. A good example is the Shuttle Radar Topography Mission (SRTM) offering a free high-quality 90-m resolution DEM (Rabus et al., 2003). For regional erosion studies, satellite imagery is increasingly being used, both for the detection of erosion features and eroded surfaces, and for the assessment of erosion determining factors like soil properties and vegetation cover. However, in most studies satellite data are merely applied to assess the vegetation cover, partly due to the limited visibility of the soil surface in humid environments (Vrieling, 2006). As a consequence, methods applied for spatial assessment of erosion at the regional scale still heavily rely on data sources that have a limited availability in wider regions.

The objective of this study was to evaluate the potential of readily available spatial data to analyze regional erosion risk. The erosion assessment was executed to provide a qualitative erosion risk map that can be used for prioritization of soil and water conservation efforts within the 70-km^2 study area.

5.2 Study area

The West Usambara Mountains are located in northeast Tanzania (Fig. 5.1) and form part of the system known as the East African Highlands, which comprises highland areas in Burundi, Ethiopia, Kenya, Rwanda, Tanzania, and Uganda. This highland system was formed during and after the Tertiary period. The West Usambara Mountains are an upraised horst of Precambrian metamorphic rocks, consisting mainly of gneisses (Pfeiffer, 1990). Because of a favourable climate and fertile soils, these mountains are very important for food, fibre, and fodder production. However, high population pressure (> 100 persons/km^2) has resulted in overexploitation of natural resources causing deforestation and land degradation (Conte, 1999; Kaoneka and Solberg, 1994). Currently, soil erosion is widespread and forms the major limiting factor for agricultural production (Tenge et al., 2004). In spite of several governmental, non-governmental and international donor programmes aiming at tackling the soil erosion problem by construction of soil and water conservation measures, adoption of such practices by farmers has been poor, particularly due to the incompatibility of the measures with socio-economic conditions and limited farmer participation (Mbaga-Semgalawe and Folmer, 2000; Tenge et al., 2004). Following the Kenyan example, during recent years the Catchment Approach has been applied to increase farmer participation and effectiveness of soil conservation programmes (Johansson, 2001). In this approach, a small focal area (about 200 ha in West Usambara Mountains) is selected where the soil erosion

Figure 5.1   Location, boundary, and drainage pattern of Baga watershed

problem is addressed in a participatory manner and joint farmer action towards soil and water conservation is envisaged (Pretty et al., 1995).

The Baga watershed is a 70-km^2 hydrological watershed situated in the humid warm agro-ecological zone of the West Usambara Mountains (Fig. 5.1). Average annual rainfall is approximately 1000 mm falling in a bimodal pattern. The two rainy seasons are locally named short rains (October-November), and long rains (March to May), and a dry spell occurs in January-February. Average monthly temperatures vary between 18°C (July) and 23°C (March), with high diurnal variation. The elevation within the watershed ranges from 1200 to 2000-m above mean sea level. The terrain is highly dissected with local slopes of up to 90%. A detailed soil survey in a small part of the Baga watershed (2 km^2) showed that Humic and Haplic Acrisols occur on the slopes and ridges, Haplic Lixisols on the footslopes, and Eutric Fluvisol and Umbric Gleysols in the river valley, using the FAO classification system (Meliyo et al., 2002). Possibly other soil types occur in the Baga watershed, but besides this soil survey only coarse-scale soil maps (1:500,000) are available.

Land use principally consists of agriculture, although mountain rain forest is present in the higher parts of the watershed. Agricultural land is mostly composed of small-scale fields that are generally cultivated with maize, intercropped with beans, banana, cassava, and sugarcane. The combination of coffee, banana, and coco yam occurs on some steeper slopes. Irrigated vegetables are intensively planted in the valley bottoms. Furthermore, large mono-crop tea plantations are present in the area. Dispersed trees of different species are found in varying densities throughout the watershed. Erosion occurs mainly in the form of sheet and rill erosion on fields that are cultivated with annuals. It is most severe at the onset of the long rains, when high-intensity rainstorms occur and the soil cover is poor due to antecedent land preparation (Vigiak et al., 2005). Very few soil and water conservation measures were found in the Baga watershed.

5.3 Materials and methods

5.3.1 Data

Three main data sources were used for the erosion risk analysis: a Shuttle Radar Topography Mission (SRTM) DEM, a Landsat Enhanced Thematic Mapper (ETM+) image, and field data. The only additional data applied were a set of orthophotos (i.e. orthorectified aerial photographs) covering the complete study area, which allowed precise georefencing of the Landsat image.

SRTM was flown in February 2000 onboard the Space Shuttle Endeavour. During the 11-day mission, two antenna pairs operating in C- and X-band (5.6 and 3.0 cm wavelength) simultaneously transmitted and received radar signals. Good quality DEMs were obtained from the received signals using interferometric synthetic aperture radar processing (Rabus et al., 2003). DEMs derived from C-band radar are freely available from the internet at 90-m resolution for any land mass between 60°N and 57°S latitude. The DEM containing the study site was selected.

The Landsat series of satellites started to acquire images in 1972 with the launch of Landsat-1. Large archives of Landsat imagery exist, that can be easily accessed and bought through the internet, and for some regions free scenes are available. The Landsat-7 ETM+ image used in this study, was acquired on 6 February 2003 (path/row: 167/73), slightly before the start of the long rains. At that moment, many agricultural fields were bare, causing high erosion risks at the onset of the rains. The image was of good quality with no clouds present in the study area. Only the 30-m resolution multispectral bands number 3 and 4 were used, which capture respectively red (0.63-0.69 μm) and near infrared (NIR: 0.76-0.90 μm) reflection.

A detailed field survey was executed during late February to early March 2003, before the start of the long rains. Three reasons existed for the timing of the survey: (1) the high erosion risk at the onset of the long rains, which is caused by the concurrence of high intensity rainfall and the high presence of bare fields that are prepared for cultivation in January-February, (2) the easier accessibility of many locations as compared to the wet season, and (3) the availability of a good Landsat image with a maximum deviation of 28-days from the last survey performed. Prior to the field survey, several field visits were carried out in presence of extension officers and different groups of local farmers. The purpose of these field visits was to understand the local perception of erosion, its causes, and the locally used indicators of erosion. This knowledge assisted in assigning qualitative estimates to erosion risk throughout the survey. During the survey, 151 points with an approximately uniform vegetation cover were located within the Baga watershed using a Global Positioning System (GPS). At each point the following characteristics were recorded: land cover, fractional vegetation cover (FVC), presence of soil and water conservation measures, slope gradient, and erosion indicators. The assessment of FVC was done through visual estimation, and slope was measured with an inclinometer. Erosion risk was qualitatively estimated jointly with an extension officer on a scale ranging from 1 (very low) to 5 (very high), based

on the recorded surface characteristics and the presence of local erosion indicators (Okoba, 2005). Used indicators of high erosion risk included stony soil, exposed roots, and the presence of rills and pedestals (although at many locations limited due to dry period and ploughing).

5.3.2 Preprocessing

The SRTM DEM contained minor data voids within the study area. These occurred due to radar shadows that are caused by steep terrain. The voids were filled by interpolating neighbouring elevation values. Slope was calculated from the DEM using the slope definition of Zevenbergen and Thorne (1987). Subsequently the slope map was reprojected to a UTM projection, using nearest neighbour resampling and a 30-m output pixel size. This reprojection was executed to be consistent with available base data, including a topographic map and aerial orthophotos. The 30-m pixel size was chosen to match the Landsat ETM+ image. A coarse (90-m) DEM normally results in lower slope values for steep slopes and slightly higher slope values for gentle slopes, but slope values are generally well correlated when compared to a finer DEM (e.g. Thompson et al., 2001; Wolock and McCabe, 2000). Because slope values were to be used in a qualitative way, it was assumed that the calculation of slope from the 90-m DEM would provide a proper approximation of slope classes in the Baga watershed.

The Landsat ETM+ image was orthorectified to reduce geometric distortions caused by the steep topography. The process of orthorectification calculates a horizontal correction to the image data by combining information on the elevation and viewing geometry of each image point (Tucker et al., 2004). Elevation was obtained from the SRTM DEM and viewing geometry was derived from the path definition of the Landsat-7 satellite. The geometric reference of the Landsat image was determined by visually relating 23 control points on the available orthophoto to the same points on the Landsat image. The root mean square error of the orthorectification model using these control points was 23.6-m, which is lower than the image resolution. Nearest neighbour resampling was applied with an output pixel size of 30-m. The 30-m image resolution was maintained to allow the representation of small-scale changes in vegetation cover.

The digital numbers of the orthorectified Landsat image bands 3 and 4 were converted into reflectance (ρ) values (i.e. radiometric calibration) using a straightforward procedure described in Chander and Markham (2003). Subsequently, the Normalized Difference Vegetation Index (NDVI) was calculated using the following equation:

$$NDVI = \frac{\rho(NIR) - \rho(red)}{\rho(NIR) + \rho(red)} = \frac{\rho(band\,4) - \rho(band\,3)}{\rho(band\,4) + \rho(band\,3)} \tag{5.1}$$

For healthy green vegetation $\rho(NIR)$ is high, while $\rho(red)$ is low, resulting in a high NDVI, whereas for bare soil $\rho(NIR)$ and $\rho(red)$ are similar causing a low NDVI. Because the NDVI
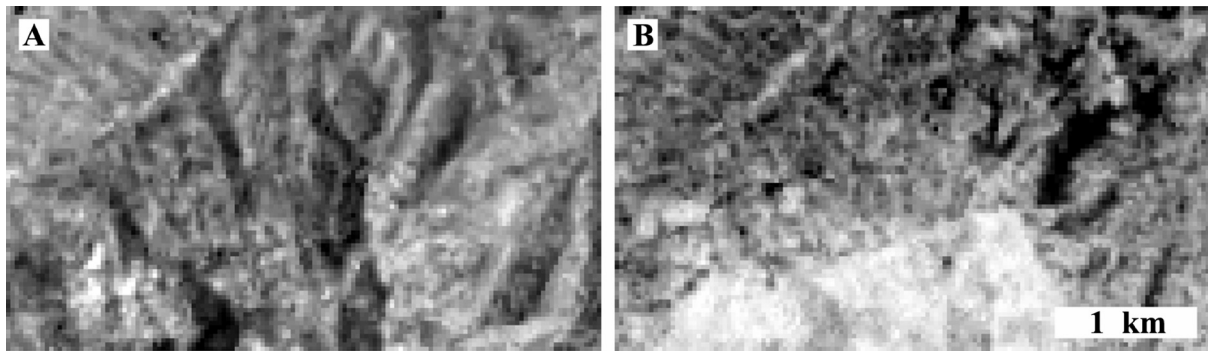
Figure 5.2   Area near study site to illustrate the reduction of the topographic effect. (A) Landsat band 4 reflectance stretched between 0.15 (black) and 0.35 (white); (B) NDVI stretched between 0.4 and 0.8 of same area. In (A) several dark shadows are present, which are nearly absent in (B). In B, dark areas are related to limited vegetation cover.

is an image ratio, it reduces the effect of topography (Holben and Justice, 1981). Due to variation of slope inclination and aspect in rugged terrain, spectral reflection is different for a similar vegetation cover. Although more sophisticated approaches exist towards topographic normalization (e.g. Riaño et al., 2003; Sandmeier and Itten, 1997), these approaches require a DEM with a spatial resolution that is as high, or higher than the image resolution. For the Baga watershed, the NDVI resulted in a good reduction of the topographic effect (Fig. 5.2).

5.3.3 Erosion risk assessment using field data (Method 1)

The construction of the soil erosion risk map for the Baga watershed with Method 1 was achieved through a qualitative integration of the slope map and a fractional vegetation cover (FVC) map. The choice of these two variables does not imply that we consider factors like soil properties, rainfall characteristics, land use, tillage operations, and presence of conservation practices, of little importance for erosion. There are however three main rationales for using only these two variables: (1) the relative ease with which the variables can be obtained from readily available data, (2) the reported high correlation between these variables and the occurrence of erosion features in a region within the Kenyan Highlands (Okoth, 2003), and (3) the frequency by which these variables were mentioned by both farmers and extension officers as important causes of erosion within the region during the field visit. Furthermore, FVC is strongly correlated with several other factors (e.g. soil properties and presence conservation measures). A third cause of erosion that was often mentioned by farmers and extension officers is heavy rainfall. On an annual basis, this factor can be assumed uniform in the Baga watershed, and thus does not contribute to spatial differences of erosion risk. In larger regions, spatial variability of rainfall characteristics may be accounted for using readily available data products from the Tropical Rainfall Measuring Mission (TRMM: Kummerow et al., 1998).

Regression analysis was performed between the 151 field estimates of FVC and the corresponding NDVI values derived from the Landsat image. The resulting relationship was applied to obtain an FVC-map of the complete watershed. The FVC and the slope map were both reclassified resulting in five classes for each variable. The class limits were set at multiples of 10, in such a way that the class range was of equal size for each class, and that each class was represented in 5 to 35 % of the study area. For slope this resulted in the following classes: 0-10 %, 10-20 %, 20-30 %, 30-40 %, and more than 40 %. For FVC the classes were: 0-20 %, 20-40 %, 40-60%, 60-80 %, and 80-100 %.

Erosion risk classes were assigned to FVC and slope class combinations using a decision tree. The same five erosion risk classes as of the field survey assessments were used, ranging from very low (1) to very high (5). The construction of the decision tree was achieved through comparing 100 field estimates of erosion risk with the corresponding FVC-slope class combinations derived from the spatial data sources. A logical sequence of erosion risk classifications was always maintained, e.g. assuming the same FVC class, a steeper slope class cannot be assigned a lower erosion risk as a less steep class. The 100 locations used for the calibration of the decision tree were randomly selected from the 151 available field estimates. The remaining 51 locations were used for validation. The erosion risk map was subsequently constructed through applying the decision tree to the classified FVC and slope map of the Baga watershed.

5.3.4 Erosion risk assessment without field data (Method 2)

A second method was tested to assess the requirement of using field data for accurate erosion risk mapping. In most cases field data are not readily available, and therefore Method 1 may be difficult to extrapolate and apply to other areas, unless a detailed field survey is performed. Method 2 is also a qualitative approach and addresses the same factors as Method 1, but in a very simple straightforward manner that can easily be applied to other areas.

NDVI was used directly as a measure of vegetation cover, thus no processing was done to determine FVC. Both NDVI-values and slope-values were automatically classified into five classes that occupy an equal area within the study area. For both factors, an erosion risk class – five classes ranging from very low (1) to very high (5) – was assigned based on the relative erosion susceptibility. For example, very steep slopes obtained a very high factorial erosion risk class, whereas flat areas and very gentle slopes received a very low risk class. For NDVI it was the other way around, i.e. very high NDVI values obtained a very low risk class. The erosion risk map was constructed by simply taking the minimum of the NDVI-based and the slope-based risk classes at each location. The minimum-operator was chosen for two reasons: (1) it was assumed that the lowest of the two factorial risk classes is determinative for the final erosion risk, because e.g. a good vegetation cover on a steep slope and a poor cover on a very gentle slope both result in a relatively little erosion, and (2) this operator effectively limited the occurrence of high and very high erosion risk classes, resulting in a similar occurrence histogram as Method 1.

5.3.5 Accuracy assessment

To assess the accuracy of the erosion risk maps, field estimates of erosion risk were compared against mapping results for the same locations. The frequency of occurring combinations of estimates and mapping results were tabulated in a confusion matrix. Two definitions were used to obtain a quantitative measure of accuracy (A). The first (A_1) strictly defines a correct classification as one where the field estimate of erosion risk is the same as the mapping result. For a confusion matrix, this implies the sum of the diagonal elements divided by the total number of observations, or in an equation:

$$A_1 = \frac{\sum\limits_{i=1}^{5} u_{i,i}}{\sum\limits_{i=1}^{5} \sum\limits_{j=1}^{5} u_{i,j}} \cdot 100\% \tag{5.2}$$

where $u_{i,j}$ represents a specific number in the confusion matrix. The second definition (A_2) is more flexible and assumes that a one-class difference is acceptable. This may be justified because the classes are not defined on a nominal scale, but on an ordinal scale. If we state that a classified pixel with a certain erosion risk is considered correctly classified when there is a maximum difference of one class (e.g. low erosion risk in classification is correct if field estimate is very low, low, or medium), we obtain the following equation:

$$A_2 = \frac{\sum\limits_{i=1}^{5} u_{i,i} + \sum\limits_{i=2}^{5} u_{i,i-1} + \sum\limits_{i=1}^{4} u_{i,i+1}}{\sum\limits_{i=1}^{5} \sum\limits_{j=1}^{5} u_{i,j}} \cdot 100\% \tag{5.3}$$

To assess the accuracy of the erosion risk map constructed with Method 1, 51 field estimates of erosion risk were used that were not included for calibrating the decision tree. To assess the accuracy of Method 2, all 151 field estimates were included.

5.4 Results and discussion

5.4.1 Results Method 1

The classified slope map is presented in Fig. 5.3a. The map shows steep slopes, which at several places are more than 40 %. In the field, steeper slopes of up to 90 % were measured. However, the high local slope variations cannot be represented with the relatively coarse SRTM DEM. Consequently, very low correlations were found between field measurements
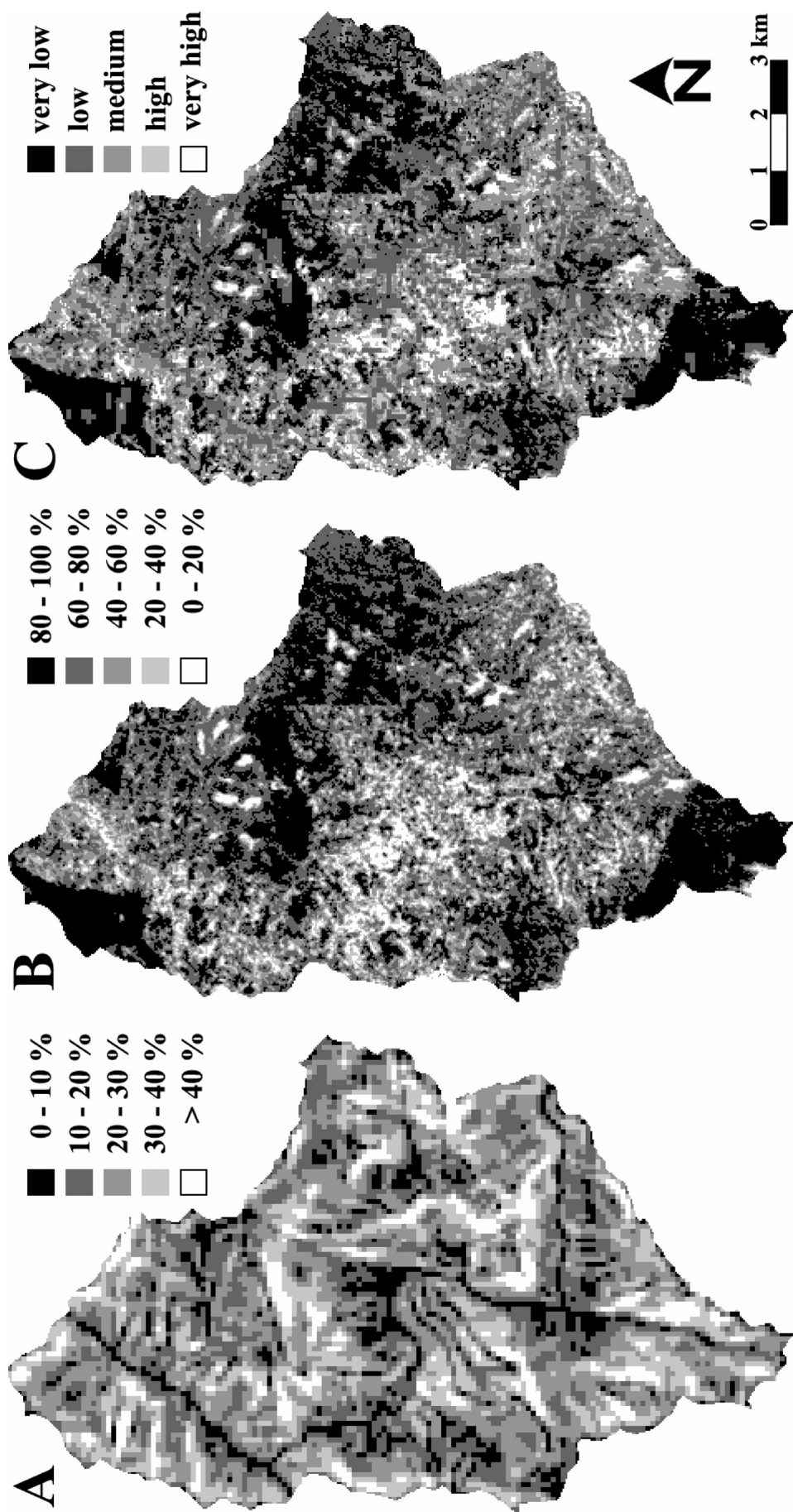
Figure 5.3   *Results of Method 1: (A) slope map from SRTM DEM; (B) Landsat-derived fractional vegetation cover (FVC) map; and (C) erosion risk map.*

and calculated slopes from the DEM, with slope inclinations derived from the DEM generally being lower than the field measurements. This is supported by other studies, which showed that reduced DEM resolution negatively affects slope accuracy especially in areas of steep elevation changes like in the Baga watershed (e.g. Chang and Tsai, 1991; Gao, 1997) and cause a systematic underestimation of slope (Hill and Neary, 2005). Nevertheless, from the acquired field knowledge on the watershed it can be concluded that the general slope pattern is well represented. Although for physically-based erosion modelling exact slope values are very important (Warren et al., 2004), for the qualitative approach presented here a proper representation of slope pattern is sufficient.

The relationship between FVC and NDVI was determined using linear regression and yielded the following equation:

$$NDVI = 0.00325FVC + 0.437 \tag{5.4}$$

having a R^2 of 0.80 (Fig. 5.4). Linear relationships between NDVI and FVC with comparable correlation coefficients were also found for, e.g., semi-arid grassland regions in Kansas (Rundquist, 2002) and in China (Zha et al., 2003) and for agricultural and forested areas in Germany (Wittich and Hansing, 1995). Others have suggested that a second order polynomial regression provides a better relationship (e.g. Carlson and Ripley, 1997; Purevdorj et al., 1998), but no evidence was found for this in our study (Fig. 5.4).

The fractional vegetation cover was calculated for the complete Baga watershed through inversion of Eq. 5.4. Classification of the outcomes resulted in the FVC map (Fig. 5.3b). The highest FVC is found in the forested areas, generally on high elevations. The lowest FVC class corresponds largely to bare fields that are cleared for cultivation of annual crops during the upcoming long rains.
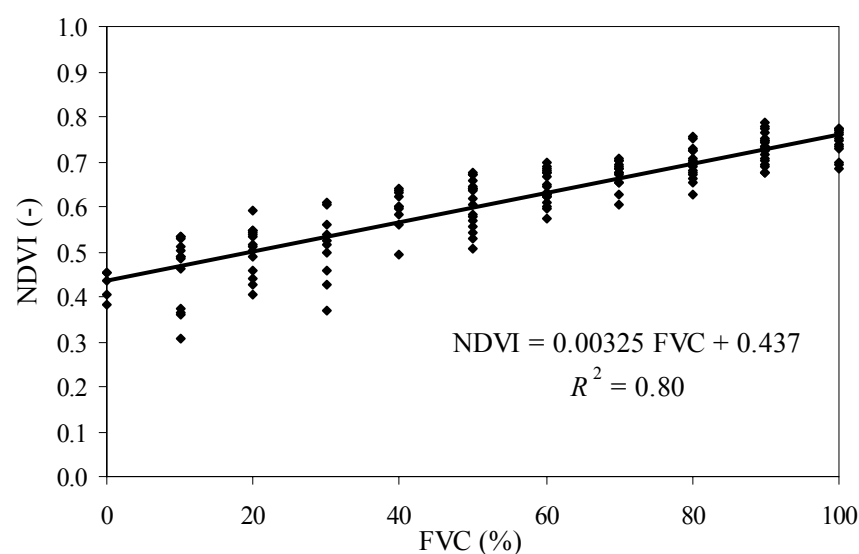

Figure 5.4   *Relationship between fractional vegetation cover (FVC), estimated in the field, and calculated NDVI-values from the Landsat image (n=151)*

The erosion risk map was constructed using a decision tree that combined the obtained FVC and slope classes. The development of this decision tree followed a calibration procedure, in which for each FVC-slope class pair (in total 25 different possible pairs) the optimal erosion risk class was determined, using the 100 field estimates set aside for calibration. Optimal refers to the number of field estimates falling in the different risk classes. For instance, six field locations coincided with the pair 'FVC = 80-100 %; slope = 30-40 %'. Of these six locations, the field estimate of erosion risk was four times 'very low' and two times 'low'. Therefore the decision tree assigns 'very low' to this FVC-slope class pair. However, some pairs did not coincide with any field estimates, e.g. 'FVC = 0-20 %; slope = >40 %'. For such cases the assigned class was based on surrounding pairs. For the previous example this resulted in the class 'very high', because this class was already assigned to the pair 'FVC = 0-20 %; slope = 30-40 %'. If the optimal classification of a certain pair, based on the field estimates, differed from surrounding pairs, the class was changed to obtain a logical sequence. The resulting decision tree is presented in Table 5.1. The confusion matrix of the calibration points is shown in Table 5.2.

Applying the decision tree to the FVC and slope map yielded the erosion risk map (Fig. 5.3c). Although the map has a similar appearance as the FVC map, close examination reveals several differences from which the effect of the slope becomes clear. The large areas of very low erosion risk correspond mostly to the forested areas, whereas very high erosion risk is mainly found on sloping fields of annual crop cultivation that were bare at the time the Landsat image was taken.

Table 5.1   Decision tree for the construction the erosion risk map (Method 1)

FVC (%)	Slope (%)	Erosion risk
80–100	0–40	Very low
80–100	>40	Low
60–80	0–30	Low
60–80	>30	Medium
40–60	0–10	Low
40–60	10–40	Medium
40–60	>40	High
20–40	0–10	Low
20–40	10–20	Medium
20–40	20–30	High
20–40	>30	Very high
0–20	0–10	Low
0–20	10–20	High
0–20	>20	Very high

Table 5.2   *Confusion matrix comparing field-based estimates of erosion risk with classification results for the 100 locations used for calibrating the decision tree (Method 1)*

Erosion risk map	Field estimate of erosion risk					
	Very low	Low	Medium	High	Very high	Total
Very low	10	3	1	0	0	14
Low	8	16	9	1	1	35
Medium	4	6	9	6	2	27
High	1	3	5	5	0	14
Very high	0	1	0	5	4	10
Total	23	29	24	17	7	100

The accuracy of the erosion risk map was analyzed with 51 independent field estimates of erosion risk. Table 5.3 presents the confusion matrix comparing these field estimates with the mapping results for the same locations. Using the accuracy definition of Eq. 5.2, A_1 becomes 35 %, which is low. However, under the assumption that a one-class difference is acceptable, the accuracy (A_2 from Eq. 5.3) increases to 80 %. This value seems to indicate that areas with respectively low and high erosion risk can be reasonably well identified for the Baga watershed using Method 1. Misclassifications with more than one class difference from the field estimates (10 points) appeared to be randomly distributed within the study area. No clear reason was found for this misclassification.

Table 5.2   *Confusion matrix for validation of the erosion risk map (Method 1)*

Erosion risk map	Field estimate of erosion risk					
	Very low	Low	Medium	High	Very high	Total
Very low	6	5	0	0	0	11
Low	7	6	3	2	0	18
Medium	2	3	3	2	2	12
High	0	1	0	2	0	3
Very high	0	1	2	3	1	7
Total	15	16	8	9	3	51

5.4.2 Results Method 2

The automatic classification of NDVI and slope values in equal frequency classes resulted in the class limits presented in Table 5.4. The interval for each range is different because the only classification criterion is that each class occupies 20 % of the study area. An erosion risk class was assigned to both factors based on the relative susceptibility of erosion. Fig. 5.5a and 5.5b show respectively the erosion risk class for the slope factor and the NDVI. The overall patterns are similar as Fig. 5.3a and 5.3b, but the appearance is different due to the distinct class limits and sizes.

The erosion risk map (Fig. 5c) was created by taking the minimum value of Fig. 5.5a and 5.5b for each location. Relatively flat or highly vegetated areas show a very low erosion risk, including river valleys and forested areas. The highest erosion risk is found on steep slopes with limited vegetation cover at the time of image acquisition. Table 5.5 presents the confusion matrix comparing 151 field estimates of erosion risk with the classification results for the same locations. From this matrix the accuracy was calculated: A_1 is 38 %, whereas A_2 is 81 %. This shows that Method 2 allows for a proper identification of areas with low and high erosion risk within the Baga watershed. Erroneous classifications that differ by more than one class showed a random distribution within the study area. Obvious causes for these misclassifications could not be identified.

Table 5.4   *Factorial erosion risk classes based on equal frequency of each class (Method 2)*

Factorial erosion risk classes	NDVI (–)	slope (%)
Very low (1)	> 0.735	< 14.6
Low (2)	0.695 – 0.735	14.6 – 20.9
Medium (3)	0.649 – 0.695	20.9 – 26.2
High (4)	0.580 – 0.649	26.2 – 32.9
Very high (5)	< 0.580	> 32.9

Table 5.5   *Confusion matrix for validation of the erosion risk map (Method 2)*

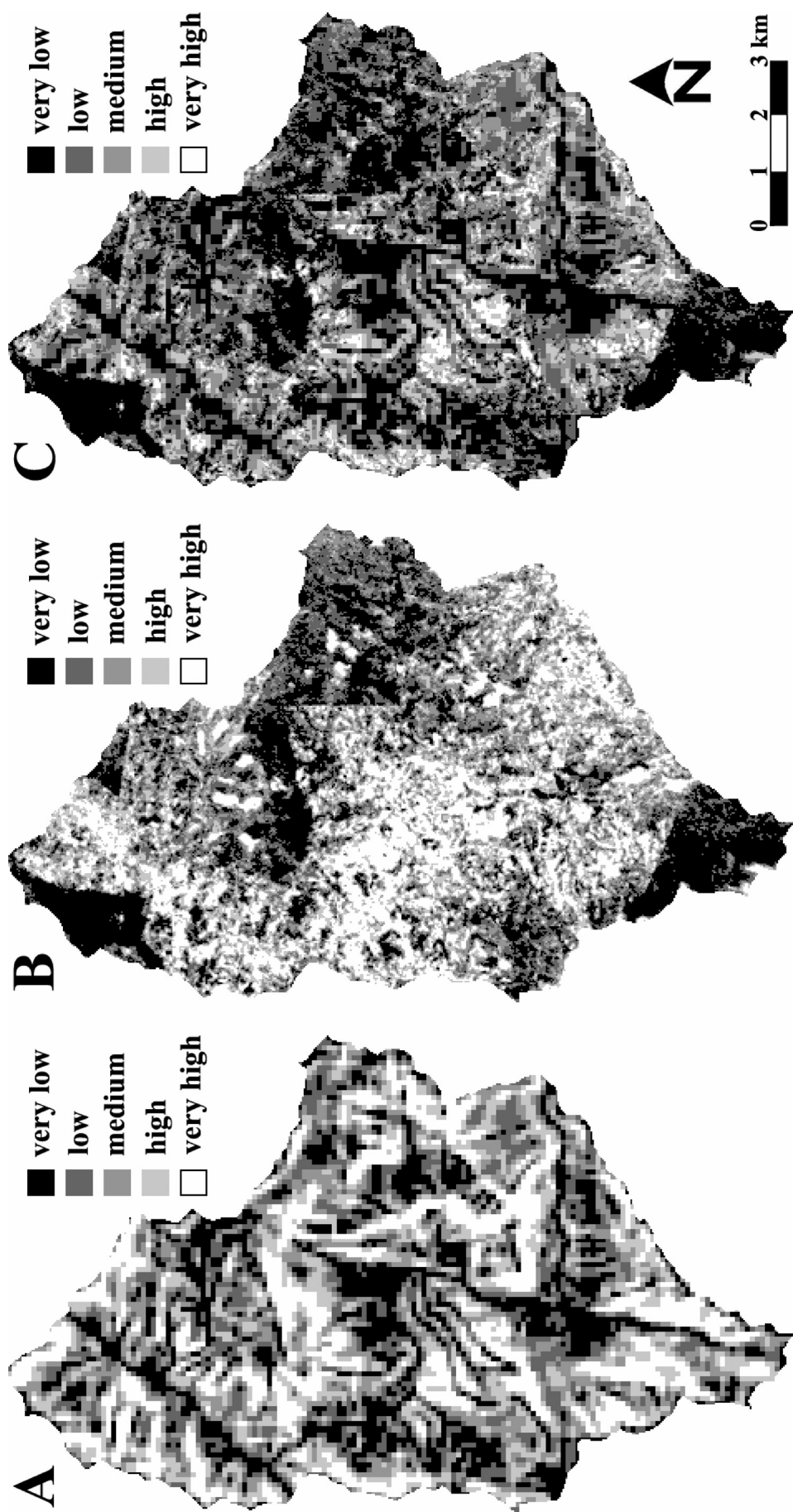| Erosion risk map	Field estimate of erosion risk					
	Very low	Low	Medium	High	Very high	Total
Very low	25	16	9	3	1	54
Low	8	13	6	5	2	34
Medium	5	13	9	8	1	36
High	0	3	8	8	3	22
Very high	0	0	0	2	3	5
Total	38	45	32	26	10	151

Figure 5.5   Results of Method 2: (A) erosion risk classes for slope; (B) erosion risk classes for NDVI; (C) erosion risk map created by taking the minimum of A and B.

93

5.4.3 Comparison of Method 1 and 2

Two methods for regional erosion risk mapping were presented that are similar in several ways: (1) the use of slope information derived from a SRTM DEM; (2) the use of the NDVI derived from a Landsat image to obtain a measure of vegetation cover; (3) the classification of slope and vegetation information in five classes; and (4) the application of a qualitative decision rule for integration of slope and vegetation factors. The main differences are: (1) Method 1 transforms the NDVI to fractional vegetation cover (FVC) using field data, whereas Method 2 uses NDVI directly; (2) Method 1 creates "logical" classes for slope and FVC, whereas Method 2 automatically assigns classes of equal area; (3) the decision rule for Method 1 is a decision tree that is constructed using field estimates of erosion risk, whereas the decision rule for Method 2 is a simple minimum-operator.

The relative occurrence of the resulting five erosion risk classes within the Baga watershed is presented in Fig. 5.6. The histograms of both methods are similar, with major differences occurring in classes 'very low' and 'medium'. The erosion risk maps of Method 1 and 2 (Fig. 5.3c and 5.5c) show some differentiating features. For example Method 1 is more sensitive to the vegetation factor, whereas Method 2 clearly shows the location of river valleys as a strong determining factor for low erosion risk. This is not surprising because of the different methods used for data integration. However, when both maps are compared quantitatively, differences appear to be small. Fig. 5.7 shows the absolute class difference between both maps, and the percentage of the study area where these class differences occur. Nearly 93 % of the study area has a maximum class difference between both methods of only one class. This implies that both maps are rather comparable. Higher class differences occur scattered over the watershed, and are mostly areas with relatively little vegetation cover and low slopes.
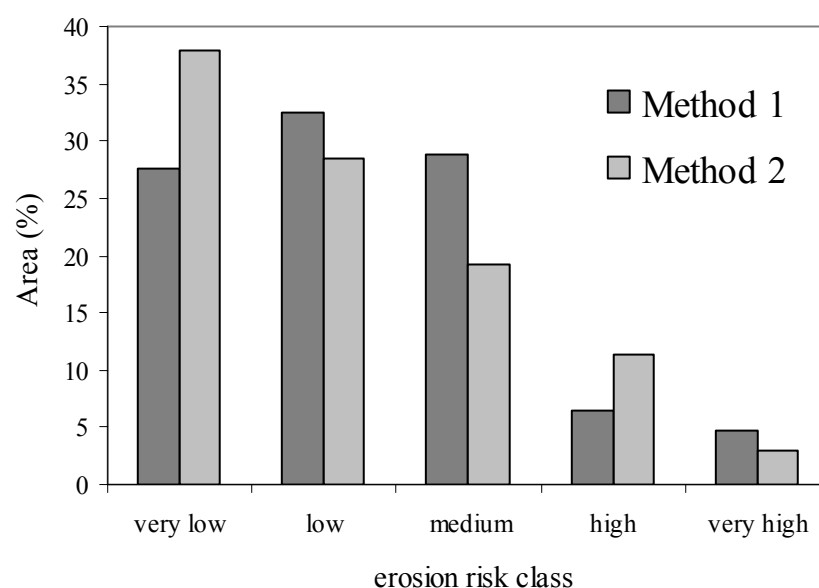

Figure 5.6   Histogram of erosion risk class occurrence within Baga watershed for both methods
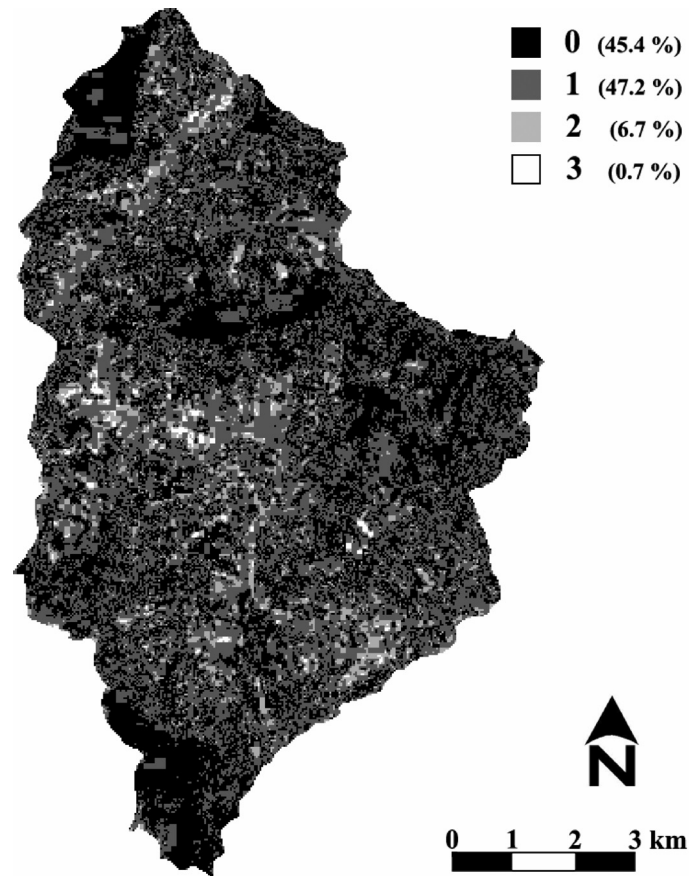
Figure 5.7   Absolute class difference between Method 1 and 2. Within brackets the frequency of occurrence is indicated for the Baga watershed.

In spite of the low accuracy A_1 for both methods (35 % for Method 1, and 38 % for Method 2), the accuracy A_2 is rather high (80% and 81 %). This means that both erosion risk classifications have a similar accuracy. The use of field data within the methodology did therefore not contribute to increased map quality, judging from the field estimates of erosion risk. Based on the accuracy assessment, both methods seem to provide a proper identification of respectively high and low erosion risk areas. Because of the ease of application, the slightly higher accuracy, and the high correspondence between both results, Method 2 is preferred over Method 1 for the mapping of erosion risk within the Baga watershed.

5.4.4 General discussion

The assessment of the map accuracy for both methods was solely based on a limited number of field estimates of erosion risk. Ideally the field survey would include all the locations (pixels) shown in the map, but this is practically impossible. Nevertheless, it would be of interest to obtain field knowledge on the locations that show a high difference between both maps in Fig. 5.7. In this study however, the field survey was executed before the map construction, and the area has not been revisited later.

The qualitative estimates of erosion risk in the field are no hard figures, because the estimates depend to some extent on the person executing the survey. Although the criteria for the estimation were clear, it is possible that a different person assigns more importance to a particular factor at a specified location. For that reason, only five classes were differentiated and the estimates were executed in collaboration with a local extension officer, to obtain a more balanced estimate of erosion risk. It was believed that this resulted in a proper qualitative estimate. It makes sense however to apply a flexible definition of accuracy when using such ordinal qualitative estimates, as was done here through the use of Eq. 5.3. Okoba (2005) performed a study to standardise a field-based approach for qualitative erosion assessment based on local indicators, but this has not been applied during this study.

Other possibilities for validating the constructed erosion risk maps include the execution of erosion measurements (Stroosnijder, 2003) or the performance of more quantitative surveys for example through the repetitive measurement of rill volumes (Herweg, 1996). However, such measurements are extremely labour intensive, and require long time series of data in order to make a proper assessment of the occurring erosion at a certain location. In most cases it is therefore not feasible to perform measurements in many different locations in order to validate regional erosion risk maps. For this reason many regional erosion studies create maps but do not provide any validation of these maps (e.g. Jürgens and Fander, 1993; Lu et al., 2004; Reusing et al., 2000; Shrimali et al., 2001; Vaidyanathan et al., 2002). This makes it hard, if not impossible, to assess the validity of the methods applied for the region and scale under study. Therefore, we believe that the qualitative field-based estimation of erosion risk provides a good alternative for validating regional erosion maps and mapping methodologies. Proper timing of the field survey is very important, because erosion determining factors and erosion features show a strong temporal trend. Here a clear choice was made to execute the survey at a moment of high erosion risk (little soil cover due to land preparation), but when few erosion features occurred.

In this study two simple methods for regional erosion risk mapping were presented that only address the factors slope and vegetation, which could be derived from readily available data. In spite of using only these factors, we recognize that other factors are important for the occurrence and intensity of erosion processes, like soil properties and rainfall intensity. Moreover important additional information could potentially be derived from the data sources used, such as land cover classes and topographic attributes. For the West Usambara Mountains accurate land cover classification using Landsat imagery is however difficult, due to the small-scale fields covered with a variety of crops, the presence of dispersed trees, and the rugged topography causing shadowing effects. For this purpose, also additional detailed field data would be required. Additional topographic attributes like slope length do not have much physical meaning when using a 90-m resolution DEM because important micro-topography features reducing the slope length are not represented. Therefore, the use of such additional information would likely introduce additional uncertainty into the erosion risk assessment, due to the limited quality of the information that can be obtained.

Following the accuracy assessment it appears that the combination of the two measures used for slope and vegetation allowed for a good representation of the spatial distribution of erosion risk. This underlines the conclusion of Van Rompaey and Govers (2002), which state that for optimal predictions of erosion at the regional scale the complexity of the mapping method has to be in balance with the quality of the available input data. Therefore, with limited availability of input data, as was the case in this study, a simple method is required. For a different part of the East African Highlands, in Kenya, Okoth (2003) used regression analysis to relate erosion determining factors to erosion features recorded in the field and from aerial photographs. Both for the field scale and the landscape scale, the factors that were selected and best explained the presence of the erosion features, were slope and vegetation cover. This seems to indicate that for regional scale erosion risk mapping in different parts of the East African Highlands, integration of the factors slope and vegetation cover provides accurate results. It would be of interest to test whether this is true for other regions of the East African Highlands.

Potentially even outside the East African Highlands, particularly Method 2 may be useful for obtaining a quick identification of high erosion risk areas within a region, especially when otherwise little information is available. As classes are defined automatically based on equal occurrence in the region, the method has a high flexibility to adapt to other environments with different slope and vegetation cover characteristics. The method simply pinpoints the areas where relatively steep slopes coincide with limited vegetation cover. For environments where spatial variability of erosion processes is for an important part determined by other factors (such as soil characteristics) this approach will probably fail, unless there is a strong correlation between the soil characteristics and vegetation cover. A great advantage of applying such an approach over the application of e.g. erosion models, is the readily availability of the data, at least for regions between 60°N and 57°S latitude. Obviously, a proper validation of the method in other environments would be required.

The purpose of the erosion assessment, as defined in the introduction, was to provide a qualitative risk map to be used for prioritizing soil and water conservation efforts. The erosion risk maps presented in Fig. 5.3c and 5.5c should not necessarily be seen as the end product for this particular case study. The presented raster-based maps show where problem areas are located with respect to erosion. However, as soil and water conservation programmes in the area function through the application of the Catchment Approach, it may be of more interest for the local extension agency to construct a map showing erosion risk per focal area, through e.g. averaging the pixel values per focal area. This approach resembles the vast amount of literature from India on (large) watershed prioritization (e.g. Jain and Goel, 2002; Khan et al., 2001). Here, we did not present the results in this way, because focal areas were not clearly defined and do not always coincide with hydrological catchments. However, the presented map is a base map that can be elaborated on for increased utility and improved readability by involved agencies.

Many possible ways exist for qualitative data integration. In this study Method 1 used a decision tree, whereas Method 2 applied the minimum-operator. Other options include e.g.

the averaging, addition, or multiplication of factors. There is no standard method for qualitative erosion risk mapping, and it is often a personal choice of the cartographer or scientist which approach is chosen. Although most approaches are clearly documented, the fact that there is so much variability complicates their comparison. This is worsened by the different techniques applied for validation, and the often-encountered lack of validation. In this study two different methods that use the same data sources are compared using the same source of validation data. It appears that depending on the method chosen, results show some differences. However, the accuracy of both maps was comparable, for both around 80 %, and in nearly 93 % of the study region the two maps did not differentiate by more than one class. This may imply that the factors used and the way these factors can be described by the available data, are more important than the specific manner in which the data are integrated.

The two main data sources used in this study were the SRTM DEM and a Landsat image. Field data was used within the methodology for Method 1, but Method 2 did not require these data, and performed equally well. The only additional data used in this study were the aerial orthophotos for the precise georeferencing of the Landsat image. This was necessary for creating a correct link with the GPS-points recorded in the field. Therefore stating that we only used readily available data would not be entirely correct. For the application of the methodology in other areas we cannot assume that orthophotos are always available. However, a good fit of the data can generally also be obtained when using 1:50,000 topographic maps which exist for most East African countries. Otherwise, the georeferencing information that is contained in both the SRTM DEM and Landsat imagery usually allows for an acceptable overlay of the two sources.

A static representation of erosion risk is given in this study through the use of only one Landsat image. The timing of the image is therefore very important. Although here the image was taken just before the start of the long rains, which is thought to be the most erosive period, it is known that more fields were cleared for cultivation of annual crops between the image date and the start of the rains. Ideally the image would thus have been taken a month later to include the bareness of those fields in the analysis. However, availability of good-quality optical satellite images is quite low in the area due to frequent cloud cover. The image used was therefore the optimal solution, and the timing can be considered quite good. When analyzing vegetation cover for the purpose of assessing erosion risk in any region, it is of utmost importance to obtain a properly timed image with respect to the most erosive season. Besides Landsat, other optical satellite images like ASTER or SPOT are equally good options. Although synthetic aperture radar (SAR) data also has the potential to assess vegetation characteristics (e.g. Brisco and Brown, 1998; Kasischke et al., 1997), the radar lay-over and shadow effects complicate its effective use in mountainous environments. Multi-temporal optical imagery acquired during the same season in different years would allow a monitoring of changes in erosion risk due to e.g. improved soil and water conservation. In the case of method validation through the execution of field surveys, the fieldwork should ideally be planned near the image acquisition date.

5.5   Conclusions

The main conclusions to be drawn from this study are the following:

- The qualitative integration of the factors vegetation cover and slope allows for an accurate mapping of soil erosion risk in the Baga watershed.
- Good-quality information on these factors can be derived from a limited amount of readily available data, including an SRTM DEM and a Landsat image.
- A method that mapped erosion risk as the minimum of automatically defined NDVI and slope classes performed very similar to a more sophisticated approach that used a decision tree, which combined slope and NDVI-derived fractional vegetation cover classes.
- The simpler method has a high potential to provide a quick and proper identification of erosion risk in different regions within the East African Highlands, and possibly also in other environments.
- Timing of the Landsat image is very important for accurate risk assessment and should be during or just before the most erosive season, when soils are less protected and rainfall intensity becomes high.

References

Ananda J, and Herath G. 2003. Soil erosion in developing countries: a socio-economic appraisal. *Journal of Environmental Management* 68 (4): 343-353.

Brazier RE, Beven KJ, Freer JF, and Rowan JS. 2000. Equifinality and uncertainty in physically based soil erosion models: application of the GLUE methodology to WEPP - the Water Erosion Prediction Project - for sites in the UK and USA. *Earth Surface Processes and Landforms* 25 (8): 825-845.

Brisco B, and Brown RJ. 1998. Agricultural applications with radar. *In*: Henderson FM, and Lewis AJ (Editors), Principles and Applications of Imaging Radar - Manual of Remote Sensing. John Wiley & Sons, Inc., New York (NY), USA: pp. 381-406.

Carlson TN, and Ripley DA. 1997. On the relation between NDVI, fractional vegetation cover, and leaf area index. *Remote Sensing of Environment* 62 (3): 241-252.

Chander G, and Markham B. 2003. Revised Landsat-5 TM radiometric calibration procedures and postcalibration dynamic ranges. *IEEE Transactions on Geoscience and Remote Sensing* 41 (11): 2674-2677.

Chang KT, and Tsai BW. 1991. The effect of DEM resolution on slope and aspect mapping. *Cartography and geographic information systems* 18 (1): 69-77.

Conte CA. 1999. The forest becomes desert: forest use and environmental change in Tanzania's West Usambara Mountains. *Land Degradation & Development* 10 (4): 291-309.

De la Rosa D, Mayol F, Moreno JA, Bonsón T, and Lozano S. 1999. An expert system/neural network model (ImpelERO) for evaluating agricultural soil erosion in Andalucia region, southern Spain. *Agriculture, Ecosystems and Environment* 73 (3): 211-226.

Gao J. 1997. Resolution and accuracy of terrain representation by grid DEMs at a micro-scale. *International Journal of Geographical Information Science* 11 (2): 199-212.

Herweg K. 1996. Field Manual for Assessment of Current Erosion Damage. SCRP Ethiopia, and Centre for Development and Environment, University of Berne, Switzerland: 69 pp.

Hill AJ, and Neary VS. 2005. Factors affecting estimates of average watershed slope. *Journal of Hydrologic Engineering* 10 (2): 133-140.

Holben B, and Justice C. 1981. An examination of spectral band ratioing to reduce the topographic effect on remotely sensed data. *International Journal of Remote Sensing* 2 (2): 115-133.

Jain SK, and Goel MK. 2002. Assessing the vulnerability to soil erosion of the Ukai Dam catchments using remote sensing and GIS. *Hydrological Sciences Journal* 47 (1): 31-40.

Jetten V, De Roo A, and Favis-Mortlock D. 1999. Evaluation of field-scale and catchment-scale soil erosion models. *Catena* 37 (3-4): 521-541.

Jetten V, Govers G, and Hessel R. 2003. Erosion models: quality of spatial predictions. *Hydrological Processes* 17 (5): 887-900.

Johansson L. 2001. Ten Million Trees Later: land use change in the West Usambara Mountains. The Soil Erosion Control and Agroforestry Project in Lushoto District 1981-2000. GTZ, Eschborn, Germany: 163 pp.

Jürgens C, and Fander M. 1993. Soil erosion assessment and simulation by means of SGEOS and ancillary digital data. *International Journal of Remote Sensing* 14 (15): 2847-2855.

Kaoneka ARS, and Solberg B. 1994. Forestry related land use in the West Usambara mountains, Tanzania. *Agriculture, Ecosystems and Environment* 49 (2): 207-215.

Kasischke ES, Melack JM, and Dobson MC. 1997. The use of imaging radars for ecological applications - a review. *Remote Sensing of Environment* 59 (2): 141-156.

Khan MA, Gupta VP, and Moharana PC. 2001. Watershed prioritization using remote sensing and geographical information system: a case study from Guhiya, India. *Journal of Arid Environments* 49 (3): 465-475.

Kirkby MJ, Imeson AC, Bergkamp G, and Cammeraat LH. 1996. Scaling up processes and models from the field plot to the watershed and regional areas. *Journal of Soil and Water Conservation* 51 (5): 391-396.

Kummerow C, Barnes W, Kozu T, Shiue J, and Simpson J. 1998. The Tropical Rainfall Measuring Mission (TRMM) sensor package. *Journal of Atmospheric and Oceanic Technology* 15 (3): 809-817.

Lal R. 1988. Soil degradation and the future of agriculture in sub-Saharan Africa. *Journal of Soil and Water Conservation* 46 (6): 444-451.

Lu D, Li G, Valladares GS, and Batistella M. 2004. Mapping soil erosion risk in Rondonia, Brazilian Amazonia: Using RUSLE, remote sensing and GIS. *Land Degradation & Development* 15 (5): 499-512.

Mbaga-Semgalawe Z, and Folmer H. 2000. Household adoption behaviour of improved soil conservation: the case of North Pare and West Usambara Mountains of Tanzania. *Land Use Policy* 17 (4): 321-336.

Meliyo J, Kabushemera W, and Tenge AJ. 2002. Characterization and mapping soils of Kwalei subcatchment, Lushoto District, Agricultural Research Institute Mlingano, Tanga, Tanzania.

Merritt WS, Letcher RA, and Jakeman AJ. 2003. A review of erosion and sediment transport models. *Environmental Modelling & Software* 18 (8-9): 761-799.

Okoba BO. 2005. Farmers' indicators for soil erosion mapping and crop yield estimation in central highlands of Kenya. Ph.D. Thesis, Wageningen University, Wageningen, The Netherlands: 143 pp.

Okoth PF. 2003. A hierarchical method for soil erosion assessment and spatial risk modelling: a case study of Kiambu District in Kenya. Ph.D. Thesis, Wageningen University, Wageningen, The Netherlands: 213 pp.

Oldeman LR, Hakkeling RTA, and Sombroek WG. 1991. World map of the status of human induced soil degradation. ISRIC/UNEP, Wageningen, The Netherlands.

Pfeiffer R. 1990. Sustainable agriculture in practice: the production potential and the environmental effects of macro-contourlines in the West Usambara Mountains of Tanzania. Ph.D. Thesis, University Hohenheim, Stuttgart, Germany.

Pretty JN, and Shah P. 1997. Making soil and water conservation sustainable: from coercion and control to partnerships and participation. *Land Degradation & Development* 8 (1): 39-58.

Pretty JN, Thompson J, and Kiara JK. 1995. Agricultural regeneration in Kenya: the catchment approach to soil and water conservation. *Ambio* 24 (1): 7-15.

Purevdorj T, Tateishi R, Ishiyama T, and Honda T. 1998. Relationships between percent vegetation cover and vegetation indices. *International Journal of Remote Sensing* 19 (18): 3519-3535.

Rabus B, Eineder M, Roth A, and Bamler R. 2003. The shuttle radar topography mission: a new class of digital elevation models acquired by spaceborne radar. *ISPRS Journal of Photogrammetry and Remote Sensing* 57 (4): 241-262.

Renschler CS, and Harbor J. 2002. Soil erosion assessment tools from point to regional scales - the role of geomophologists in land management research and implementation. *Geomorphology* 47: 189-209.

Reusing M, Schneider T, and Ammer U. 2000. Modelling soil loss rates in the Ethiopian Highlands by integration of high resolution MOMS-02/D2-stereo-data in a GIS. *International Journal of Remote Sensing* 21 (9): 1885-1896.

Riaño D, Chuvieco E, Salas J, and Aguado I. 2003. Assessment of different topographic correction in Landsat-TM data for mapping vegetation types. *IEEE Transactions on Geoscience and Remote Sensing* 41 (5): 1056-1061.

Rundquist BC. 2002. The influence of canopy green vegetation fraction on spectral measurements over native tallgrass prairie. *Remote Sensing of Environment* 81 (1): 129-135.

Sandmeier S, and Itten KI. 1997. A physically-based model to correct atmospheric and illumination effects in optical satellite data of rugged terrain. *IEEE Transactions on Geoscience and Remote Sensing* 35 (3): 708-717.

Schoorl JM, Sonneveld MPW, and Veldkamp A. 2000. Three-dimensional landscape process modelling: the effect of DEM resolution. *Earth Surface Processes and Landforms* 25 (9): 1025-1034.

Shrimali SS, Aggarwal SP, and Samra JS. 2001. Prioritizing erosion-prone areas in hills using remote sensing and GIS - a case study of the Sukhna Lake catchment, Northern India. *International Journal of Applied Earth Observation and Geoinformation* 3 (1): 54-60.

Sonneveld BGJS. 2003. Formalizing expert judgements in land degradation assessment: a case study from Kenya. *Land Degradation & Development* 14 (4): 347-261.

Stroosnijder L. 2003. Measurement of erosion: is it possible? In: Gabriels D, and Cornelis W (Editors), Proceedings of the International Symposium on 25 Years of Assessment of Erosion. Ghent University, Ghent, Belgium: pp. 53-59.

Tenge AJ, De Graaff J, and Hella JP. 2004. Social and economic factors affecting the adoption of soil and water conservation in West Usambara highlands, Tanzania. *Land Degradation & Development* 15 (2): 99-114.

Thompson JA, Bell JC, and Butler CA. 2001. Digital elevation model resolution: effects on terrain attribute calculation and quantitative soil-landscape modeling. *Geoderma* 100 (1-2): 67-89.

Tucker CJ, Grant DM, and Dykstra JD. 2004. NASA's global orthorecticified Landsat data set. *Photogrammetric Engineering and Remote Sensing* 70 (3): 313–322.

Vaidyanathan NS, Sharma G, Sinha R, and Dikshit O. 2002. Mapping of erosion intensity in the Garhwal Himalaya. *International Journal of Remote Sensing* 23 (20): 4125-4129.

Van Rompaey AJJ, and Govers G. 2002. Data quality and model complexity for regional scale soil erosion prediction. *Geomorphology* 16 (7): 663-680.

Vigiak O, Okoba BO, Sterk G, and Groenenberg S. 2005. Modelling catchment-scale erosion patterns in the East African highlands. *Earth Surface Processes and Landforms* 30 (2): 183-196.

Vrieling A. 2006. Satellite remote sensing for water erosion assessment: a review. *Catena* 65 (1): 2-18.

Vrieling A, Sterk G, and Beaulieu N. 2002. Erosion risk mapping: a methodological case study in the Colombian Eastern Plains. *Journal of Soil and Water Conservation* 57 (3): 158-163.

Warren A. 2002. Land degradation is contextual. *Land Degradation & Development* 13 (6): 449-459.

Warren SD, Hohmann MG, Auerswald K, and Mitasova H. 2004. An evaluation of methods to determine slope using digital elevation data. *Catena* 58 (3): 215-233.

Wittich K-P, and Hansing O. 1995. Area-averaged vegetative cover fraction estimated from satellite data. *International Journal of Biometeorology* 38 (4): 209-215.

Wolock DM, and McCabe GJ. 2000. Differences in topographic characteristics computed from 100-and 1000-m resolution digital elevation model data. *Hydrological Processes* 14 (6): 987-1002.

Yair A, and Raz-Yassif N. 2004. Hydrological processes in a small arid catchment: scale effects of rainfall and slope length. *Geomorphology* 61 (1-2): 155-169.

Zevenbergen LW, and Thorne CR. 1987. Quantitative analysis of land surface topography. *Earth Surface Processes and Landforms* 12 (1): 47-56.

Zha Y, Gao J, Ni S, Liu Y, Jiang J, and Wei Y. 2003. A spectral reflectance-based approach to quantification of grassland cover from Landsat TM imagery. *Remote Sensing of Environment* 87 (2-3): 371-375.

Chapter 6

TIMING OF EROSION AND SATELLITE DATA: A MULTI-RESOLUTION APPROACH TO SOIL EROSION RISK MAPPING

Vrieling A, de Jong SM, Sterk G, and Rodrigues SC

6. Timing of erosion and satellite data: a multi-resolution approach to soil erosion risk mapping

Abstract

Erosion is an erratic process and occurs when high-intensity rainfall coincides with limited vegetation cover. The timing of erosion events has implications on the selection of satellite imagery, used to describe spatial patterns of protective vegetation cover. This study proposes a method for erosion risk mapping using multi-temporal and multi-resolution satellite data. The specific objectives of the study are: (1) to determine when during the year erosion risk is highest using coarse-resolution data, and (2) to assess the optimal timing of available medium-resolution images to spatially represent vegetation cover during the high erosion risk period. The analyses were performed for a 100-km^2 pasture area in the Brazilian Cerrados during one full growing season. The first objective was studied by qualitatively comparing 3-hourly TRMM rainfall estimates with MODIS NDVI time series. November and December were identified as the months with highest erosion risk. The second objective was investigated using a time series of six available ASTER images acquired between August 2002 and August 2003. Persistent cloud cover clearly limited image acquisition during high erosion risk periods. For each ASTER image the NDVI was calculated and classified into five equally-sized classes. Low NDVI was related to high erosion risk and vice versa, while a DEM was used to set approximately flat zones to very low erosion risk. The six resulting risk maps were compared with erosion features, visually interpreted from a fine-resolution QuickBird image. Results from the October ASTER image gave highest accuracy (84%), indicating that images acquired shortly before the first erosion events show best results for the Brazilian Cerrados. The presented approach for erosion risk mapping using both coarse-resolution temporal data for determining erosion periods and medium-resolution data for effective mapping uses only readily available data and is fast and straightforward, and may thus easily be applied in other areas with high spatial and temporal variability of vegetation cover.

6.1 Introduction

In many regions around the world, soil erosion by runoff is one of the main processes reducing the soil productivity by removing fertile topsoil layers, thus decreasing levels of organic matter and nutrients. Furthermore, it often causes negative downstream impacts, such as the sedimentation of soil material in reservoirs or damage to infrastructural facilities like houses, roads and canals (Morgan, 2005). Because soil erosion has a high spatial variability, it is useful to obtain knowledge on where erosion is occurring, for example for the planning of mitigation measures. Many efforts have been made to map erosion at different scales and in different regions around the world. Although sometimes maps are constructed with deterministic erosion models describing the erosion processes and resulting in quantitative

outcomes, especially for larger regions (> 50 km^2) it is more common to construct erosion risk maps. Erosion risk usually indicates the relative risk that erosion will occur at a certain location as compared to other locations in the region mapped. Erosion risk maps are constructed using either erosion models or more qualitative approaches (e.g. Vrieling et al., 2002). Although erosion models yield absolute soil loss values, their outcome is generally used in qualitative terms.

Satellite remote sensing can offer important inputs for the mapping of erosion risk (Vrieling, 2006). Some options exist for direct detection of erosion, but these are mostly limited to semi-arid environments (Liu et al., 2004) or detection of large features such as permanent gullies (Vrieling et al., 2006a). High-resolution imagery like QuickBird (< 1 m) may however detect smaller features such as rills and signs of overland flow, but neither the price of these data nor the data volume would currently allow timely erosion detection over large areas. Therefore, the most important role of satellite data for erosion risk mapping is the assessment of erosion controlling factors. Although in semi-arid areas soil properties may be assessed with satellite data, for more vegetated (tropical) areas the use of satellite data is generally limited to assessing slope (from DEMs) and particularly vegetation (Vrieling, 2006). However, depending on the region this limitation need not be a constraint for erosion risk mapping, as some factors may be assumed spatially constant or directly related to vegetation cover. For example Vrieling et al. (2006b) showed that for a mountainous region in northeast Tanzania, erosion risk could be accurately mapped using only information on slope and vegetation cover.

Erosion is an erratic process and occurs usually during high-intensity rainfall events. Given a certain slope and soil type, much erosion occurs when high-intensity rainfall coincides with limited soil protection. Vegetation cover is one of the most important factors offering protection of the soil against erosion. Vegetation cover, and thus erosion risk, can however be highly variable during the year, depending on seasonal effects and land management. Using satellite data, different ways exist to deal with the spatial and temporal dynamics of vegetation cover. One approach is to create a land use map and apply a vegetation growth model for the different mapping units (e.g. using WEPP: Laflen et al., 1991). However, growth models cannot account for within-class spatial variability, nor for the effects of varying management practices and ad-hoc changes by land users, like for instance land clearing, burning, late sowing, or mismanagement. In many land use- and ecosystems, this variability cannot be discarded.

A different approach is the use of spectral vegetation indices. Unlike land use, a vegetation index is a continuous variable which allows detailed spatial and temporal comparison. Vegetation indices like the NDVI (normalized difference vegetation index) can easily be derived from data acquired by a variety of satellites operating at different spatial resolutions and long time series are available. Although the NDVI is affected by soil reflectance (Escadafal, 1994) and vegetation vitality (De Jong, 1994), it can give a proper relative indication of the spatial and temporal variability of vegetation cover (e.g. Carlson and Ripley, 1997; Purevdorj et al., 1998). NDVI has therefore often been used for assessing

the protective vegetation cover within erosion studies (e.g. De Jong et al., 1999; Jain and Goel, 2002; Symeonakis and Drake, 2004).

Time series of NDVI images, combined with temporal rainfall data, allow determining where and when erosion can be expected to occur. Erosion risk is high, if low NDVI values coincide with high rainfall intensities. However, a problem for detailed temporal analysis of NDVI is the persistent cloud cover, which especially in humid (tropical) regions hampers frequent observation of the land surface. In these regions, cloud cover is particularly problematic during periods of high-intensity rainfall. At coarse resolution (250-m and above) images are acquired frequently and thus good opportunities may exist for obtaining cloud-free scenes (either individual scenes or composite products), also during difficult periods. However, at medium (10-30 m) resolution image acquisition is far less frequent, often only once every 14 days and hence cloud cover often reduces image availability to less than five scenes per year. For mapping at the regional scale (50-10,000 km^2), medium-resolution data is required.

A detailed quantitative description of spatial and temporal changes of vegetation cover is not always necessary for effective mapping of erosion risk as we will show in this paper, because erosion risk is normally expressed in qualitative terms. Although vegetation cover may change, relative spatial patterns of vegetation cover may remain fairly constant during certain periods. What is required therefore is an accurate spatial representation of relative vegetation cover within a region, which is valid for the period when most erosion is expected to occur.

This paper proposes a new, two-step method for erosion risk mapping using multi-resolution multi-temporal satellite data. The method is applied in a 100-km^2 area in the Brazilian Cerrados and consists of (1) coarse-scale evaluation of the timing of erosive periods and (2) medium-resolution erosion risk mapping. At the medium resolution, vegetation patterns during the erosive period need to be accurately described. The timing of the erosive period thus dictates medium-resolution image selection, but due to limited image availability often at best an image can be obtained before or after this period. The specific objectives of this study are:

1. to determine during which period of the year erosion risk is highest, based on a combined analysis of rainfall and NDVI time series derived from coarse-resolution satellite data;
2. to assess which of the differently-timed available medium-resolution images allows for the optimal spatial representation of erosion risk and how does this optimal image timing relate to the erosive period found under the first objective.

All analyses were performed for one full year ranging from August (dry season) 2002 to August 2003. Erosion in this study is limited to processes of rill and sheet erosion. Gully erosion is a more complex phenomenon (Valentin et al., 2005) and was subject of another study in the same region (Vrieling et al., 2006a) and is not considered here.

6.2   Study area

The selected study area is located in the Brazilian Cerrados (Fig. 6.1). The Cerrados are a natural ecosystem of woody savannahs, which vary from nearly treeless grasslands with small shrubs to woodlands of semi-deciduous trees, with inclusions of gallery forest. The Cerrados cover nearly 23% of the land surface of Brazil (Furley, 1999). Since the 1970s the ecosystem increasingly suffered from the expansion of agriculture, cattle raising and forestry, not in the last place due to active government policies (Klink and Moreira, 2002). Current estimates of land conversions indicate that between 40 and 80 % of the Cerrados region has been affected by human activities (Jepson, 2005). Soil erosion is one of the major environmental impacts of these conversions (Rodrigues, 2002).

The 10 by 10 km study area is situated near the city of Uberlândia in the Triângulo Mineiro (Fig. 6.1). Slopes are between 0 and 15 % in a slightly undulating topography. Most soils consist of loamy sand, and are generally deep, with soil depths of up to 25 m. Average annual rainfall amounts 1500 mm, mostly falling during the rainy season between October and April. The seasonal changes in rainfall have a large effect on the vegetation cover, which is generally poor during the dry season (Ferreira and Huete, 2004). The present vegetation consists mainly of introduced pastures, with varying amounts of scattered trees and shrubs. Most pastures are degraded, thus having a high fraction of weeds and shrubs, and a relatively limited vegetative cover, including bare patches. Fig. 6.2 shows a nadir view of both a degraded pasture and a well-maintained pasture with good ground cover. Pasture degradation is caused by several factors, including inadequate management and overgrazing (Costa and Rehman, 1999). Because of this degradation, pastures are often renovated a number of years (5-10) after pasture installation. Pasture renovation signifies cutting and burning of present weeds, shrubs and trees, leaving the soil bare for several months. After ploughing new grass seeds are sown and the pasture develops during the rainy season.   Besides pastures, other vegetation types in the area include open and dense woodland, gallery forest, and some small patches of agricultural fields with principally maize or sugarcane.
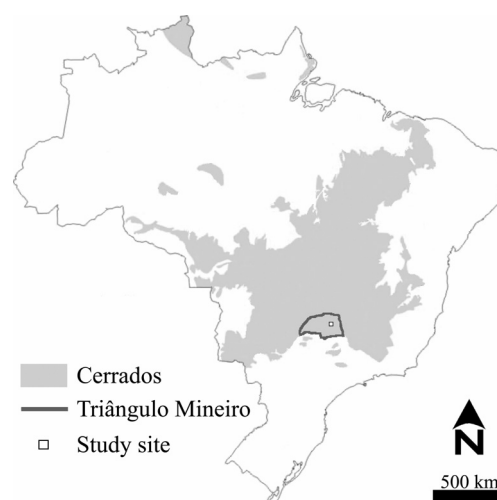

Figure 6.1   Location of the study site in Brazil (map source: EMBRAPA)
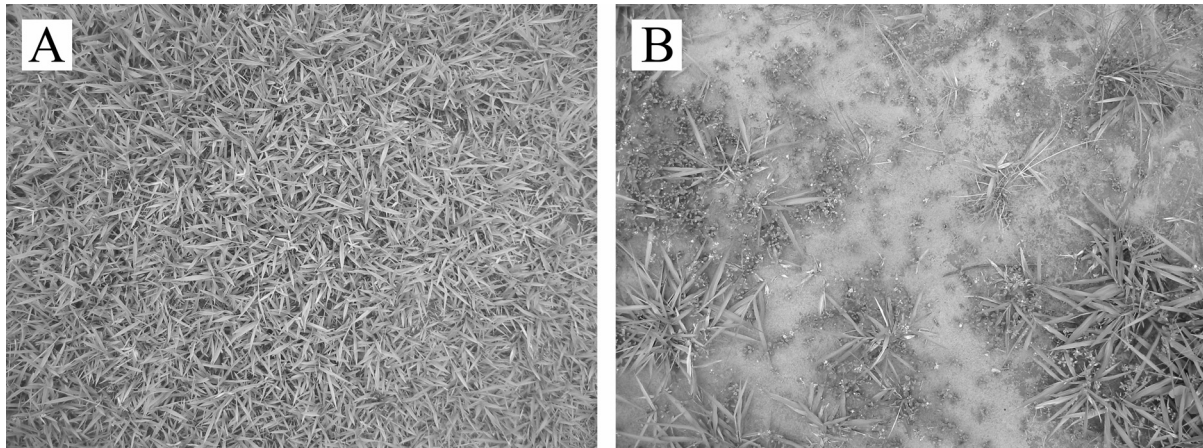
Figure 6.2   *Nadir photographs showing the vegetative ground cover of a well-maintained pasture (A), and of a degraded pasture with many bare parts having crusted soil (B). Both photographs were taken in January 2004 (wet season).*

Erosion occurs in the study area in several forms. The most visible form is gully erosion. Several large permanent erosion gullies are present with gully depths ranging from 4 to 25 m. The other forms are sheet and rill erosion and occur at many locations in the landscape at different rates (Baccaro, 1999). Sheet and rill erosion are caused by high rainfall intensity storms in combination with limited infiltration of water into the soil, generating Hortonian overland flow. Infiltration rate is low especially at areas with little vegetation cover where raindrop impact on the soil causes rapid crust formation and soil permeability is low due to the absence of a well-developed rooting system (Bezerra and Rodrigues, 2006). Resulting runoff concentrates and entrains sediments, causing the formation of rills.

Figure 6.3   *Strong rill development during the start of the rainy season (2003-2004) on a field prepared for pasture renovation.*

Erosion decreases pasture productivity and causes decline of soil nutrients and organic matter, which also negatively impacts options for future pasture renovation. Pasture renovation practices create periodically bare surfaces where strong erosion may occur during the beginning of the rainy season (Fig. 6.3). At many places, farmers try to reduce or control the erosion process by the construction of earthen contour bunds of about 0.50 to 1.00 m high, favouring infiltration and sedimentation of soil particles behind the bund. Nevertheless, poor construction and maintenance of the contour bunds often worsen the situation, due to minor depressions behind the bund where water concentrates and subsequently can cause ruptures. These bund failures can even trigger gully formation or gully advance in some cases.

6.3   Materials and methods

6.3.1 Assessment of high erosion risk periods with coarse-resolution data

Moments of high erosion risk between August 2002 and August 2003 were determined with low-resolution NDVI data, and rainfall intensity data, both freely available and acquired from satellite missions. MODIS (Moderate-Resolution Imaging Spectroradiometer) imagery from the Terra platform was used to determine the temporal variation of NDVI during the year. Two different MODIS products were used: MOD09GQK and MOD13Q1. MOD09GQK is a daily surface reflectance product at 250-m resolution with two spectral bands, red (620-670 nm) and NIR (841-876 nm), allowing NDVI calculation. Scenes were selected that were cloud-free and of good-quality for the entire study area. MOD13Q1 is a 16-day composite vegetation index product derived from daily surface reflectance data (using amongst others MOD09GQK as an input). The NDVI for the 16-day period is calculated on a pixel-by-pixel basis, in which images are selected or excluded based on quality, cloud cover and viewing geometry as described by Huete et al. (2002). MOD09GQK data therefore show NDVI values when cloudless scenes are available, whereas MOD13Q1 always provides a well-timed NDVI value for each pixel even during poor conditions (such as persistent cloud cover or bad quality during 16-day period, but not necessarily over the full study area at every instance).

Average NDVI time series were derived from both MODIS data sources for the most important land cover classes in the area, including forest, well-maintained pasture, degraded pasture, and new pasture. The only reason for using land cover classes in this study is to assess differences in temporal NDVI signatures and to analyse at what time of the year protective vegetation cover is limited. Forest is found along drainage lines and on some higher-lying flat areas, whereas pastures dominate the landscape. Section 6.2 describes the degraded and new pastures. Well-maintained pastures are characterized by a good vegetative ground cover with a low presence of weeds and are often found on less sloping land. Field knowledge obtained during the execution of field surveys was used as the basis for visual

interpretation of medium-resolution ASTER (Advanced Spaceborne Thermal Emission and Reflection Radiometer) imagery. In this way large representative areas of the above-mentioned classes were identified, thus allowing the generation of average NDVI time series with MODIS for each class.

The temporal variability of rainfall intensity was assessed using 3-hourly rainfall estimates obtained from the Tropical Rainfall Measurement Mission (TRMM) in combination with other satellites. These data are available starting from January 1998 and were obtained through the TRMM Online Visualization and Analysis System (TOVAS: http://disc2.nascom.nasa.gov/Giovanni/tovas/). TRMM is the first satellite carrying a precipitation radar. Active and passive instantaneous microwave measurements made by instruments onboard the satellite are combined with geosynchronous infrared rainfall estimates to obtain the 3-hourly data (Kummerow et al., 2000). The integration of the various data sources into one product is achieved using specific merging techniques described by Adler et al. (2000). The data are available at a 0.25° grid and the single grid-cell was selected in which the study area was completely included (in this case about 27-km resolution). Although the spatial resolution is low, it was assumed that a good indication can be obtained of when high rainfall intensities occur. Moreover, for risk mapping the exact location of the rainfall is less important than knowing the risk period. Recordings at 8-hour intervals of a rain gauge at 30-km distance from the study area showed the same period of high rainfall intensities for the 2002-2003 season as TRMM data. The advantage of using TRMM data is that these are available for any region between latitudes 50°N and 50°S, whereas rain gauge measurements do not always exist or are often hard to obtain. Three thresholds of 15, 20, and 30 mm rainfall per 3-hours were set to evaluate the moments of highest rainfall intensities. The thresholds are merely intended for clear graphical display in Fig. 6.6 and 6.7 (discussed in Section 6.4) and consequent analysis of the figures.

The two time series of information, i.e. times of low vegetation cover (low NDVI) and times of high intensity rainfall, were combined to determine high erosion risk periods in the study area. Erosion risk is considered high when high-intensity rainfall coincides with low NDVI (thus limited vegetation cover).

6.3.2 Optimal image timing for medium-resolution erosion risk mapping

After the rapid coarse-scale analysis of when erosion is expected to have occurred, we look at the implications of this for medium-resolution erosion risk mapping. A major problem is the generally low availability of cloud-free medium-resolution data in tropical regions. In this study 15-m resolution ASTER imagery was used, containing amongst others a red (630-690 nm) and a NIR (760-860 nm) spectral band, which allow NDVI calculation. ASTER is obtained from the same Terra platform as from which the MODIS images used in this study were acquired. Nearly continuous ASTER data acquisition requests were made during September 2002 until September 2003 through the Japanese ERSDAC (Earth Remote Sensing Data Analysis Center). This resulted in six good-quality images over the study area,

recorded on 9 September 2002, 11 October 2002, 4 March 2003, 23 May 2003, 24 June 2003, and 11 August 2003. The major observation gap is during the wet season between October and March, and is caused by cloud cover. ASTER surface reflectance products were used (AST_07: Thome et al., 1999) and they were geocoded using a panchromatic orthorectified QuickBird image. A first-order polynomial model with a cubic convolution resampling to a 12.5-m pixel size was applied, resulting in a positional accuracy of better than 10 m.

A DEM (digital elevation model) was obtained from 10-m interval contourlines digitized from a 1:25,000 topographic map. The DEM was constructed with the same raster definition as the ASTER images using the ArcGIS-implementation of the method of Hutchinson (1989). This DEM-source was preferred over other DEMs, like the free 90-m resolution SRTM (Shuttle Radar Topography Mission) DEM, because a similar resolution as the ASTER imagery could be obtained. An ASTER DEM was not used here because the resolution that can be obtained is 30-m (versus 15-m resolution ASTER imagery) and the quality was judged poor. Slope was calculated from the DEM using the slope definition of Zevenbergen and Thorne (1987).

Six different erosion risk maps were constructed by integrating the six individual ASTER images with the slope information based on a simple erosion risk mapping methodology described by Vrieling et al. (2006b). They used for a mountainous area in northern Tanzania a Landsat ETM+ image recorded just before the main rainy season when soils are bare, in combination with an SRTM DEM. Landsat-derived NDVI was classified into five classes, each covering 20% of the study area. Low NDVI-values corresponded with a high erosion risk and high NDVI-values with a low erosion risk. For slope (derived from the DEM) a similar classification was made, where low slope values corresponded with low erosion risk. The final qualitative erosion risk map was then constructed by taking the minimum of the two classifications at each location. High erosion risk thus occurs at places were low vegetation cover coincides with steep slopes.

For the study area in the Brazilian Cerrados a very similar approach was followed. For each ASTER image, NDVI-values were classified into five equal-area classes. These classes therefore fully depend on the relative occurrence of NDVI values within an individual ASTER scene. However, based on field knowledge and data, slope did not play such an important role here as in northern Tanzania, because clear erosion features were also observed at places with limited slope steepness. At the Tanzanian site slopes are a lot steeper (with slopes up to 90%), while at the Brazilian site the generally long slope lengths in combination with strong crust formation and consequently high runoff during rainfall events trigger erosion even on gentle slopes. Differences in slope length at the Brazilian site are greatly influenced by the good- or mal-functioning of contour bunds constructed (see Section 6.2), and may potentially only be described properly with a very detailed DEM, i.e. better than 1.0-m resolution. Because no clear indications existed for strong spatial differences of erosion based on slope length, erosion risk was based solely on the NDVI-classification, except for places were the slope was below 3%. At these very gentle slopes, erosion risk was assumed to be always very low.

The assumption that slope is of less importance in this study area, is supported by field observations at 331 locations, which were made between December 2003 and February 2004. At each location the slope was measured with an inclinometer, fractional vegetation cover (FVC) was visually evaluated, and an estimate of erosion risk was made. Erosion risk estimates were done on a scale of 1 to 5 (very low to very high erosion risk) and were based on the occurrence of erosion features (i.e. rills), and signs of concentrated overland flow. Fig. 6.4 shows how erosion risk relates to vegetation cover when discarding slopes lower than 3%. Erosion risk was generally low for low slopes, and the FVC-erosion risk relationship was optimal when using this 3% slope threshold value.

Unlike slope, vegetation cover changes substantially during the year due to seasonal changes and human impacts. Through NDVI classification, general patterns of vegetation cover are analysed, without considering exact quantitative values. These patterns also change during the year. Of course the approach followed here is rather basic to assess erosion risk almost solely on the basis of vegetation cover. However, the method is fast and easy to use and yields spatial overviews of regional erosion risk. Because a clear relationship exists between the erosion risk and vegetation cover (Fig. 6.4), the intention here is to indicate when the vegetation patterns described by the NDVI classes best correspond with patterns of erosion risk. For that purpose, the six generated maps (Fig. 6.8 to be discussed in Section 6.4.2) need to be compared individually against validation data. Thus an evaluation can be made of the optimal image timing of satellite data to describe patterns of protective vegetation cover, as related to the erosion risk during a specific year.

$$FVC = -13.9 \text{ erosion risk} + 102.0$$
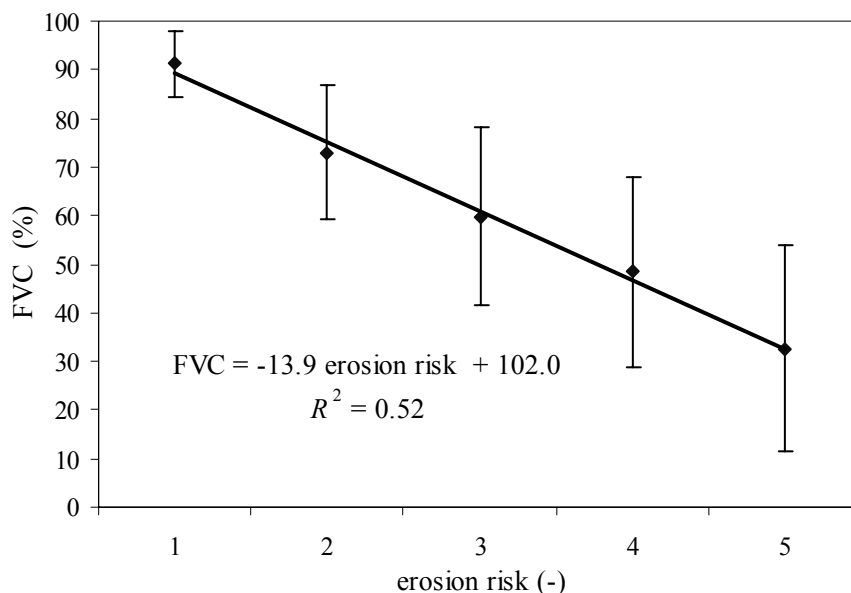$$R^2 = 0.52$$

Figure 6.4   Relationship between erosion risk and fractional vegetation cover (FVC) for slopes higher than 3%. Both erosion risk and FVC were estimated in the field. The figure shows average FVC values for each erosion risk class (1 = very low, 5 = very high) together with the standard deviation. The equation and R^2 are calculated using all 311 observations
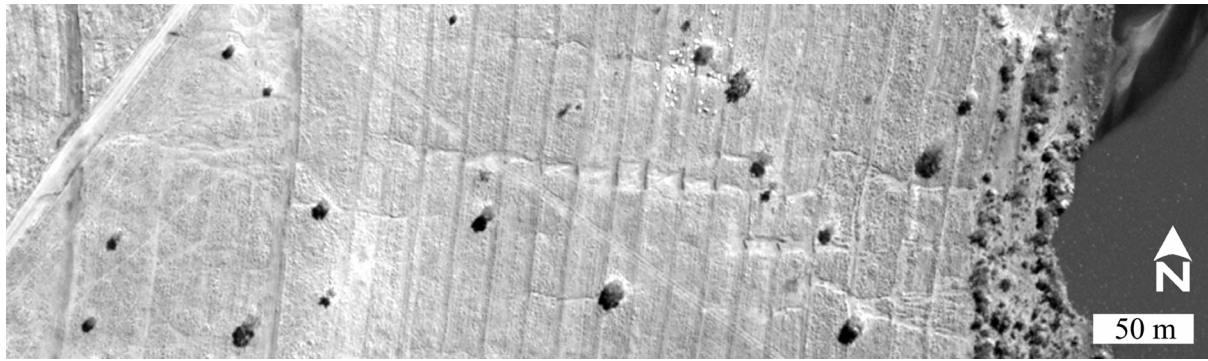
Figure 6.5   *QuickBird image (August 2003) of small part of study area. Concentrated runoff patterns can be observed, starting from the dirt road, at the left of the image. Subsequent failures of contour bunds are clearly visible, of which various were repaired later. On the right a part of a large reservoir can be seen. Pasture renovation was initiated here in the dry season of 2002.*

6.3.3 Validation of erosion risk maps with fine-resolution data

The six erosion risk maps were evaluated using information obtained from a panchromatic orthorectified QuickBird image acquired on 4 August 2003. Although field observations were also available (Section 6.3.2), it was preferred to evaluate the erosion risk maps using only the QuickBird information, which was interpreted using field knowledge. The reason is that field observations were done between December 2003 and February 2004, and therefore correspond to another wet season than when the ASTER images were acquired (from September 2002 to August 2003). As a result other erosion features may have formed which relate to more recent changes in vegetation cover and some erosion features may have been removed by tillage or pasture renovation practices. The QuickBird image was acquired after the 2002-2003 rainy season, and shows the erosion features that were formed during that year at very detailed spatial resolution.

Patterns of concentrated flow and ruptures of contour bunds could be clearly identified from the panchromatic QuickBird image as shown in Fig. 6.5. Unambiguous features related to soil erosion were visually discerned for the full 10 by 10 km QuickBird image, and their limits were digitized on-screen. Although cattle paths may also be identified and can trigger rill formation, they were not treated here as erosion features. The reason is that cattle paths are not necessarily related to erosion and including them would therefore not be correct in various cases. In general the distinction could be easily made due to the direction and the form of these paths. A set of 436 polygons was thus generated, which was rasterized to obtain the 12.5-m grid of the corrected ASTER data. The area of the erosion features totals 0.82 km^2 and the features are located throughout the study area.

The accuracy of the six erosion risk maps was evaluated by determining which erosion risk classes occurred at the locations where an erosion feature was detected from the

QuickBird image (here called erosion feature pixels). In this way, the producer's accuracy (A_p) could be assessed by dividing the number of pixels correctly classified as high and very high erosion risk, by the total number of erosion feature pixels. In this study A_p can be defined as the probability that an erosion feature pixel is correctly mapped as high or very high risk. A_p will be low if most erosion feature pixels correspond with very low, low, or medium erosion risk classes. The user's accuracy (A_u) can be defined here as the probability that a pixel classified on the erosion risk map actually represents that erosion risk class on the ground. This measure could not be evaluated here, because from the absence of erosion features we cannot infer that erosion risk will consequently be low for the specific location. Features may have been removed by human action or be too small to be observed by the QuickBird image, for instance in the case of sheet erosion. The optimal erosion risk classification and thus the optimal ASTER image timing, was therefore considered as the classification where A_p had the largest value.

6.4 Results

6.4.1 Coarse-resolution evaluation of high erosion risk periods

Erosion generally occurs when high-intensity rainfall events affect soils that are poorly protected by vegetation cover. Time series of MODIS imagery allow the monitoring of changing vegetation cover. Fig. 6.6 shows the temporal NDVI pattern for different land cover types during 2002-2003, as derived from MOD13Q1 data. The NDVI of forest is affected by seasonal changes, but throughout the year the NDVI values for forest are much more stable and higher than for pasture as might be expected. The NDVI of pasture has a high temporal variability, indicating that changes of green vegetation cover are substantial during the year. Fig. 6.6 also shows that the development of a well-maintained pasture (no overgrazing, good management of nutrients and runoff, generally little slope) starts earlier than degraded or new (renovated) pastures. Well-maintained pasture shows an important rise of NDVI starting in the beginning of November, whereas for the other pastures this rise starts mid-December. Optimal green cover is obtained for all pastures between February and April, after which NDVI-values decrease again. Degraded pasture has a low NDVI also during the wet season, while new pastures show the most significant increase during the onset of the rainy season. However, before December, their NDVI is lowest of all classes, because soils are almost completely bare at that time of the year.

The temporal NDVI signatures were compared with rainfall data from TRMM. The lower part of Fig. 6.6 shows the moments when the TRMM data indicate intensities of more than 15, 20, and 30 mm per 3-hours. During three events the rainfall intensity exceeded 30 mm per three hours. These events took place on 18 November, 10 December, and 29 December 2002. These intensities are averages for an area of about 27*27 km, as explained in Section 6.3.1. Locally, intensities may thus have been higher. The TRMM data give a good

Figure 6.6   Temporal NDVI-signature of 2002-2003 for four land cover types obtained from 16-day MODIS composites (MOD13Q1). The lower part of the figure indicates the moments when TRMM 3-hourly data show high-intensity rainfall for the study area.
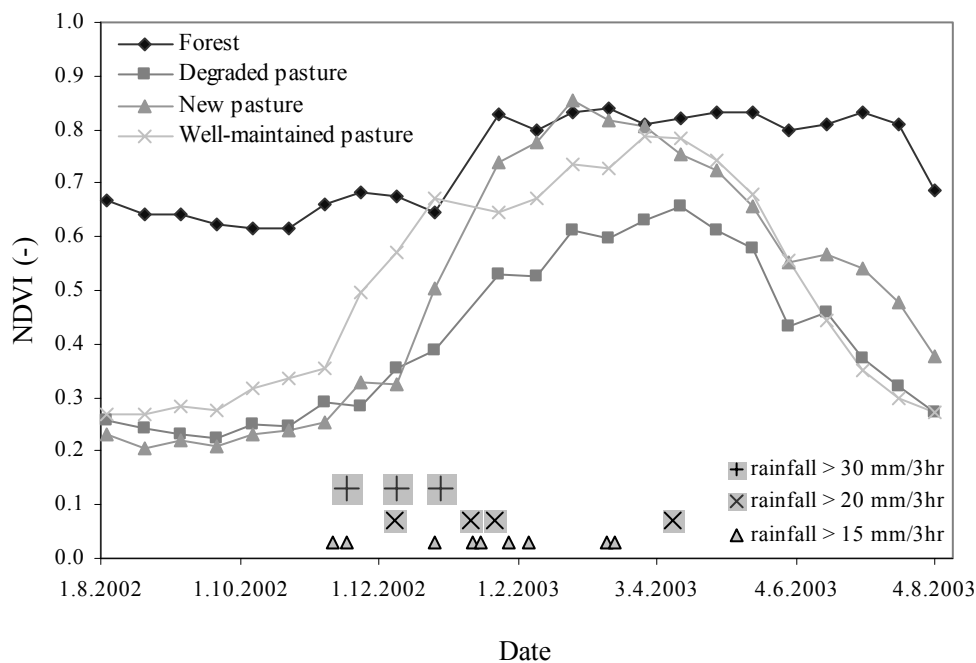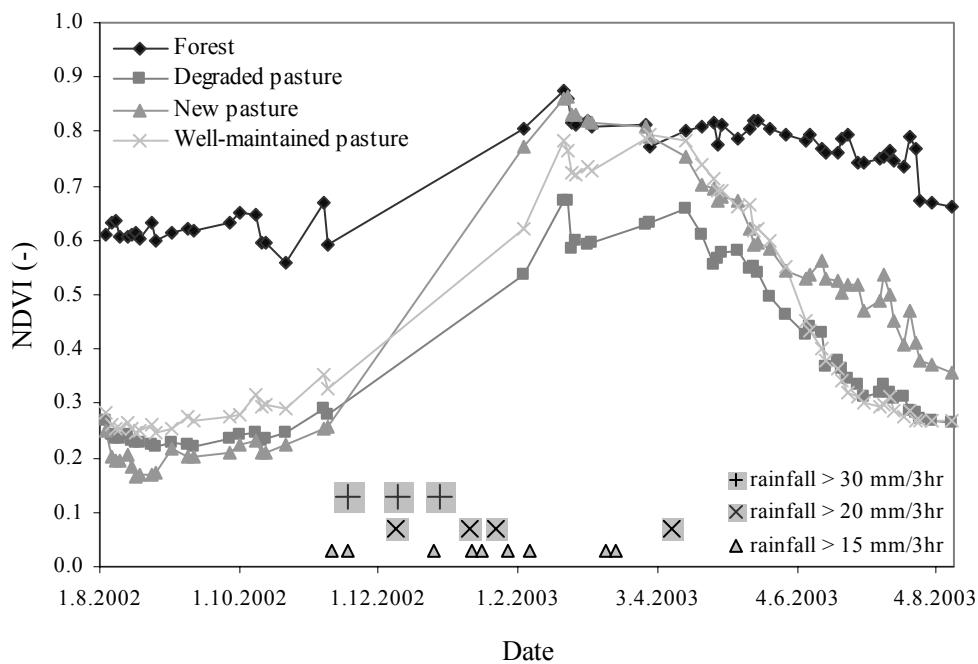

Figure 6.7   Temporal NDVI-signature of 2002-2003 for four land cover types obtained from daily MODIS composites (MOD09GQK). The lower part of the figure indicates the moments when TRMM 3-hourly data show high-intensity rainfall for the study area.

indication of when high-intensity rainfall events have occurred during the specific year within the study area. The highest intensity events of more than 30 mm per 3-hours occurred principally at the beginning of the rainy season, whereas also some smaller events can be observed in this period. Vegetation cover for the pastures is still very poor at this moment, especially for degraded and new pastures. The smaller events later in the season (February-April) have less impact on erosion, because vegetation cover offers better protection during this period. For the year 2002-2003, the period with highest erosion risk is therefore November-December.

Fig. 6.7 shows the temporal NDVI signatures of the different land cover types based on daily MOD09GQK imagery. In this case, only images were selected that were of good quality and free of clouds for the complete 10 by 10 km study area. Not surprisingly, the temporal pattern is similar to the one presented in Fig. 6.6. The most striking difference is that although many good-quality images could be selected, a large gap exists at the beginning of the rainy season. Between 9 November 2002 and 4 February 2003 no single good image was acquired due to poor weather conditions. Two conclusions may be drawn from this. The first is that MOD13Q1 is a better source for assessing the temporal changes of NDVI than MOD09GQK, because even during the period of high erosion risk a NDVI estimate is obtained. The differentiated development of the various pasture types during the early rainy season is not clear from the daily MOD09GQK images. The second conclusion is that medium-resolution imagery is very difficult to obtain for the erosion period. If from daily MODIS data no cloud-free, good-quality image is available for the area, this indicates that persistent cloud cover makes it difficult, if not impossible, to obtain medium-resolution imagery, which is acquired less-frequently (see Section 6.1). In general it should thus not be expected that a good quality optical medium-resolution image can be obtained for the period of high erosion risk, in any case not from the optical sensors of ASTER which are onboard the same Terra-platform as the MODIS instrument that acquired the images used in this study. Nevertheless, images do exist for the period shortly before the first high-intensity rainfall event. Medium-resolution spatial patterns of relative amounts of protective vegetation cover during the critical erosion period may therefore nonetheless be well represented.

6.4.2 Medium-resolution erosion risk mapping and image timing

Erosion risk was assessed using six ASTER images acquired at different moments between August 2002 and August 2003. Based on the coarse-scale NDVI analysis, the ASTER image dates correspond to the following situations:
- 9 September 2002: end of the dry season with minimal vegetation cover
- 11 October 2002: the rainy season has started but the low rainfall amounts have not yet have an important influence on vegetation development
- 4 March 2003: the middle of the rainy season when pastures and other vegetation has or is near to optimal green vegetation cover

- 23 May 2003: beginning of dry season, vegetation senescence and reduction of vegetation cover
- 24 Jun 2003: continued reduction of vegetation cover
- 11 August 2003: approaching the end of the dry season and vegetation cover is again minimal

The nearly five-month observation gap between October and March corresponds with a period of strong vegetation development and high-intensity rainfall, and consequently of high erosion risk. Quantitative changes of NDVI are presented in the first column of Fig. 6.8. This column shows that vegetation cover changes substantially in the October-March period. The quantitative NDVI maps were transformed into qualitative maps by classification of NDVI values into five equally-sized classes (Fig. 6.8, second column). Table 6.1 shows the NDVI class limits for each image. Due to differentiated development of vegetation cover within the region, the qualitative spatial patterns of vegetation cover also change. Patterns of September and October, and of June and August are very similar, whereas the differences between the spatial patterns of September 2002 and August 2003 can be mainly attributed to pasture renovation. Pasture renovation results in a very low NDVI during the dry season when vegetation is burnt and removed, and a high NDVI during the wet season when pasture develops. This explains the black area in the centre of the March NDVI class image (very high NDVI), whereas for previous dates the NDVI class was very low (white).

Erosion risk maps were created by inversely relating the NDVI classes to erosion risk, while setting the erosion risk to 'very low' for areas with slopes less than 3% (Fig. 6.8, third column). High erosion risk areas on the different maps mostly correspond with degraded pastures or bare areas, which are generally related to pasture renovation and some small agricultural fields. Nevertheless, also within these classes strong spatial and temporal variability exists in vegetation cover and therefore in erosion risk. Gallery forest and dense woodlands always show a very low erosion risk. The six erosion risk maps were compared with the erosion features derived from the QuickBird image. Table 6.2 shows for each risk map the percentage of erosion feature pixels (pixels where an erosion feature was detected) that fall within the different risk classes. The producer's accuracy (A_p) is the percentage of

Table 6.1   *NDVI class limits for the six ASTER images*

Image date	NDVI class				
	Very low	Low	Medium	High	Very high
9 Sep 2002	<0.271	0.271-0.297	0.297-0.342	0.342-0.448	>0.448
11 Oct 2002	<0.275	0.275-0.302	0.302-0.349	0.349-0.462	>0.462
4 Mar 2003	<0.595	0.595-0.660	0.660-0.719	0.719-0.785	>0.785
23 May 2003	<0.465	0.465-0.532	0.532-0.599	0.599-0.693	>0.693
24 Jun 2003	<0.364	0.364-0.421	0.421-0.495	0.495-0.617	>0.617
11 Aug 2003	<0.268	0.268-0.299	0.299-0.349	0.349-0.477	>0.477

Column labels: NDVI, NDVI class, erosion risk

Row labels: 9 Sep 2002, 11 Oct 2002, 4 Mar 2003, 23 May 2003, 24 Jun 2003, 11 Aug 2003

NDVI scale: 0.20 — 0.85

0 2 4 6 km

N

NDVI class:
- very low
- low
- medium
- high
- very high

erosion risk:
- very low
- low
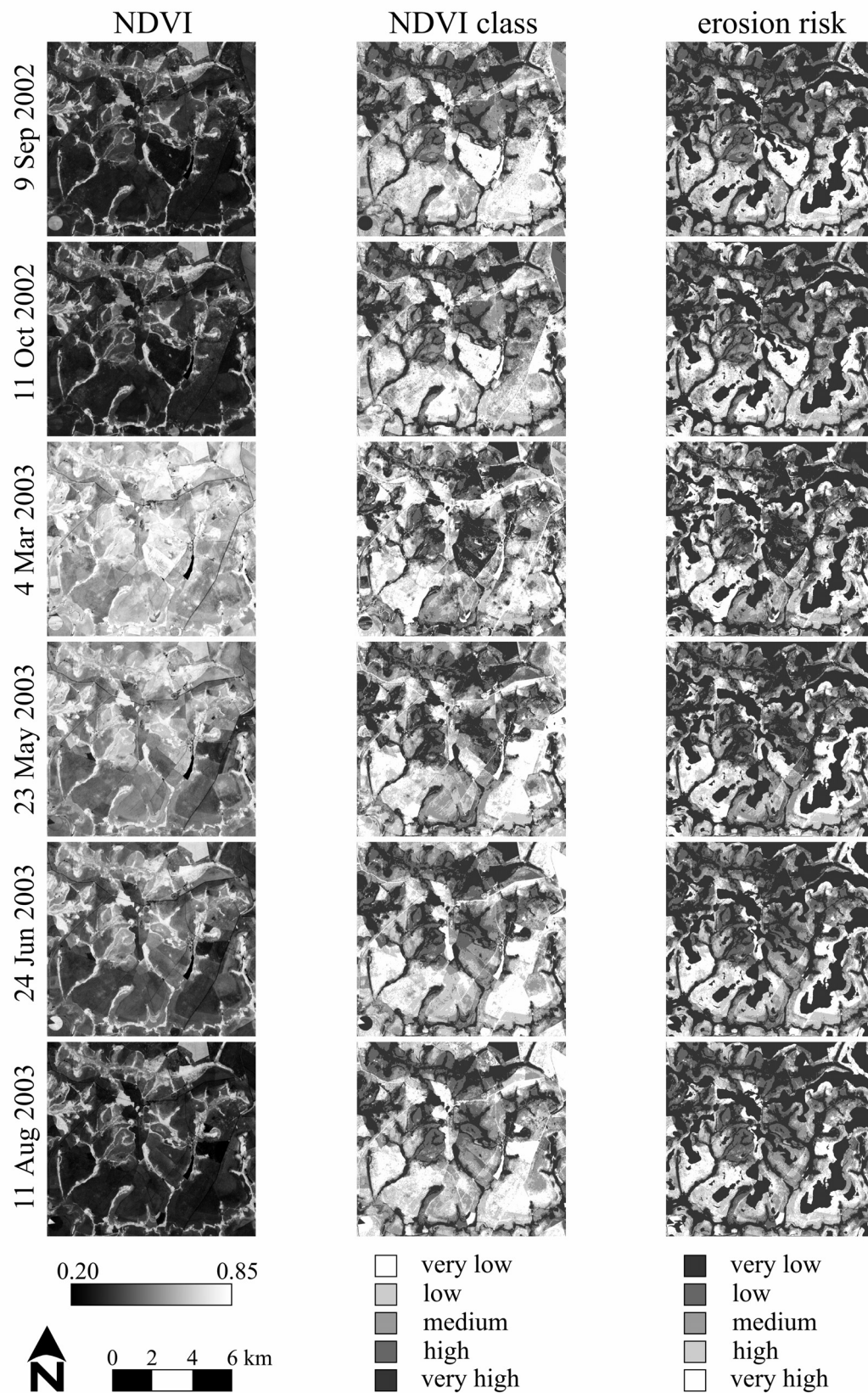- medium
- high
- very high

Figure 6.8   Erosion risk map construction for six different ASTER images. Column 1 shows the scaled NDVI, column 2 the NDVI divided in five classes, and column 3 the erosion risk maps, which integrate slope information with the NDVI classes.

Table 6.2   *Percentage of erosion feature pixels falling within the different risk classes for each erosion risk map. The producer's accuracy (A_p) is the percentage falling in the classes 'high' and 'very high'.*

Image date	Erosion risk					Accuracy
	Very low	Low	Medium	High	Very high	(A_p)
9 Sep 2002	4.9	3.7	9.5	21.9	60.0	81.9
11 Oct 2002	4.9	2.5	8.6	18.5	65.5	84.0
4 Mar 2003	14.5	8.4	12.2	17.8	47.1	64.9
23 May 2003	8.4	17.2	9.4	22.6	42.4	65.0
24 Jun 2003	4.9	6.3	24.2	30.9	33.7	64.6
11 Aug 2003	5.0	5.1	24.7	32.5	32.7	65.2

erosion feature pixels falling in erosion risk class 'high' or 'very high'. The map of 11 October 2002 shows the highest A_p (84.0%) closely followed by the map of 9 September 2002 (81.9%). All other maps have lower A_p-values of about 65%, while the percentage falling in the class 'very high erosion risk' is gradually decreasing from 47.1% to 32.7%. This indicates that the later the image is acquired (after October 2002), the worse spatial NDVI patterns match erosion feature patterns.

Reasons for the time-dependency of A_p-values are related to the specific timing of the ASTER image acquisitions and to the timing of the QuickBird image. The QuickBird image was acquired during August 2003, and therefore shows erosion features that were formed during the erosion events of the previous rainy season. The distribution of vegetation cover in August 2003 does therefore not tell much about the erosion features encountered at that same moment, resulting in a low A_p for the 11 August 2003 image. From Section 6.4.1 we learned that the erosion period is at the start of the rainy season when soils are poorly protected by vegetation. In the case of renovated pasture, vegetation shows strong development during the rainy season, but offers little protection during November and December when high-intensity rainfall occurs. The ASTER image of 11 October 2002 is acquired shortly before this period and thus gives a good description of vegetation patterns at the moment when the first high-intensity rainfall events occur. However, because relative differences of NDVI between August and November 2002 are small (Fig. 6.6), the A_p for 9 September 2002 is only slightly lower. If images would be available for late October or November, A_p can be expected to show a slight increase. During the rainy season however, vegetation patterns change substantially and thus the March 2003 image and subsequent images show a poor relation with the digitized erosion features. Optimal image timing for this case study of erosion risk mapping in pasture areas of the Cerrados is therefore during late dry season/ start of wet season (September to November).

An important factor for differences between A_p-values of the ASTER image dates is the location of pasture renovation practices during a specific year, although factors such as local overgrazing also play a role. Nonetheless, all classifications correctly classify an

important amount of erosion feature pixels as 'high' or 'very high'. This is because many features are found on degraded pastures which have relatively low NDVI-values at any instance during the year. Field observations affirmed that degraded pastures have a poor vegetation cover also during the wet season (see Fig. 6.2), and that many erosion features are present in these areas.

6.5   Discussion and conclusions

The new method presented in this paper shows that it is possible to produce accurate soil erosion risk maps of the Brazilian Cerrados using satellite derived information of rainfall and vegetation cover. Such a method is valuable for areas where data availability on land use, land management, vegetation cover, soil type and rainfall is poor. The method also illustrates that timing of satellite images for erosion risk mapping is critical. The protective cover of vegetation can be well described by a satellite image if the spatial patterns of vegetation cover at the time of image acquisition are similar to the vegetation patterns present at the time of the major erosion events.

The timing of major erosion events was assessed by qualitatively comparing temporal NDVI-signatures with high-intensity rainfall events for a specific year. This was performed using coarse-resolution multi-temporal MODIS-images in combination with rainfall intensity data from TRMM. The 16-day MODIS composites (MOD13Q1) performed better than daily MODIS data (MOD09GQK) for obtaining NDVI time series, because the composites showed no temporal gaps. The MODIS/TRMM analysis provided a quick overview of when erosion is likely to occur in a specific region. For the study area, the major erosion period for season 2002-2003 is November-December. This corresponds well with measurements performed by Baccaro (1990) during 1984-1986 using several Gerlach troughs in an area about 10 km south of the study region. Gerlach troughs are a type of unbounded erosion plots consisting of a collecting gutter in the soil surface, which is connected to a collecting container on the downstream side. They are used to measure runoff and erosion (Hudson, 1993). Baccaro found that despite high rainfall intensities and high runoff in other periods of the year, the highest erosion was measured generally during the months November-January.

The vegetation patterns were well described by NDVI classes derived from ASTER imagery of October, and to a lesser extent of September. For pasture areas in the Cerrados, optimal image timing is therefore during late dry season/ start of wet season (September to November). During the wet season, image availability is low in these areas, but judging from accuracy values of above 80%, this does not seem to constitute an important problem for mapping areas with high erosion risk. Actually late dry season imagery performed much better than an image acquired during the wet season. As optimal timing is before the erosion occurs, the resulting risk maps will have a predictive value for erosion occurrence during the upcoming rainy season.

Although a general indication of optimal image timing is given for pasture areas in the Cerrados, we recommend that for any erosion risk mapping activity the timing of satellite images is clearly considered in relation to the erosive season. This may alternatively be derived from temporal field measurements or local knowledge. Here however, a very straightforward and promising qualitative evaluation was presented that uses readily available data (MODIS and TRMM), and can therefore be easily applied in other regions. We stress that the optimal timing depends on specific regional characteristics, such as climate, vegetation types, and land management. Moreover, for a specific region important differences may exist in climate and vegetation development, which would require a multi-year analysis to determine whether the high-erosion period is always at the same moment.

The method presented for erosion risk mapping is straightforward and easy to apply, based on a mono-temporal evaluation of NDVI-values at the moment of high erosion risk, in combination with masking of low slope values. By no means do we intend to deny the importance of other factors controlling the erosion process. Especially for large-scale studies and quantitative erosion studies we believe factors such as climatic differences and soil properties need to be accounted for. For quantitative modelling in small catchments, accurate data on all erosion factors are needed. Nevertheless, for qualitative erosion risk mapping in the 100-km^2 region, we assumed additional factors to be constant, which according to the high accuracy (84%) of the optimal erosion risk map seems to be a valid assumption. Moreover, soil properties are also often related to vegetation cover, as for example under forest the soil organic matter is higher than under pasture.

Instead of mono-temporal evaluation of NDVI-values for erosion risk mapping for a specific year, multi-temporal erosion risk mapping would also be a possibility. Multi-temporal mapping would signify the combined evaluation of rainfall intensity and NDVI data during different moments of a year to construct one final erosion risk map. However, the major problem, at least for tropical regions, is the uncertainty of the availability of medium-resolution optical images during specified moments of a year which are of importance for vegetation development. For 2002-2003 a total of six ASTER images was recorded. For other years or areas however, it is unlikely that optical images exist for the same moments, especially for the wet season when cloud cover is persistent. Therefore, if erosion risk for a particular year can be assessed quite accurately with only one well-timed image per year, this is a much better option for monitoring during consecutive years. Late dry season imagery of different years can thus show the changes occurring in erosion risk patterns. Based on the differences between NDVI patterns of 9 September 2002 and 11 August 2003 (Fig. 6.8), it can be expected that in the study area spatial erosion risk patterns change substantially from year to year. This implies that the erosion risk assessments are valid for a specific year, and for each growing season a different assessment is required.

Synthetic aperture radar (SAR) imagery seems a logical alternative to optical satellite data, because its acquisition is not hindered by cloud cover and thus in principal images may be required at any moment during the year. The assessment of vegetation cover and related parameters is possible using spaceborne SAR systems. However the SAR backscatter is

dependent not only on vegetation parameters, such as crop biomass and plant structure, but also on soil parameters, such as soil moisture and soil roughness, and on sensor configuration parameters, like polarization, frequency, and incidence angle (Brisco and Brown, 1998; Paloscia, 2002). Some recent studies have investigated the potential of multi-polarisation SAR data in order to retrieve vegetation parameters (McNairn and Brisco, 2004). Good results were obtained for regular vegetation types such as agricultural crops, such as wheat and sugar beet, in the retrieval of the biomass and leaf area index (e.g. Mattia et al., 2004; Vyas et al., 2003). However it was also shown that the structure of the plants plays an important role in the retrieval capability and that for vegetation characterised by low density and low biomass the soil contribution to the multi-polarisation SAR backscatter is dominant. This means that over irregular vegetated areas (e.g. degraded pastures with scattered shrubs and trees) the retrieval becomes much more difficult. Our study site showed a large variety of scattered vegetation types and irregular elements and accurately estimating vegetation cover with SAR data would therefore be extremely difficult and require much additional field data.

This study has shown that regional erosion studies can benefit from the use of multi-resolution satellite imagery. Coarse-resolution data (MODIS, TRMM) allow for a temporal assessment of vegetation cover and rainfall intensity, thus knowledge can be obtained of when erosion risk is high for a particular area. Medium-resolution imagery (ASTER) can describe the more detailed spatial variability of vegetation cover at different moments of the year. The cover patterns of slightly before or at the start of the rainy season can be used for mapping of erosion risk. Fine-resolution imagery (QuickBird) may subsequently be applied for validating erosion risk maps by assessing where erosion features occur. The approach followed here is fast and straightforward and may be easily applied to other areas, although the precise medium-resolution data integration method may vary according to specific regional characteristics. The approach is especially useful for areas where spatial and temporal variability of vegetation is significant and cannot be captured merely by land use classification.

References

Adler RF, Huffman GJ, Bolvin DT, Curtis S, and Nelkin EJ. 2000. Tropical rainfall distributions determined using TRMM combined with other satellite and rain gauge information. *Journal of Applied Meteorology* 39 (12): 2007-2023.

Baccaro CAD. 1990. Estudo dos processos geomorfológicos de escoamento pluvial em área de Cerrado - Uberlândia - MG. Ph.D. Thesis, University of São Paulo, São Paulo, Brazil.

Baccaro CAD. 1999. Processos erosivos no Domínio do Cerrado. *In*: Guerra AJT, da Silva AS, and Botelho RGM (Editors), Erosão e Conservação dos Solos. Bertrand Brasil, Rio de Janeiro, Brazil: pp. 195-227.

Bezerra JFR, and Rodrigues SC. 2006. Estudo do potencial matricial e geotêxteis aplicado a recuperação de um solo degradado, Uberlândia MG. *Revista Caminhos de Geografia* In press.

Brisco B, and Brown RJ. 1998. Agricultural applications with radar. *In*: Henderson FM, and Lewis AJ (Editors), Principles and Applications of Imaging Radar - Manual of Remote Sensing. John Wiley & Sons, Inc., New York (NY), USA: pp. 381-406.

Carlson TN, and Ripley DA. 1997. On the relation between NDVI, fractional vegetation cover, and leaf area index. *Remote Sensing of Environment* 62 (3): 241-252.

Costa FP, and Rehman T. 1999. Exploring the link between farmers' objectives and the phenomenon of pasture degradation in the beef production systems of Central Brazil. *Agricultural Systems* 61 (2): 135-146.

De Jong SM. 1994. Derivation of vegetative variables from a Landsat TM image for modelling soil erosion. *Earth Surface Processes and Landforms* 19 (2): 165-178.

De Jong SM, Paracchini ML, Bertolo F, Folving S, Megier J, and De Roo APJ. 1999. Regional assessment of soil erosion using the distributed model SEMMED and remotely sensed data. *Catena* 37 (3-4): 291-308.

Escadafal R. 1994. Soil spectral properties and their relationships with environmental parameters: examples from arid regions. *In*: Hill J, and Mégier J (Editors), Imaging Spectrometry - a Tool for Environmental Observations. Kluwer Academic Publishers, Dordrecht, The Netherlands: pp. 71-87.

Ferreira LG, and Huete AR. 2004. Assessing the seasonal dynamics of the Brazilian Cerrado vegetation through the use of spectral vegetation indices. *International Journal of Remote Sensing* 25 (10): 1837-1860.

Furley PA. 1999. The nature and diversity of neotropical savanna vegetation with particular reference to the Brazilian cerrados. *Global Ecology and Biogeography* 8 (3-4): 223–241.

Hudson NW. 1993. Field measurement of soil erosion and runoff. FAO Soils Bulletin, 68. Food and Agriculture Organization, Rome, Italy.

Huete A, Didan K, Miura T, Rodriguez EP, Gao X, and Ferreira LG. 2002. Overview of the radiometric and biophysical performance of the MODIS vegetation indices. *Remote Sensing of Environment* 83 (1-2): 195-213.

Hutchinson MF. 1989. A New Procedure for Gridding Elevation and Stream Line Data with Automatic Removal of Spurious Pits. *Journal of Hydrology* 106 (3-4): 211-232.

Jain SK, and Goel MK. 2002. Assessing the vulnerability to soil erosion of the Ukai Dam catchments using remote sensing and GIS. *Hydrological Sciences Journal* 47 (1): 31-40.

Jepson W. 2005. A disappearing biome? Reconsidering land-cover change in the Brazilian savanna. *Geographical Journal* 171 (2): 99-111.

Klink CA, and Moreira AG. 2002. Past and current human occupation, and land use. *In*: Oliveira PS, and Marquis RJ (Editors), The Cerrados of Brazil: Ecology and Natural History of a Neotropical Savanna. Columbia University Press, New York: pp. 69-88.

Kummerow C, Simpson J, Thiele O, Barnes W, Chang ATC, Stocker E, Adler RF, Hou A, Kakar R, Wentz F, Ashcroft P, Kozu T, Hong Y, Okamoto K, Iguchi T, Kuroiwa H, Im E, Haddad Z, Huffman G, Ferrier B, Olson WS, Zipser E, Smith EA, Wilheit TT, North G, Krishnamurti T, and Nakamura K. 2000. The status of the Tropical Rainfall Measuring Mission (TRMM) after two years in orbit. *Journal of Applied Meteorology* 39 (12): 1965-1982.

Laflen JM, Lane LJ, and Foster GR. 1991. WEPP - a new generation of erosion prediction technology. *Journal of Soil and Water Conservation* 46 (1): 34-38.

Liu JG, Mason P, Hilton F, and Lee H. 2004. Detection of rapid erosion in SE Spain: A GIS approach based on ERS SAR coherence imagery. *Photogrammetric Engineering and Remote Sensing* 70 (10): 1179-1185.

Mattia F, Dente L, Satalino G, and Le Toan T. 2004. Sensitivity of ASAR AP data to crop and soil parameters, Proceedings of the 2004 Envisat & ERS Symposium. SP-572. ESA, Salzburg, Austria.

McNairn H, and Brisco B. 2004. The application of C-band polarimetric SAR for agriculture: a review. *Canadian Journal of Remote Sensing* 30 (3): 525-542.

Morgan RPC. 2005. Soil erosion and conservation. Blackwell Publishing, Malden, MA: 304 pp.

Paloscia S. 2002. A summary of experimental results to assess the contribution of SAR for mapping vegetation biomass and soil moisture. *Canadian Journal of Remote Sensing* 28 (2): 246-261.

Purevdorj T, Tateishi R, Ishiyama T, and Honda T. 1998. Relationships between percent vegetation cover and vegetation indices. *International Journal of Remote Sensing* 19 (18): 3519-3535.

Rodrigues SC. 2002. Impacts of human activity on landscapes in Central Brazil: a case study in the Araguari watershed. *Australian Geographical Studies* 40 (2): 167-178.

Symeonakis E, and Drake N. 2004. Monitoring desertification and land degradation over sub-Saharan Africa. *International Journal of Remote Sensing* 25 (3): 573-592.

Thome K, Biggar S, and Takashima T. 1999. Algorithm Theoretical Basis Document for ASTER Level 2B1 - Surface Radiance and ASTER Level 2B5 - Surface Reflectance, University of Arizona, Tucson, Arizona: 45 pp.

Valentin C, Poesen J, and Li Y. 2005. Gully erosion: Impacts, factors and control. *Catena* 63 (2-3): 132-153.

Vrieling A. 2006. Satellite remote sensing for water erosion assessment: a review. *Catena* 65 (1): 2-18.

Vrieling A, Rodrigues SC, Bartholomeus H, and Sterk G. 2006a. Automatic detection of erosion gullies with ASTER imagery in the Brazilian Cerrados. *International Journal of Remote Sensing* In press.

Vrieling A, Sterk G, and Beaulieu N. 2002. Erosion risk mapping: a methodological case study in the Colombian Eastern Plains. *Journal of Soil and Water Conservation* 57 (3): 158-163.

Vrieling A, Sterk G, and Vigiak O. 2006b. Spatial evaluation of soil erosion risk in the West Usambara Mountains, Tanzania. *Land Degradation & Development* 17 (3): 301-319.

Vyas SP, Steven MD, Jaggard KW, and Xu H. 2003. Comparison of sugar beet crop cover estimates from radar and optical data. *International Journal of Remote Sensing* 24 (5): 1071-1082.

Zevenbergen LW, and Thorne CR. 1987. Quantitative analysis of land surface topography. *Earth Surface Processes and Landforms* 12 (1): 47-56.

Chapter 7

SYNTHESIS

7. Synthesis

Satellite remote sensing can offer an important input to soil erosion assessments at various spatial scales. A wide range of options for evaluating erosion with satellite data exist. This thesis has provided an extensive review on different options described in literature (Chapter 2), followed by four case studies in three tropical regions: the Brazilian Cerrados (Chapter 3 and 6), the Colombian Eastern Plains (Chapter 4), and the West Usambara Mountains of Tanzania (Chapter 5). For each case study, a different methodology was developed, taking into account the local conditions and the generally limited availability of detailed spatial data for these regions. Inevitably, only a small fraction of the thinkable ways for studying erosion with satellite data is covered by the case studies. Nevertheless, the studies clearly indicate potential alternative opportunities for mapping erosion with satellite data besides the application of often-used erosion models. The current chapter aims at synthesizing the studies presented in this thesis. The synthesis is based on three pillars: obtaining erosion related information from satellite data (Section 7.1), integrating spatial data for regional assessment of erosion (Section 7.2), and validation of the outcomes (Section 7.3). Finally, Section 7.4 expresses the author's views on future directions for satellite-based erosion assessment.

7.1 Remote sensing of erosion related variables

For any erosion study intending to use satellite data, first a thorough evaluation is required of the potential variables that may be obtained from satellite imagery for the region and scale considered. Chapter 2 gave an overview of the different variables obtained from satellite data in previous erosion studies, including presence of erosion features, and erosion factors such as slope and vegetation cover. Also the amount of additional data needed to accurately derive these variables has to be evaluated. Limited resources may imply that certain variables cannot be derived in case additional data can only be obtained through labour-intensive field campaigns. Tropical regions possess distinct characteristics which may complicate the retrieval of certain variables. Firstly, in humid tropical areas vegetation cover is generally abundant, thus hampering effective study of soil properties most of the time. Secondly, persistent cloud cover in these areas limit the options for timely acquisition of optical satellite data for at least part of the year. Also spatial resolution plays a role here: while coarse-resolution images such as obtained from the MODIS-instrument (250-1000 m) can be acquired daily over the same site, for higher resolution imagery (e.g. ASTER, 15-60 m) this frequency is much lower, thus limiting opportunities for cloud-free observations (Chapter 6). For the case studies presented in this thesis, satellite data was used for assessing the following variables: presence of erosion features (Chapter 3 and 6), vegetation type (Chapter 4) and cover (Chapter 4, 5, and 6), rainfall (Chapter 6), and slope (Chapter 5).

Erosion features of sufficient spatial size may be discerned through visual identification of distinct patterns on high-resolution satellite imagery. In Chapter 3 erosion gullies could be visually identified from a panchromatic 0.60-m resolution QuickBird image. Also smaller features could be discerned from this image, i.e. patterns of concentrated flow and contourbund ruptures, indicating the occurrence of rill erosion and potentially gully initiation (Chapter 6). However, high-resolution data are still expensive if required for large areas, whereas visual interpretation techniques demand substantial time from an interpreter. Therefore, Chapter 3 examined the possibility of automatic detection of large individual erosion features. A special application of the maximum likelihood algorithm was proposed using only two classes for training, i.e. a gully class and a large non-gully class. Gully class training sites were obtained from the QuickBird-derived gully limits, whereas the non-gully class consisted of all other pixels in the training area. The algorithm was applied to multispectral ASTER data. A combination of visible, near infrared, and middle infrared bands gave accurate classification results, especially when combining classifications from the wet and the dry season.

Vegetation is an important dynamic factor offering protection of the soil. In Chapter 4, a Landsat Thematic Mapper image was applied for land use classification using the maximum likelihood algorithm. Spatial reference data acquired in the field, allowed for the training of the algorithm and validation of the results. Six classes with different soil protection properties could be separated with an accuracy of 84%. In both Chapter 4 and Chapter 5 (method 1), field estimates of fractional vegetation cover (FVC) were related with linear regression to the normalized difference vegetation index (NDVI) calculated from a Landsat image. However, NDVI may also be used directly as an indicator of FVC, in case only FVC patterns are required. Moreover, this may circumvent problems of timing differences between satellite acquisition and field estimates, and methodological difficulties for precisely estimating FVC in the field. In Chapter 5 (method 2) and Chapter 6, NDVI was used directly as a measure of FVC. In Chapter 6 the NDVI was derived from coarse-resolution MODIS data to study the temporal dynamics of FVC for different land cover classes during one year. For this purpose, 16-day MODIS composites outperformed daily MODIS data due to better masking of cloud effects. At the medium-resolution spatial NDVI patterns were determined at different moments of the year from six available ASTER images to examine when these NDVI patterns best correlate with patterns of erosion occurrence.

Besides vegetation, rainfall is also a highly dynamic erosion factor. Erosion is an erratic process and occurs usually during high-intensity rainfall events. To reduce soil erosion, soils should be protected (e.g. by vegetation) during periods when these events occur, thus knowledge on the timing of events is required. Often rainfall data is obtained from raingauges, but for large regions in the tropics these data are not gathered or stored in a systematic way, or otherwise difficult to obtain. Until present, no erosion studies have been published that use satellite data to obtain rainfall information. In Chapter 6 periods of high-intensity rainfall periods were determined from 3-hourly precipitation data obtained from the spaceborne TRMM mission, carrying a precipitation radar. Although the data are at a coarse

resolution (0.25° corresponding with 27-km resolution for the study area), they gave a good indication of the timing of high-intensity rainfall periods. In this study, merely temporal data from a single TRMM resolution cell corresponding with the study area were used.

Without a certain slope, no runoff and thus no erosion occurs. For some environments slope is strongly related to erosion (Chapter 5), whereas for others this is less the case (Chapter 6). Also other terrain parameters, like dissection grade (Chapter 4) may explain erosion at certain scales and regions. Various studies in this thesis obtained topography-related variables from DEMs. In some cases it was chosen to use a DEM derived from contourlines digitized from a topographic map, because it offered a higher resolution or quality for the desired scale as satellite-derived DEMs (Chapter 4 and 6). Nevertheless, several satellite sources for good-quality DEMs exist, such as the SRTM, offering a free readily available 90-m resolution DEM for any land mass between 60°N and 57°S latitude. In Chapter 5 SRTM data were used for slope estimation.

7.2   Spatial data integration for erosion assessment

The strength of satellite remote sensing for erosion studies is that good-quality timely spatial information can be obtained on a variety of erosion related variables (Chapter 2). Although detection of the presence of erosion features may give direct information, a lot can be gained from integrating remotely sensed variables with additional data. These data may also be derived from satellite imagery, or have another source (e.g. field measurements, soil and topographic maps). Even if erosion features can be directly obtained from satellite imagery, integration with other variables can assist in explaining the occurrence of erosion features or to predict future erosion. As an example, visual interpretation of QuickBird imagery allowed for gully detection in Chapter 3. This formed the basis for automatic gully detection with ASTER, which then permits obtaining fast information on gully occurrence in larger regions. Coupling this knowledge to other variables (like presence of roads, terrain variables, vegetation cover, etc.) may subsequently explain why gullies occur at certain locations. Chapter 6 could also be looked at from this perspective: QuickBird was applied for extracting erosion features, while NDVI patterns in combination with slope information explained its occurrence. Detection of features from satellite data can therefore be a goal in itself, but also a way to arrive at understanding of the erosion process. Unfortunately, limitations exist for detecting erosion features from satellite imagery due to e.g. the limited size of the features, vegetation cover obscuring feature presence (e.g. in agricultural fields), feature removal by ploughing, the high cost of high-resolution data, or simply the inability of discerning certain features by current satellite systems. Nevertheless, the general factors responsible for erosion occurrence are rather well-known partly because of many decades of erosion research, but equally due to the experience of e.g. local farmers, working daily in the field.

Although the factors that play a role in the erosion process are well-known (i.e. climate, terrain, soil, vegetation), there is more confusion about how to best select parameters

describing these factors at different scales, and to integrate these parameters for accurate estimation of erosion rates or prediction of locations where erosion is likely to occur. For assessing erosion rates and erosion mapping, a variety of data-integrating erosion models have been developed for different locations worldwide. However, in Chapters 1, 2, 4, and 5 it was discussed that most erosion models have certain drawbacks that limit their adequacy for accurate erosion mapping. This is partly because specific model assumptions may not be valid for other regions and scales, and partly because the model's input data requirements are often too high as compared to data availability, even when considering the variables that may be extracted from satellite data. This may imply that more assumptions considering input variables will have to be made, thus reducing accuracy of the input and therefore of the outcomes. Erosion models give some estimate of erosion rates, but its predictive value is generally low. Often, especially for larger regions, precise erosion rates are not required, but merely a spatial (and sometimes temporal) indication of where (and when) erosion is likely to occur. This is generally expressed as erosion risk, being the relative risk that erosion will occur at a specific location (and moment) as compared to other locations in the region mapped. Therefore, qualitative data integration methods using data on regionally-important parameters can be a good option for the goal of erosion risk mapping. Local knowledge of experts (Chapter 4) or farmers (Chapter 5) can be an important input to such methods.

In Chapter 4, a qualitative erosion risk mapping methodology was presented that uses expert knowledge to select and combine locally-important parameters that can be extracted from available data sources. A generic description of the methodology was given, such that the method can be applied for other regions with different parameters of importance and different data availability. For the Colombian Eastern Plains, four erosion factors were defined, namely geology, soils, relief, and management. Through interviews with local soil experts the relevant parameters for each factor were identified and subsequently derived from a soil survey, a DEM, and a Landsat image. For each factor a decision tree was constructed allowing combination of the selected parameters into a factor rating between 1.0 (low erosion risk) and 3.0 (high erosion risk). Averaging factor ratings resulted in a potential (without management factor) and actual erosion risk map. Chapter 4 concluded that flexible methodologies using expert knowledge are valuable for erosion risk mapping as locally-important factors and processes can be accounted for effectively.

The Colombian case study still used several data sources that may not be readily available at a sufficiently detailed scale in other areas (e.g. soil map). Therefore, in Chapter 5 it was examined if accurate erosion risk mapping is possible using only readily available data obtained from spaceborne sensors. Two methods were tested that both used a well-timed Landsat image for assessing patterns of vegetation cover and a SRTM DEM to evaluate slope. During informal interviews in the 70-km^2 watershed in the West Usambara Mountains of Tanzania, both farmers and extension officers mentioned steep slopes and reduced vegetation cover during certain moments of the year as the most important causes of erosion in the region. Therefore, only these factors were addressed for assessing erosion risk. The first method was partly based on field surveys, estimating FVC, slope, and erosion risk. Field

estimates of FVC were related to NDVI-values of corresponding pixels in the Landsat image. Using multiples of 10% as class limits, FVC and slope were both classified in five classes. A decision tree was set up using part of the field surveys to optimally combine the slope and FVC classes into erosion risk classes. Although spatial erosion risk patterns are eventually derived from readily available data sources, development of method 1 greatly relies on field surveys.

Method 2 of Chapter 5 on the contrary did not require field data for its development. NDVI was used directly as an indicator of FVC. The NDVI and slope values were both automatically classified in five classes, with each class covering 20% of the watershed. For each factor, value 1 was assigned to the class with the lowest erosion risk (gentle slopes or high NDVI) and value 5 to the highest erosion risk. The final erosion risk map was subsequently created by taking the minimum class value of NDVI and slope classification for each pixel. Performance of both methods was similar in terms of accuracy, and therefore the simpler and more straightforward method 2 is preferred. Chapter 5 showed that qualitative integration of the factors vegetation cover and slope, indicated by local farmers, may allow for accurate mapping of soil erosion risk in the watershed studied. Spatial information on these factors could be easily extracted from readily available spaceborne data, while proper timing of the Landsat image to assess patterns of vegetation cover at the time of high erosion risk was considered important.

Chapter 6 assessed more in detail the importance of temporal dynamics of vegetation cover and rainfall for satellite image timing. For the 10 by 10 km Brazilian study area, multi-temporal information on rainfall intensity and vegetation cover (through NDVI) during one year was derived from coarse spatial resolution TRMM and MODIS data. Qualitative comparison of the time series allowed for identifying the period when erosion risk is highest due to limited vegetation cover and occurrence of high-intensity rainfall events. To assess the implications of this timing on the selection of available optical medium-resolution imagery, the NDVI was calculated from six medium-resolution ASTER images. For each image, the calculated NDVI was classified in five equally-sized classes the same way as in method 2 of Chapter 5. However, field surveys showed that slope is not an equally important factor for erosion at the Brazilian site as in the West Usambara Mountains. Classes with low NDVI were related to high erosion risk and vice versa, while a DEM was merely used to set pixels with gentle slopes less than 3% to very low erosion risk. Of the six erosion maps thus constructed, the one created from the image acquired at the start of the rainy season, shortly before the erosion period, best described the erosion patterns, as observed visually from the QuickBird image. The different erosion risk maps gave varying accuracy values because the spatial NDVI patterns, and not only NDVI values, change during the year. Chapter 6 showed that erosion studies can benefit from the use of multi-resolution and multi-temporal satellite data, and that temporal dynamics of vegetation cover and rainfall are to be considered for satellite image selection in erosion studies.

The different case studies of this thesis showed that various alternatives exist for erosion risk mapping besides the use of erosion models. With only a limited amount of

information that can easily be extracted from satellite imagery or other sources, often a good indication of the spatial variability of erosion risk can be obtained. While under some circumstances erosion features may be detected directly from satellite data (Chapter 3 and 6), in other cases selection and combination of information sources can be based on expert knowledge (Chapter 4), farmer's knowledge (Chapter 5), or field surveys (Chapter 6). A flexible approach that can easily be adapted to regional characteristics is therefore to be preferred over data-demanding approaches that are developed for other scales and regions. Here it is not meant to repudiate the validity of physically-based erosion models, as their development assists in understanding the erosion process. However, for the goal of regional erosion mapping they are probably not the best tool. To obtain relevant input data, especially for assessing vegetation patterns, timing of satellite imagery can be important. Coarse-resolution satellite data may assist in defining the optimal timing (Chapter 6).

7.3   Validation

The term 'accurate' was mentioned several times in Sections 7.1 and 7.2. Accuracy is the degree of conformity of the results with actual values. To determine the accuracy of output maps, results need to be validated with independent data. In this section the focus will be merely on validating erosion results, and not on validation of intermediate products, such as FVC or land use maps. Chapter 2 gave an overview of the validation techniques applied in erosion studies that use satellite remote sensing. Erosion is a difficult process to measure, because accurate measurements are generally expensive and time-consuming, standard equipment is hardly available, and measurement results may be highly variable under similar circumstances. Probably partly because of this, many of the reviewed studies in Chapter 2 did not or only slightly address the issue of validation. However, validation is essential for identifying accurate erosion mapping methodologies and closer collaboration between the remote sensing community and field-based erosion scientists may be needed for that purpose. Common techniques that have been applied to obtain validation data include soil loss measurements from plots, evaluation of sediments leaving hydrological catchments, erosion surveys, and aerial photo interpretation. Plot measurements are time-consuming and expensive to perform over large areas, whereas evaluating sediments at the outlet does not give information on what is happening inside the catchment. Therefore, and because no estimates of erosion rates were required, validation data for the case studies presented in this thesis were obtained from field surveys and high-resolution image interpretation.

Field surveys examine erosion features and possible causes of erosion, such as limited vegetation cover and steep slopes. These observations are recorded for different points or areas which are located with a Global Positioning System (GPS). Erosion features may not be visible at every moment of the year, so surveys need to be timed carefully. However, accessibility can sometimes become problematic during the rainy season, which would impose the need to execute the survey at another moment and focus more on causes of erosion (Chapter 5). In Chapter 4, surveys were performed for seven high erosion risk areas

identified by the erosion risk map. At these locations advanced signs of sheet and gully erosion were observed, and favourable conditions for erosion (e.g. steep slope, bare soil) were found. However, the need for more validation data was clearly identified in this study. In Chapter 5, field surveys were performed for 151 locations during a period of one month. At each location several characteristics were recorded, including land cover, FVC, presence of conservation measures, slope, and erosion indicators. Erosion indicators were defined locally and comprised stony soil, exposed roots, and the presence of rills and pedestals. Based on the characteristics found at a specific location, a qualitative estimate of erosion risk was made in the field together with a local extension officer on a scale ranging from 1 (very low) to 5 (very high). In Chapter 6, similar surveys as for Chapter 5 were performed at 331 locations, but were eventually not used for the accuracy assessment, due to important timing differences between image acquisition and the execution of the surveys. Nevertheless, surveys like presented in this thesis, although to some extent subjective, can be a useful tool for assessing the accuracy of regional erosion maps.

High-resolution image interpretation is another valuable tool for obtaining validation data. Although aerial photographs have been used previously for this purpose (Chapter 2), high-resolution satellite images may serve equally well. These images may be used to visually identify gullies (Chapter 3) or patterns of concentrated flow and ruptures of contourbunds (Chapter 6). For the Brazilian site a QuickBird image was used for feature detection, whereas field knowledge and observations assisted in image interpretation. Although high-resolution satellite images are still expensive, their acquisition should be considered for validation purposes in future regional erosion studies. However, important factors to take into account are the image timing in relation to erosion occurrence or presence of erosion features and the spatial size of the features encountered in the region.

7.4   Future directions

The approaches presented in this thesis constitute a small contribution towards critical thinking about regional erosion risk mapping and provide alternatives to erosion models, that are often applied to different scales and regions than for which they are developed. For several tropical regions, it was shown that erosion risk may be accurately mapped using only a limited amount of satellite- and other available data, in combination with local knowledge or field surveys. Nevertheless, much more work will be needed to obtain a good understanding of the importance of soil erosion across different regions, and at different spatial and temporal scales. Remote sensing may contribute to this understanding, but it will not alone provide the answers to the great number of uncertainties that exist in erosion science. Causes of uncertainties comprise:

- the difficulty of measuring erosion rates in the field (Stroosnijder, 2005) and extrapolating this information to larger regions (Boardman, 1998; Trimble and Crosson, 2000);

- the complexity of the erratic erosion processes and consequently failing of empirical or mathematical solutions to accurately describe and predict these processes for varying conditions (Beven, 2001);
- the problem of disaggregating the impact of soil erosion on crop productivity (Dregne, 1992; Lal, 2001), food security (Lomborg, 2001) or carbon storage (Lal, 2003), from other influences such as the use of ameliorated crop varieties, fertilizer application, soil deposition, and climatic changes, thus hampering a good appreciation of this impact.

Serious thought is required within the erosion community whether universal approaches towards assessment of erosion can be achieved, or whether its assessment is necessarily dependent on its spatial, temporal, economic, environmental and cultural context (Warren, 2002). Or in other words, can a single tool eventually be developed to evaluate erosion across different regions and scales, or are approaches intrinsically related to the purpose of the assessment, the regional characteristics, and scale? This thesis is clearly in support of the contextual approach. If ever a complete universal physical description of erosion processes can be obtained, including all relevant factors and processes (which is very doubtful due to the causes of uncertainties mentioned above), a model based on this description would have such a high requirement for good-quality data at a detailed spatial and temporal resolution, that it will prove practically impossible to apply the model anywhere. Notwithstanding, the development of physically-based models is important for increasing our understanding of the erosion processes. For spatial erosion assessments however, the starting point should not be the correct physical description or a pre-defined model developed for a very specific context, but rather the relevant spatial and temporal data that may be obtained for a specific region and scale. For areas larger than about 50 km^2, satellite remote sensing is one of the principle sources of spatial and temporal data. Because potential remote sensing observables depend on scale and regional characteristics, a data-driven approach is necessarily region-dependent. For example for arid environments SAR interferometry to detect random surface changes and linear spectral unmixing of optical data to assess status of soil and vegetation are promising methods (Chapter 2), and it would thus be unwise to discard their use in erosion assessment just because their applicability is not universal. Specific approaches may however prove useful for larger regions having a similar regional context, like e.g. the Brazilian Cerrados.

Based on the experience acquired within the framework of this thesis, future progress of regional erosion risk mapping is considered to depend on (1) improved techniques for retrieving erosion-related variables from remote sensing data, (2) the ongoing development of spaceborne sensors, (3) improved region-dependent data integration methods, and (4) the increase of proper validation activities.

1. Information retrieval algorithms from satellite remote sensing data are under strong development. Any progress in the retrieval of parameters describing the erosion factors may benefit erosion research. Promising fields of interest include the mapping of

senescent vegetation (Arsenault and Bonn, 2005; French et al., 2000), soil moisture assessment (Le Hégarat-Mascle et al., 2002; Mattia et al., 2006), but also improved techniques for erosion detection (chapter 3; Liu et al., 2004). Without doubt, many of the algorithms will work better for some regions than for others, and thus erosion risk mapping activities should follow the state-of-the-art knowledge on the conditions for retrieving specific observables. Relevant observables may then be selected for the local situation. With the increasing size and accessibility of current satellite data archives, also options for change detection and monitoring increase (Coppin et al., 2004). Assessment of dynamic soil and vegetation parameters may thus allow monitoring of erosion, although detailed field studies would be required to identify whether a clear relationship exists between observed changes and accelerated soil erosion. An operational monitoring system would be in need of reliable satellite recordings for a long time period, which may require much more similar land-observing satellites to be brought into orbit (Landgrebe, 2005).

2. Development of instruments and satellites is ongoing, and many new land-observing satellites have recently been launched or are planned to be launched in the near future, such as ALOS, RADARSAT-2, SMOS, OrbView-5, and TerraSAR-X. The instruments carried by these satellites will provide new capabilities, either through increased spatial or temporal resolution, through offering continuity for specific types of observation, or through the use of innovative imaging principles. Some satellite missions are mainly intended for technology demonstration (e.g. hyperspectral sensors like CHRIS-PROBA or Hyperion), whereas others provide data on an operational basis. Several potentially interesting instruments that are tested on airborne platforms, are awaiting financing opportunities for becoming spaceborne. Erosion research may take advantage of these developments, that may provide innovative ways for the retrieval of erosion factors and erosion detection.

3. Proper data integration methods are of utmost importance for accurate regional erosion risk mapping. Erosion models have their merit for the particular region and scale for which they were developed, but good validated methodologies for larger regions are scarce. More benefit is expected from region-specific selection and integration of parameters derived from current and future earth observation missions in combination with other data sources. This selection and integration may be based on expert knowledge (Chapter 4) or potentially on statistical relationships (Okoth, 2003). However, statistical relationships require a substantial amount of field data, which may be hard to obtain. A better dialogue between the remote sensing community and (local) erosion experts would allow determination of the remotely sensed variables required for erosion assessment under different conditions. In this way, various approaches would evolve for different regions and contexts, while similar techniques and integration methods may be used for comparable environments. Special attention should be paid to multi-scale assessments (e.g. Chapter 6), in which relevant temporal information is obtained from coarse-resolution satellite data, medium-resolution data are used for actual erosion risk mapping,

and fine-resolution data offer ground-truth information. Hierarchical erosion risk mapping approaches can thus be envisaged, where the coarser assessment defines areas of particular interest, while the more detailed assessment can provide validation of the coarser-scale results.

4. Advance in satellite-based erosion assessments is not possible if the performance of different methodologies is unknown. Multi-scale validation as presented above should be used to validate multi-scale assessments, but at the lowest level the options are largely restricted to the use of erosion field measurements, erosion surveys, and high-resolution image interpretation. Especially the last option could be used much more frequently in erosion studies, although limitations for discerning certain features exist. Standardisation of erosion measurement techniques (Stroosnijder, 2005) and a general format for erosion surveys (e.g. Herweg, 1996) that may be adapted to include local indicators, could be a step in the right direction. Moreover, construction of a global geo-database with field observations, measurements, and a clear description of the measurement and survey techniques used, is a conceivable option for the future. This would serve both for testing of a variety of mapping methodologies in different areas, and for defining generally-accepted good practices for acquiring validation data.

The time seems to be ripe for defining a clear research agenda and vision for future erosion mapping and monitoring across different scales. Under the proposed European Union Soil Framework Directive for example, the Member States will be required to identify areas of high erosion risk within their country and take appropriate measures for erosion reduction (CEC, 2006). At present, satellite remote sensing is still poorly used by erosion scientists, which may partly be explained by the fact that too high expectations were raised in the past considering remote sensing. Nevertheless, satellite remote sensing constitutes the major source of timely spatial information, and is necessarily part of potential monitoring schemes at larger scales. It is striking that a recent symposium on erosion assessment (Gabriels and Cornelis, 2003) hardly addressed remote sensing, while most presentations at a remote sensing conference on land degradation (Röder and Hill, 2006) focussed primarily on studying temporal vegetation patterns, which do not have a straightforward relation with erosion occurrence. A step forward for regional assessment and monitoring can only be made when close collaboration between erosion scientists, geographers, and the remote sensing community takes place. Interesting frameworks are currently being defined, bringing together space and ground observations to create better services. These include among others the European GMES (Global Monitoring for Environment and Security) and the global GEOSS (Global Earth Observation System of Systems) initiatives. Linking up of a large community of erosion scientists with these initiatives could provide a good means to critically enhance current methodologies and thus improve regional erosion mapping and monitoring capabilities.

References

Arsenault E, and Bonn F. 2005. Evaluation of soil erosion protective cover by crop residues using vegetation indices and spectral mixture analysis of multispectral and hyperspectral data. *Catena* 62 (2-3): 157-172.

Beven K. 2001. On modelling as collective intelligence. *Hydrological Processes* 15 (11): 2205-2207.

Boardman J. 1998. An average soil erosion rate for Europe: Myth or reality? *Journal of Soil and Water Conservation* 53 (1): 46-50.

CEC. 2006. Proposal for a Directive of the European Parliament and of the Council establishing a framework for the protection of soil and amending Directive 2004/35/EC. Commission of the European Communities, Brussels, Belgium: 30 pp.

Coppin P, Jonckheere I, Nackaerts K, Muys B, and Lambin E. 2004. Digital change detection methods in ecosystem monitoring: a review. *International Journal of Remote Sensing* 25 (9): 1565-1596.

Dregne HE. 1992. Erosion and soil productivity in Asia. *Journal of Soil & Water Conservation* 47 (1): 8-13.

French AN, Schmugge TJ, and Kustas WP. 2000. Discrimination of senescent vegetation using thermal emissivity contrast. *Remote Sensing of Environment* 74 (2): 249-254.

Gabriels D, and Cornelis W (Editors). 2003. Proceedings of the International Symposium on 25 Years of Assessment of Erosion: 22-26 September 2003. Ghent University, Ghent, Belgium: 555 pp.

Herweg K. 1996. Field Manual for Assessment of Current Erosion Damage. SCRP Ethiopia, and Centre for Development and Environment, University of Berne, Switzerland: 69 pp.

Lal R. 2001. Soil degradation by erosion. *Land Degradation & Development* 12 (6): 519-39.

Lal R. 2003. Soil erosion and the global carbon budget. *Environment International* 29 (4): 437-450.

Landgrebe DA. 2005. Multispectral land sensing: Where from, where to? *IEEE Transactions on Geoscience and Remote Sensing* 43 (3): 414-421.

Le Hégarat-Mascle S, Zribi M, Alem F, Weisse A, and Loumagne C. 2002. Soil moisture estimation from ERS/SAR data: Toward an operational methodology. *IEEE Transactions on Geoscience and Remote Sensing* 40 (12): 2647-2658.

Liu JG, Mason P, Hilton F, and Lee H. 2004. Detection of rapid erosion in SE Spain: A GIS approach based on ERS SAR coherence imagery. *Photogrammetric Engineering and Remote Sensing* 70 (10): 1179-1185.

Lomborg B. 2001. The skeptical environmentalist: measuring the real state of the world. Cambridge University Press, Cambridge, UK.

Mattia F, Satalino G, Dente L, and Pasquariello G. 2006. Using a priori information to improve soil moisture retrieval from ENVISAT ASAR AP data in semiarid regions. *IEEE Transactions on Geoscience and Remote Sensing* 44 (4): 900-911.

Okoth PF. 2003. A hierarchical method for soil erosion assessment and spatial risk modelling: a case study of Kiambu District in Kenya. Ph.D. Thesis, Wageningen University, Wageningen, The Netherlands: 213 pp.

Röder A, and Hill J (Editors). 2006. Proceedings of the 1st International Conference on Remote Sensing and Geoinformation Processing in the Assessment and Monitoring of Land Degradation and Desertification: 7-9 September 2005. University of Trier, Trier, Germany: 635 pp.

Stroosnijder L. 2005. Measurement of erosion: is it possible? *Catena* 64 (2-3): 162-173.

Trimble SW, and Crosson P. 2000. U.S. soil erosion rates - myth and reality. *Science* 289 (5477): 248-250.

Warren A. 2002. Land degradation is contextual. *Land Degradation & Development* 13 (6): 449-459.

SUMMARY

Summary

Chapter 1: Introduction

Accelerated soil erosion by water is a major land degradation problem in many regions around the world, creating negative impacts on agricultural production, infrastructure, and water quality. For defining effective soil and water conservation strategies, spatial information on the importance of erosion is required at various scales. Satellite data can provide a valuable input for spatial erosion assessment. One option for this is by identifying eroded areas, which is possible for specific conditions. More common is the satellite-based assessment of erosion factors, such as vegetation characteristics. In this case, erosion risk may be obtained by integrating the derived information with additional spatial data sources. Tools that are currently used for data integration are mostly limited to erosion models, which frequently have a high data requirement. Generally, these models are developed for smaller scales and other regions than for which they are applied. Therefore, model outcomes are questionable in many cases, especially if no validation is performed. As erosion processes are complex and vary between regions, new approaches are required that can incorporate locally-relevant information. The main objective of the research described in this thesis was to develop new methodologies for qualitative erosion mapping using satellite remote sensing. To this end, several tropical regions were studied that, except for satellite data, have poor data availability.

Chapter 2: Satellite remote sensing for water erosion assessment: a review

During the past 30 years, many studies have been published that in some way or another used satellite data for assessing soil erosion. This chapter provides an overview of the different methodologies used in these studies. Erosion detection was achieved by visually identifying large erosion features and eroded areas from satellite images. For specific cases, eroded areas could be automatically discerned mainly due to reduced vegetation cover or changing soil properties. Erosion consequences were assessed by determining sedimentation volumes or sediment concentrations in downstream lakes and reservoirs. However, most studies applied satellite data for the evaluation of erosion factors, including topography, soil, management practices, but in particular vegetation. The specific satellite sensor used and site characteristics determine which variables may be extracted. For example in more humid tropical environments, soils are often not visible from space due to the abundant vegetation cover. Remote sensing derived variables can subsequently be integrated with other data sources to map erosion risk. This has been achieved through erosion models and qualitative methods. The latter are generally more flexible in terms of data requirements and adaptability to regional characteristics, and allow incorporation of local expert knowledge. Validation of output results is important for evaluating the performance of different approaches, but was

not or only poorly done in most studies. It was concluded that satellite remote sensing can contribute to erosion assessment in many ways, but that a general lack of validation is a main concern.

Chapter 3: Automatic identification of erosion gullies with ASTER imagery in the Brazilian Cerrados

Although automatic identification of large eroded areas from satellite data has been performed in previous studies, individual erosion features were merely detected using visual interpretation techniques. The objective of this chapter was to determine whether it is possible to automatically identify large permanent erosion gullies from satellite data for the Brazilian Cerrados. For that purpose, a common algorithm called maximum likelihood classification was applied to a wet- and a dry-season optical ASTER image. Training of the algorithm was done by calculating the spectral statistics of the classes 'gullies' and 'non-gullies' from a 16-km^2 portion of the ASTER scene. Visual interpretation of a high-resolution QuickBird image allowed for precise delineation of class limits, which for a non-overlapping 36-km^2 area resulted in a gully map that was used for validation. The wet-season performed better than the dry-season classification, but best results were obtained when both classifications were combined. User's accuracy was above 90%, while only two out of 17 actual gullies were not detected and two small locations were erroneously identified as gully. It was therefore concluded that accurate identification of permanent erosion gullies is possible with optical satellite data. It is furthermore expected that the approach may be applied to larger areas with similar characteristics.

Chapter 4: Erosion risk mapping: a methodological case study in the Colombian Eastern Plains

Because erosion models are generally developed for a specific region and small scales (plot-scale to maximum 2 km^2), qualitative data integration may be a better option for erosion risk mapping at larger scales (>50 km^2) and for different regions where model assumptions are not valid. This chapter presents a qualitative erosion risk mapping methodology that uses expert knowledge to select and combine locally-important parameters, which can be extracted from available data sources. A generic description of the methodology was given, such that the method may be applied for other regions with different parameters of importance and different data availability. For the Puerto López municipality in the Colombian Eastern Plains, four erosion factors were defined, namely geology, soils, relief, and land management. Through interviews with local soil experts the relevant parameters for each factor were identified and subsequently derived from a soil survey, a digital elevation model (DEM), and an optical Landsat satellite image. The Landsat image was used for classifying land use and estimating fractional vegetation cover (FVC). For each factor a decision tree was constructed to combine the selected parameters into a factor rating,

reflecting the relative susceptibility to erosion for that factor. Erosion risk maps were obtained through averaging factor ratings, where actual risk used all factors and potential risk excluded the management factor. The maps showed good agreement with field observations, although more field observations would be required for thorough validation. The chapter concludes that flexible methodologies using expert knowledge are valuable tools for erosion risk mapping as locally-important factors and processes can be accounted for effectively.

Chapter 5: Spatial evaluation of soil erosion risk in the West Usambara Mountains, Tanzania

Poor availability of good-quality spatial data is common in regions like sub-Saharan Africa, and complicates effective regional erosion assessment. The aim of this chapter was to evaluate whether a limited amount of readily available data from spaceborne sensors may allow for accurate erosion risk mapping. For a 70-km^2 watershed in the West Usambara Mountains of Tanzania, a DEM from the Shuttle Radar Topography Mission and a Landsat image, recorded slightly before the erosive season, were used. Two qualitative data integration methods were tested. The first method derived slope classes from the DEM and fractional vegetation cover (FVC) classes from the Landsat image and FVC field estimates. Data integration was achieved with a decision tree that was calibrated using field observations. The second method did not require field data, but automatically classified slope and a spectral vegetation index called NDVI (normalized difference vegetation index) into five classes, with each class covering 20% of the watershed. Low NDVI and steep slopes were related to high erosion risk and vice versa. For each pixel the lowest value of both classes was retained to create the final erosion risk map. High erosion risk areas are thus places with both a steep slope and a low vegetation cover. Resulting maps both showed a high accuracy of about 80%. The second method is therefore preferred because its application requires less field data. The study demonstrated that qualitative integration of the factors vegetation cover and slope allows for accurate mapping of soil erosion risk in the watershed studied. Proper timing of the Landsat image to assess patterns of vegetation cover at the time of high erosion risk was considered important.

Chapter 6: Timing of erosion and satellite data: a multi-resolution approach to erosion risk mapping

Erosion is an erratic process and occurs when high-intensity rainfall coincides with low vegetation cover. When mapping erosion risk, the timing of the major erosion events can have implications for the selection of satellite images, used to describe the spatial patterns of FVC. This chapter presents a method for erosion risk mapping using multi-temporal satellite data at various resolutions. The analyses were performed for a 100-km^2 pasture area in the Brazilian Cerrados during a full growing season from August 2002 to August 2003. At the coarse spatial scale, 3-hourly rainfall estimates, obtained from the spaceborne TRMM

mission, were compared with NDVI time series derived from daily and 16-day 250-m resolution MODIS imagery. This comparison indicated that highest erosion risk occurred during the months November and December. At the medium spatial scale, the NDVI was calculated from a time series of six 15-m resolution ASTER images available for the year studied. Due to persistent cloud cover no recordings were made between October and March. NDVI was classified in five equally-sized classes, of which the low NDVI classes were related to high erosion risk, while a DEM was merely used to set approximately flat zones to very low erosion risk. The six resulting erosion risk maps were evaluated with data on erosion features that were visually interpreted from a 0.61-m resolution QuickBird image. Results from the ASTER image of October gave the highest accuracy (84%), which is shortly before the first erosion events. The presented approach for erosion risk mapping applies coarse-resolution temporal data for determining erosion periods, which subsequently assists in the selection of medium-resolution data for effective mapping. High-resolution data allows for validation of the results, at least for the situation of Brazilian Cerrados. The approach may easily be applied in other areas with high spatial and temporal variability of vegetation cover.

Chapter 7: Synthesis

Based on the studies presented in this thesis, it can be concluded that satellite remote sensing has much to offer to spatial erosion assessments, especially for data-poor regions. Variables that may be derived from satellite data depend on the sensor type, specific regional characteristics, and the possibility of obtaining additional data. While in some cases direct detection of erosion features is possible, and automatic methods may achieve this, the general input of satellite data is to assess erosion factors that may be integrated with additional spatial data. The thesis showed that qualitative data integration methods that address regionally-important parameters can be a good option for erosion risk mapping, while local knowledge and field surveys can provide important input to such methods. A flexible approach that can easily be adapted to regional characteristics is to be preferred over data-demanding erosion models, developed for other scales and regions. Validation of results is however highly important for defining appropriate mapping techniques. Because erosion is a difficult process to measure, simple qualitative field surveys or high-resolution image interpretation constitute good alternatives for obtaining validation data. Timing of satellite imagery and of surveys is important and needs to be considered carefully in any erosion study. Coarse-resolution satellite data can assist in obtaining a quick overview of the most erosive periods. Future progress of regional erosion risk mapping is considered to depend on (1) improved techniques for retrieving erosion-related variables from remote sensing data, (2) the ongoing development of spaceborne sensors, (3) improved region-dependent data integration methods, and (4) the increase of proper validation activities. A clear research agenda and vision for future erosion mapping and monitoring activities across different scales should be developed. A step forward for these activities can only be made when close collaboration between erosion scientists, geographers, and the remote sensing community takes place.

Samenvatting

Hoofdstuk 1: Inleiding

Versnelde bodemerosie door water is een aanzienlijk landdegradatie-probleem in veel gebieden wereldwijd en veroorzaakt negatieve effecten voor agrarische productie, infrastructuur, en waterkwaliteit. Ruimtelijke informatie over bodemerosie is noodzakelijk op verschillende schaalniveaus om effectieve strategieën voor bodem- en waterconservering te ontwikkelen. Satellietdata kunnen een belangrijke bijdrage leveren aan de ruimtelijke evaluatie van bodemerosie. Enerzijds kan dit door geërodeerde gebieden te identificeren, wat mogelijk is onder bepaalde omstandigheden. Gebruikelijker is het echter om erosiefactoren, zoals vegetatiekenmerken, te bepalen met behulp van satellietbeelden. In dit geval kan erosierisico verkregen worden door de verworven informatie te integreren met andere bronnen van ruimtelijke data. Tegenwoordig gebeurt deze integratie voornamelijk door middel van erosiemodellen, die voor hun toepassing doorgaans veel invoergegevens vereisen. Over het algemeen zijn dergelijke modellen ontwikkeld voor kleinere schaalniveaus en andere gebieden dan waar ze op toegepast worden. Daardoor zijn modeluitkomsten in veel gevallen twijfelachtig, vooral wanneer deze niet zijn gevalideerd. Aangezien erosieprocessen complex zijn en variëren tussen gebieden, zijn er nieuwe benaderingen nodig die gebiedsrelevante informatie benutten. De voornaamste doelstelling van het onderzoek, beschreven in dit proefschrift, was om nieuwe methodologieën te ontwikkelen voor kwalitatieve kartering van bodemerosie, gebruik makend van satelliet remote sensing. Hiertoe werden verschillende tropische gebieden onderzocht die behoudens satellietgegevens een lage beschikbaarheid van ruimtelijke data hebben.

Hoofdstuk 2: Satelliet remote sensing voor het bepalen van watererosie: een overzicht

Gedurende de afgelopen 30 jaar zijn er een groot aantal studies gepubliceerd die op de één of andere manier satellietgegevens hebben toegepast om bodemerosie door water te bepalen. Dit hoofdstuk geeft een overzicht van de verschillende methodologieën die deze studies gebruikten. Erosiedetectie werd bereikt door visuele identificatie van grote erosievormen en geërodeerde gebieden vanaf satellietbeelden. In speciale gevallen was het mogelijk om geërodeerde gebieden automatisch te onderscheiden vanwege verminderde vegetatiebedekking of veranderende bodemeigenschappen. Gevolgen van erosie werden geëvalueerd door sedimentatievolumes of -concentraties in benedenstroomse meren of stuwmeren te bepalen. De meeste studies gebruikten satellietgegevens echter voor het analyseren van erosiefactoren, met inbegrip van topografie, bodem, landbeheerspraktijken, maar in het bijzonder vegetatie. De specifieke satellietsensor die gebruikt wordt alsmede gebiedskarakteristieken bepalen welke variabelen verkregen kunnen worden. In nattere

tropische gebieden bijvoorbeeld, belet de dichte vegetatiebedekking dikwijls de zichtbaarheid van de bodems vanuit de ruimte. De door remote sensing verkregen variabelen kunnen vervolgens met andere databronnen geïntegreerd worden teneinde erosierisico te karteren. Dit is gedaan met behulp van erosiemodellen en kwalitatieve methoden. De laatstgenoemden zijn doorgaans flexibeler wat betreft datavereisten en de aanpasbaarheid aan regionale kenmerken, en kunnen gebruik maken van de kennis van lokale experts. Het valideren van uitkomsten is belangrijk om de waarde van verschillende karteringsbenaderingen in te schatten, maar de meeste studies hebben dit niet of slecht gedaan. Er werd geconcludeerd dat satelliet remote sensing op vele manieren kan bijdragen aan erosiebepalingen, maar dat een algemeen gebrek aan validatie een belangrijk probleem is.

Hoofdstuk 3: Automatische detectie van erosiegeulen met ASTER beelden in de Braziliaanse Cerrados

Hoewel in eerdere studies grote geërodeerde gebieden automatisch konden worden geïdentificeerd met behulp van satellietgegevens, zijn individuele erosievormen tot dusverre slechts gedetecteerd door middel van visuele interpretatietechnieken. Dit hoofdstuk had tot doel om te bepalen of het mogelijk is om met satellietdata automatisch grote permanente erosiegeulen te detecteren in de Braziliaanse Cerrados. Daartoe werd een gangbaar algoritme, genaamd *maximum likelihood* classificatie, toegepast op een optisch ASTER-beeld van het natte en van het droge seizoen. Het algoritme werd getraind door de spectrale statistieken van de klassen 'geul' en 'niet-geul' te berekenen voor een gedeelte van 16 km^2 van het ASTER-beeld. De exacte ruimtelijke limieten van deze klassen werden bepaald door visuele interpretatie van een QuickBird-beeld van hoge resolutie. Voor een niet-overlappend gebied van 36 km^2 resulteerde de QuickBird-interpretatie in een geulkaart, die gebruikt werd voor validatie. Het ASTER-beeld van het natte seizoen gaf betere classificatieresultaten dan het beeld van het droge seizoen, hoewel de beste resultaten verkregen werden wanneer beide classificaties werden gecombineerd. In dit geval waren 90% van de als geul geclassificeerde pixels correct geclassificeerd, terwijl slechts twee van de 17 feitelijke geulen niet werden gedetecteerd en twee kleine gebieden foutief als geul geïdentificeerd werden. Hieruit kan worden opgemaakt dat nauwkeurige detectie van permanente erosiegeulen mogelijk is met optische satellietdata. Bovendien wordt verwacht dat de methode toegepast kan worden op grotere gebieden met gelijksoortige kenmerken.

Hoofdstuk 4: Erosierisico-kartering: een methodologische case studie in de Colombiaanse Llanos

Aangezien erosiemodellen doorgaans ontwikkeld zijn voor specifieke gebieden en kleine schaalniveaus (plotschaal tot maximaal 2 km^2), kan kwalitatieve data integratie een betere keuze zijn voor erosierisico-kartering op grotere schaal (>50 km^2) en voor andere gebieden waar modelaannames niet geldig zijn. Dit hoofdstuk presenteert een kwalitatieve

methodologie voor erosierisico-kartering, die gebruikt maakt van kennis van lokale experts om plaatselijk belangrijke parameters te selecteren en integreren. Ruimtelijke informatie met betrekking tot deze parameters kan verkregen worden uit beschikbare databronnen. De methodologie werd generiek beschreven, zodat deze toegepast kan worden voor andere gebieden met verschillen in belangrijke parameters en beschikbaarheid van gegevens. Voor de gemeente Puerto López in de Colombiaanse Llanos werden vier erosiefactoren gedefinieerd, namelijk geologie, bodem, topografie, en landbeheer. Door interviews met lokale bodemexperts werden de relevante parameters voor elke factor geïdentificeerd. Informatie over deze parameters werd vervolgens afgeleid van een bodemstudie, een digitaal hoogtemodel, en een optisch Landsat-beeld. Het Landsat-beeld werd gebruikt voor landgebruiksclassificatie en voor het schatten van de fractie vegetatiebedekking. Voor elke factor werd een beslissingsboom gemaakt met als doel de geselecteerde parameters te combineren tot een factorwaarde, die de relatieve vatbaarheid voor erosie uitdrukt voor de desbetreffende factor. Erosierisico-kaarten werden verkregen door de factorwaarden te middelen, waarbij actueel risico alle factoren gebruikte, en potentieel risico alle factoren behalve de landbeheer factor. De kaarten kwamen goed overeen met veldwaarnemingen, hoewel meer waarnemingen nodig zijn voor grondige validatie. De conclusie uit dit hoofdstuk is dat flexibele methoden, die kennis van lokale experts benutten, waardevolle middelen zijn voor erosierisico-kartering, aangezien er effectief rekening gehouden kan worden met plaatselijk belangrijke factoren en processen.

Hoofdstuk 5: Ruimtelijke evaluatie van bodemerosierisico in het westelijk Usambara Gebergte, Tanzania

Ruimtelijke data van goede kwaliteit is slecht beschikbaar voor gebieden zoals Afrika ten zuiden van de Sahara, en dit bemoeilijkt doeltreffende regionale erosiebepalingen. Het doel van dit hoofdstuk was te evalueren of nauwkeurige erosierisico-kartering mogelijk is met een beperkte hoeveelheid goedtoegankelijke satellietgegevens. Voor een vanggebied van 70 km^2 in het westelijk Usambara Gebergte van Tanzania, werd een digitaal hoogtemodel van de Shuttle Radar Topography Mission en een kort voor het erosieseizoen opgenomen Landsat-beeld gebruikt. Twee kwalitatieve data-integratiemethoden werden getest. Voor de eerste methode werden hellingsklassen afgeleid van het hoogtemodel, en fractionele vegetatiebedekking (FVC) van het Landsat-beeld en FVC-veldschattingen. Data-integratie werd gedaan door middel van een beslissingsboom, welke gecalibreerd was met veldwaarnemingen. Voor de tweede methode waren geen veldgegevens nodig, aangezien in dit geval hellingshoeken en een spectrale vegetatie-index genaamd NDVI automatisch werden ingedeeld in vijf klassen, welke elk 20% van het vanggebied omvatten. Lage NDVI-waarden en steile hellingen werden gerelateerd aan een hoog erosierisico en vice versa. De uiteindelijke erosierisico-kaart werd gegenereerd door voor elk pixel de laagste erosierisico-klasse van de helling en NDVI classificatie te behouden. Gebieden met hoog erosierisico zijn dus plekken die een steile helling en een geringe vegetatiebedekking hebben. De resulterende

erosierisico-kaarten lieten voor beide methoden een hoge nauwkeurigheid van ongeveer 80% zien. De voorkeur gaat daarom uit naar de tweede methode, omdat minder veldgegevens nodig zijn voor de toepassing hiervan. De studie toonde aan dat nauwkeurige kartering van erosierisico mogelijk is voor het bestudeerde vanggebied door de factoren vegetatiebedekking en helling op een kwalitatieve manier te integreren. Een correcte timing van het Landsat-beeld om patronen van vegetatiebedekking te schatten op het moment van hoog erosierisico werd als belangrijk beschouwd.

Hoofdstuk 6: Timing van erosie en satellietdata: een multi-resolutie benadering van erosierisico-kartering

Erosie is een onregelmatig proces en vindt plaats wanneer regenval van hoge intensiteit samenvalt met een geringe vegetatiebedekking. Bij het karteren van erosierisico, kan de timing van grote erosiegebeurtenissen consequenties hebben voor de selectie van satellietbeelden, die gebruikt worden om ruimtelijke patronen van vegetatiebedekking te beschrijven. In dit hoofdstuk wordt een methode voor erosierisico-kartering gepresenteerd, die multi-temporele satellietdata van verschillende resoluties gebruikt. De analyses werden uitgevoerd voor een graslandgebied ter grootte van 100 km^2 in de Braziliaanse Cerrados en besloegen een volledig groeiseizoen van augustus 2002 tot augustus 2003. Op de groffe ruimtelijke schaal werden 3-uurlijkse regenvalschattingen van de TRMM satellietmissie vergeleken met NDVI tijdsseries verkregen uit dagelijkse en 16-dagelijkse 250-m resolutie MODIS-beeldproducten. Deze vergelijking liet zien dat het hoogste erosierisico optreedt gedurende de maanden november en december. Op de middelgrote schaal werd de NDVI berekend voor een tijdreeks van zes 15-m resolutie ASTER-beelden die beschikbaar waren voor het bestudeerde groeiseizoen. Vanwege aanhoudende wolkenbedekking waren er tussen oktober en maart geen ASTER-opnames gemaakt. De NDVI werd geclassificeerd in vijf even grote klassen, waarbij de klassen met lage NDVI werden gerelateerd aan hoog erosierisico. Een digitaal hoogtemodel werd slechts gebruikt om zeer laag erosierisico toe te kennen aan bij benadering vlakke gebieden. De zes resulterende erosierisico-kaarten werden geëvalueerd met gegevens over aanwezige erosieverschijnselen, die door middel van visuele interpretatie waren gedigitaliseerd van een 0,61-m resolutie QuickBird-beeld. De hoogste nauwkeurigheid (84%) werd bereikt met de resultaten van het ASTER-beeld van oktober. Dit moment valt kort voor de eerste erosiegebeurtenissen van het seizoen. De gepresenteerde benadering voor erosierisico-kartering gebruikt temporele data van lage ruimtelijke resolutie om erosieperioden te bepalen, hetgeen vervolgens kan helpen in de selectie van satellietbeelden van gemiddelde resolutie voor effectieve kartering. Validatie van de resultaten was in het geval van de Braziliaanse Cerrados mogelijk met een hoogresolutie satellietbeeld. De benadering kan eenvoudig toegepast worden in andere gebieden met sterke ruimtelijke en temporele variabiliteit van vegetatiebedekking.

Hoofdstuk 7: Synthese

Gebaseerd op de gepresenteerde studies in dit proefschrift, kan geconcludeerd worden dat satelliet remote sensing veel te bieden heeft voor erosie-kartering, vooral voor gebieden met geringe beschikbaarheid van ruimtelijke data. De variabelen die uit satellietdata afgeleid kunnen worden zijn afhankelijk van het type sensor, specifieke gebiedskenmerken, en de mogelijkheid om aanvullende data te verkrijgen. In sommige gevallen is directe detectie van erosievormen mogelijk, en kunnen automatische methoden dit bewerkstelligen. Echter, het voornaamste gebruik van satellietdata is om erosiefactoren te analyseren die vervolgens geïntegreerd kunnen worden met additionele ruimtelijke gegevens. Dit proefschrift liet zien dat kwalitatieve data-integratiemethoden, die gebruik maken van regionaal belangrijke parameters, een goede optie zijn voor erosierisico-kartering. Lokale kennis en veldstudies kunnen een belangrijke bijdrage leveren aan dergelijke methoden. Een flexibele benadering die gemakkelijk aangepast kan worden aan regionale kenmerken zou verkozen moeten worden boven erosiemodellen met een hoge databehoefte, die ontwikkeld zijn voor andere gebieden en schaalniveaus. Om te komen tot adequate karteringstechnieken is validatie van resultaten echter onontbeerlijk. Aangezien erosie een lastig proces is om te meten, kunnen eenvoudige kwalitatieve veldstudies of interpretatie van remote sensing beelden van hoge resolutie goede alternatieven zijn ter verkrijging van validatiegegevens. De timing van satellietbeelden en van veldstudies is belangrijk en moet zorgvuldig overwogen worden voor iedere erosiestudie. Satellietdata van lage ruimtelijke en hoge temporele resolutie kunnen bijdragen om een snel overzicht te krijgen van de periodes waarin de meeste erosie verwacht kan worden. Toekomstige verbetering van regionale erosierisico-kartering wordt beschouwd afhankelijk te zijn van (1) verbeterde technieken om erosie-gerelateerde variabelen uit remote sensing data af te leiden, (2) de voortgaande ontwikkeling van satellietsensoren, (3) verbeterde gebiedsafhankelijke data-integratiemethoden, en (4) een toename van goede validatie-activiteiten. Een duidelijke onderzoeksagenda en een visie voor toekomstige erosie-kartering en monitoring activiteiten voor verschillende schaalniveaus zal ontwikkeld moeten worden. Een stap voorwaarts kan alleen gezet worden voor deze activiteiten wanneer nauwe samenwerking plaatsvindt tussen erosiewetenschappers, geografen, en de remote sensing gemeenschap.

Curriculum Vitae

Anton Vrieling was born on the 16th of November 1977 in Smilde, a village in the north of the Netherlands. After finishing secondary school in Assen in 1995, he started to study at Wageningen University (WU). During his studies he gained research experience in several countries. In 1998 he spent six months at the International Crops Research Institute for the Semi-Arid Tropics (ICRISAT) in Niamey, Niger, to perform a study on wind erosion variability in a farmer's field. His interest in larger-scale assessments and GIS brought him in 1999 to the International Center for Tropical Agriculture (CIAT) in Cali, Colombia. The work he carried out there on spatial erosion risk assessment formed the basis of Chapter 4 in this thesis. To gain more experience on remote sensing techniques, in 2000 Anton went for six months to the Canada Centre for Remote Sensing in Ottawa, Canada, where he studied coastline dynamics of the Beaufort Sea coast using multi-temporal satellite data. In 2001, he graduated cum laude in Tropical Land Use, and obtained an MSc degree in Geo-Information Science, both at WU. In the same year, he was awarded a scholarship of the European Space Agency (ESA) to attend the two-month Summer Session Program of the International Space University (ISU). In October 2001, Anton was contracted as a Junior Scientist by the Erosion and Soil & Water Conservation (ESW) Group at WU. The major part of his activities consisted of the PhD research, but he also gave courses, supervised students, and guided excursions and practicals in Tunisia and Spain. During the course of his PhD studies, he performed fieldwork in Brazil and Tanzania, and attended several international courses and conferences. This thesis is the final outcome of his PhD research. Since April 2006, he is working at SarVision in Wageningen on forest monitoring with satellite remote sensing.

Anton can be contacted at: anton.vrieling@gmail.com

PE&RC PhD Education Statement Form

With the educational activities listed below the PhD candidate has complied with the educational requirements set by the C.T. de Wit Graduate School for Production Ecology and Resource Conservation (PE&RC) which comprises of a minimum total of 22 credits (= 32 ECTS = 22 weeks of activities)

The C.T. De Wit Graduate School PE&RC

PRODUCTION ECOLOGY

& RESOURCE CONSERVATION
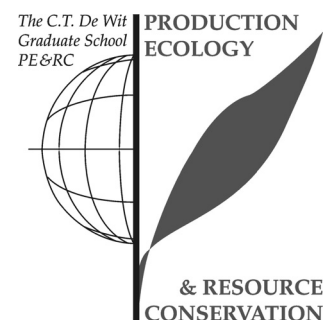
Review of Literature (3 credits)
- Remote sensing for soil erosion studies (2003)

Writing of Project Proposal (5 credits)
- Regional erosion risk mapping in tropical environments though integrated use of multi-temporal SAR in a GIS (2001)

Post-Graduate Courses (6 credits)
- MODLUC-modelling land use change (Université catholique de Louvain, Belgium) (2002)
- Wind and water erosion: modelling and measurement (Wageningen University, The Netherlands & Ghent University, Belgium) (2003)
- ENVISAT summer school (ESRIN-ESA, Frascati, Italy) (2004)
- Multivariate analysis (Wageningen University, The Netherlands) (2004)

Deficiency, Refresh, Brush-up and General Courses (1 credits)
- Career perspectives (Meijer & Meijaard) (2005)

PhD Discussion Groups (3 credits)
- Sustainable land-use and resource management (2004-2005)
- Advances in land management (seminar series at the ESWC Group) (2004-2005)

PE&RC Annual Meetings, Seminars and Introduction Days (1 credit)
- Annual meeting: "The truth of science" (PE&RC) (2005)
- Meeting for "10 years anniversary" (PE&RC) (2005)
- Master classes (PE&RC) (2005)

International Symposia, Workshops and Conferences (5 credits)
- 25 Years of assessment of erosion (Ghent, Belgium) (2003)
- ENVISAT symposium (Salzburg, Austria) (2004)
- International symposium on land degradation and desertification (Uberlândia, Brazil) (2005)
- Remote sensing and geoinformation processing in the assessment and monitoring of land degradation (Trier, Germany) (2005)
- Remote sensing and spatial analysis tools on erosion processes (Samos, Greece) (2006)

Laboratory Training and Working Visits (1 credits)
- Radar interferometry processing (Delft University of Technology, The Netherlands) (2002)